2023

UNDERSTANDING THE ROLE OF PEROXIREDOXIN IV IN COLORECTAL CANCER DEVELOPMENT

Pratik Thapa

STUDENT AGREEMENT:

I represent that my thesis or dissertation and abstract are my original work. Proper attribution has been given to all outside sources. I understand that I am solely responsible for obtaining any needed copyright permissions. I have obtained needed written permission statement(s) from the owner(s) of each third-party copyrighted matter to be included in my work, allowing electronic distribution (if such use is not permitted by the fair use doctrine) which will be submitted to UKnowledge as Additional File.

I hereby grant to The University of Kentucky and its agents the irrevocable, non-exclusive, and royalty-free license to archive and make accessible my work in whole or in part in all forms of media, now or hereafter known. I agree that the document mentioned above may be made available immediately for worldwide access unless an embargo applies.

I retain all other ownership rights to the copyright of my work. I also retain the right to use in future works (such as articles or books) all or part of my work. I understand that I am free to register the copyright to my work.

REVIEW, APPROVAL AND ACCEPTANCE

The document mentioned above has been reviewed and accepted by the student's advisor, on behalf of the advisory committee, and by the Director of Graduate Studies (DGS), on behalf of the program; we verify that this is the final, approved version of the student's thesis including all changes required by the advisory committee. The undersigned agree to abide by the statements above.

Pratik Thapa, Student

Dr. Qiou Wei, Major Professor

Dr. Isabel Mellon, Director of Graduate Studies

UNDERSTANDING THE ROLE OF PEROXIREDOXIN IV IN COLORECTAL CANCER DEVELOPMENT

DISSERTATION

A dissertation submitted in partial fulfillment of the
requirements for the degree of Doctor of Philosophy in the
College of Medicine
at the University of Kentucky

By
Pratik Thapa
Lexington, Kentucky
Director: Dr. Qiou Wei, Associate Professor of Toxicology and Cancer Biology
Lexington, Kentucky
2023

https://orcid.org/0000-0002-4266-0125

ABSTRACT OF DISSERTATION

UNDERSTANDING THE ROLE OF PEROXIREDOXIN IV
IN COLORECTAL CANCER DEVELOPMENT

Reactive oxygen species (ROS) are oxygen-containing free radicals and/or molecules that are more reactive than O_2. ROS such as hydroxyl radical ($^{\bullet}OH$) and hydrogen peroxide (H_2O_2) are produced naturally in the body as a result of reactions such as aerobic respiration and oxidative protein folding. ROS undergo reduction-oxidation (redox) reactions and mediate cell signaling. Accumulation of excessive ROS can damage DNA, RNA, protein and lipids. Antioxidants are enzymes and small molecules that react with ROS to modulate redox signaling and to prevent and repair oxidative damage. Examples of antioxidants include glutathione, thioredoxin, superoxide dismutase, catalase, vitamin C and peroxiredoxin (Prx).

In mammals, there are six Prxs that reduce hydrogen peroxide, alkyl hydroperoxide and peroxynitrite to maintain redox balance and protect against oxidative stress. Different Prxs have similar functions but different subcellular distribution. Peroxiredoxin IV (Prx4) scavenges ROS and participates in oxidative protein folding in the endoplasmic reticulum. We hypothesized that Prx4 plays an oncogenic role in colorectal cancer. To understand the significance of the Prx4 in colorectal cancer formation, wildtype and Prx4-/- mice of FVB/N background were subjected to a standard protocol of colorectal carcinogenesis induced by sequential exposure to Azoxymethane and Dextran sulfate sodium (AOM/DSS). Compared with wildtype littermates, Prx4-/- mice had significantly fewer and smaller tumors. Histopathological analysis revealed that loss of Prx4 leads to increased cell death through lipid peroxidation and lower infiltration of inflammatory cells in the knockout tumors compared to wildtype. We also examined the role of Prx4 in the progression of colorectal cancer. Loss of Prx4 reduced migration and invasion of colon cancer cell lines in vitro. Additionally, orthotopic implantation of HCT116 cells into immunodeficient NSG mice resulted in significantly lower metastasis after Prx4 knockdown. Mechanistic studies showed the involvement of tumor suppressor DKK1 in reducing migration and invasion in Prx4 knockdown cells. Thus, Prx4 plays a pro-tumorigenic role in colorectal cancer initiation and progression. This dissertation identifies Prx4 as a promising therapeutic target for prevention and treatment of colorectal cancer and highlights the need for further research to bridge the gap to clinical application.

KEYWORDS: Peroxiredoxin, Sulfiredoxin, DKK1, Oxidative Stress, Inflammation, Colorectal Cancer

Pratik Thapa

(Name of Student)

05/02/2023

Date

UNDERSTANDING THE ROLE OF PEROXIREDOXIN IV IN COLORECTAL CANCER DEVELOPMENT

By
Pratik Thapa

Qiou Wei, M.D., Ph.D.
Director of Dissertation

Isabel Mellon, Ph.D.
Director of Graduate Studies

05/02/2023
Date

DEDICATION

To my family.

ACKNOWLEDGMENTS

The following dissertation, while an individual work, benefited from the insights and direction of several people. First, my Dissertation Chair, Dr. Qiou Wei, exemplifies the high quality scholarship to which I aspire. If I am a better scientist than I was five years ago, it is thanks to Dr. Wei. Thank you so much for your continuous guidance and encouragement! Next, I wish to thank the Dissertation Committee: Dr. Daret St. Clair, Dr. Tianyan Gao, Dr. Jin-Ming Yang, and Dr. Nathan Vanderford for providing timely and instructive comments and evaluation at every stage of the dissertation process, allowing me to complete this project on schedule. Each individual provided insights that guided and challenged my thinking, substantially improving the finished product. Lastly, I would like to give a special thanks to Dr. Young-Sam Lee for serving as Outside Examiner of my final exam.

I would like to thank all the current and former members of the Wei lab. My special thanks to Dr. Hong Jiang, Dr. Yanning Hao, Na Ding and Aziza Alshahrani- your collaboration was instrumental in completion of this work, and I feel lucky to have your support and friendship in my work and in my life. I also want to thank Dr. Xiaoqi Liu, Dr. Isabel Mellon and the Department of Toxicology and Cancer Biology for educational, financial and administrative support.

The Shared Resource Facilities at the University of Kentucky Markey Cancer Center (P30CA177558) and the Sanders-Brown Center on Aging supported this work. In addition, this dissertation research would not have been possible without the funding support from: The National Institutes of Health (NCI R01CA222596, NIEHS T32ES07266), Department of Defense (W81XWH-16-1-0203), American Cancer

Society (RSG-16-213-01-TBE), and the Kentucky Lung Cancer Research Program (KLCRP2016).

In addition to the technical and instrumental assistance above, I received equally important assistance from family and friends. I also want to thank all the amazing teachers I have had over the years. Finally, I wish to thank my parents and my sister for their unconditional love. Thank you for instilling a love for learning and importance of honesty and hard work in me! None of my achievements would be possible without your support.

TABLE OF CONTENTS

LIST OF TABLES

LIST OF FIGURES

CHAPTER 1. INTRODUCTION

1.1 Introduction to Oxidative Stress and Peroxiredoxins

Reactive oxygen species (ROS) are oxygen-containing molecules that are unstable and highly reactive. Some examples of ROS include hydrogen peroxide (H_2O_2), superoxide radical ($O_2^{\bullet-}$), and hydroxide radical ($^{\bullet}OH$). ROS are natural byproducts of certain cellular processes such as oxidative protein folding in the endoplasmic reticulum and aerobic respiration in the mitochondria. Cells can also produce ROS in response to tissue damage or inflammation caused by external agents such as pathogen or ionizing radiation. Living systems use ROS for regulation of cell signaling and defense against microorganisms. However, excess ROS can damage DNA, RNA, proteins and lipids. The reduction-oxidation (redox) imbalance and/or the disruption in the regulation of cell signaling by ROS is known as oxidative stress, and it is an important risk factor for disease and ageing. Hence, it is critical to maintain a proper balance in the levels of ROS in the body.

The molecules utilized by the body to prevent or neutralize excess ROS and repair damage caused by oxidative stress are known as antioxidants. Living systems have evolved to possess several different types of enzymatic and non-enzymatic antioxidants. Some examples of antioxidants include glutathione (GSH), ascorbic acid (vitamin C), superoxide dismutase (SOD), catalase (CAT), glutathione peroxidase (GPx), and Peroxiredoxin (Prdx or Prx). Glutathione is the most abundant antioxidant in cells [1]. It can directly reduce various ROS and reactive nitrogen species (RNS), and it serves as a co-factor for several antioxidant enzymes. SOD catalyzes the conversion of superoxide anion radicals to hydrogen peroxide and molecular oxygen [2]. Catalase reduces hydrogen peroxide to water

and molecular oxygen [3]. GPx reduces hydrogen peroxide to water and lipid peroxides to their corresponding alcohols [4].

Peroxiredoxins (Prxs) are a family of thiol proteins that catalyze reduction of H_2O_2, alkyl hydroperoxides and peroxynitrite to water, corresponding alcohols and nitrite respectively, using Thioredoxin (Trx) or Glutathione (GSH) as reductants [5-7]. In addition to peroxidase function, Prxs can also function as chaperones and regulators of circadian clock [8, 9]. Prx was first identified in yeast in 1987 and in *S. typhimurium* in 1990 [10, 11]. In the following years, it was discovered that Prxs are ubiquitously expressed in all living organisms, and the name Peroxiredoxin was first suggested in 1994 [12, 13]. All Prxs contain a highly reactive Cysteine called 'peroxidatic' Cysteine (C_P) that is oxidized by peroxides to form sulfenic acid (C_PSOH). Some Prxs contain a second reactive Cysteine called 'resolving' Cysteine (C_R) that forms disulfide bond with C_PSOH. In mammalian cells, six isoforms of Prxs have been discovered, Prx 1-6. They can be classified into three subfamilies based on the location of C_R:

1) Typical 2-Cys Prx. Prx1 to Prx4 fall under typical 2-Cys Prxs. A catalytic unit consists of a homodimer where both subunits contain both C_P and C_R. Oxidized C_P (for example C_PSOH) of one subunit forms disulfide with C_RSH of another subunit. This disulfide bond is typically reduced by thioredoxin- Trx Reductase (TrxR) or GSH-Glutaredoxin (Grx) reductase systems. Typical 2-Cys Prxs exist in dimers and decamers (do-decamers for Prx3), with the ratio influenced by oxidation of C_P. These Prxs can also function as protein chaperones.

2) Atypical 2-Cys Prx. Prx5 is considered atypical 2-Cys Prx. Oxidized C_P of a Prx5 molecule forms disulfide with C_RSH in the same molecule. This disulfide bond is also reduced by Trx-TrxR system. Prx5 does not form decamers like typical 2-Cys Prxs.

3) 1-Cys Prx. Prx6 does not contain C_R, therefore disulfide bond formation takes place with other thiol proteins such as π Glutathione-S-Transferase (πGST) and is reduced by GSH. Unlike other Prxs, Prx6 also expresses phospholipase A_2 (PLA_2) activity.

A different classification system exists based on profiling of active site structure and sequence information: 1) Prx1 2) Prx5 3) Prx6 4) Tpx 5) PrxQ and 6) AhpE [14]. Mammalian Prx1-Prx4 belong to Prx1 subfamily, while mammalian Prx5 and Prx6 are classified under Prx5 and Prx6 subfamilies, respectively. The other subfamilies are not expressed in mammalian cells.

1.2 Structural Aspects of Prxs

Comparison of vertebrate Prxs shows that human Prxs have a highly similar nucleotide and amino acid sequences as commonly used animal models such as mice and zebrafish (Table 1.1) [15]. Prx protein core comprises of seven β-strands and five α-helices [16]. Prxs also contain a Trx-like fold that is essential for peroxidatic function. Trx fold is composed of a central core of five β-sheets that are surrounded by four α-helices [17]. Multiple variations of Trx fold are observed in proteins such as Arsenate reductase, Protein disulfide isomerase and Prxs. Prxs contain an N-terminal extension and an insertion between the α2 and β2 of the Trx fold [18]. C_P is found on the N-terminus, surrounded by three highly conserved residues, Proline, Threonine and Arginine, leading to stabilization of this Cysteine and pKa of 5-6 [19]. A conformational change occurs when C_P is oxidized so it can form disulfide bond with C_R of another subunit, or in case of Prx6, with another

thiol protein. In Prx1- Prx4, C_R is located 121 amino acid residues away from C_P on a conserved region of Trx-like fold. In Prx5, C_R is found 104 residues away from C_P on a less conserved region of the Trx-like fold [20].

Table 1.1 Summary of human Prx4 homologues and conservation relative to human Prx4 (generated using Homologene).

Species	**Gene Symbol**	**% Sequence Similarity**	
		Protein	DNA
H. Sapiens	PRDX4		
M. mulatta (Rhesus macaque)	PRDX4	98.5	98.4
C. lupus (Wolf)	PRDX4	93	89.2
B. taurus (Cattle)	PRDX4	93.8	90.8
M. musculus (House mouse)	Prdx4	95	89.1
R. norvegicus (Brown rat)	Prdx4	94.5	90.3
G. gallus (Red junglefowl)	PRDX4	91.9	81.6
X. tropicalis (Western clawed frog)	prdx4	93.6	81.1
D. rerio (Zebrafish)	prdx4	88.7	74.8
D. melanogaster (Common fruit fly)	Jafrac2	71	64.4

Human Prx1 is located in chromosome 1 (1p34.1), and it is transcribed from seven exons Prx1 is distributed mainly in the cytosol, but it has also been detected in nucleus, plasma membrane and centrosome (Figure 1.1) [21]. In addition to overoxidation, Prx1 activity is also inhibited by phosphorylation. Prx1 at the plasma membrane was phosphorylated at Tyr194 by a Src kinase resulting in decreased peroxidase activity [22]. Prx1 in centrosome can also be inactivated by phosphorylation by at Thr90 Cyclin dependent kinases [23]. Human Prx2 is located on chromosome 19 (19p13.13) and consists of six exons. Prx2 is distributed mainly in the cytosol and it has also been detected in nucleus and plasma membrane [21, 24]. Prx2 is reported to be more sensitive to hyperoxidation than Prx1 and Prx3 [25, 26]. Human Prx3 is located in chromosome 10 (10q26.11) and consists of seven exons. Prx3 is found in the mitochondria where it is

estimated to neutralize of 90% of mitochondrial hydrogen peroxide [27]. Human Prx4 is found on chromosome X (Xp22.11). Two variants of Prx4 are expressed: somatic Prx4 which contains conventional exon 1 and exons 2–7, and testis-specific Prx4 which contains alternative exon 1 along with exons 2–7. Prx4 is distributed mainly in the endoplasmic reticulum, but it has also been detected in extracellular matrix, cytosol and lysosome [28, 29]. We have recently summarized the roles of Prx4 in inflammation and cancer [30]. Human Prx5 is found on chromosome 11 (11q13.1) and consists of six exons. In the cells, it is distributed widely in cytosol, mitochondria, peroxisome and nucleus [20, 31]. Unlike other Prxs which form antiparallel homodimers, Prx5 forms nonantiparallel homodimers [32]. Human Prx6 is located on chromosome 1 (1q25.1), and it is transcribed from five exons. Prx6 is distributed in cytosol, lysosome and extracellular matrix [33, 34]. Prx6 has PLA_2 activity in addition to peroxidase activity. PLA2 function is active at acidic conditions, and it is shown to be increased by phosphorylation at Thr177 [35]. Thr 177 phosphorylation does not affect the peroxidase activity of Prx6.

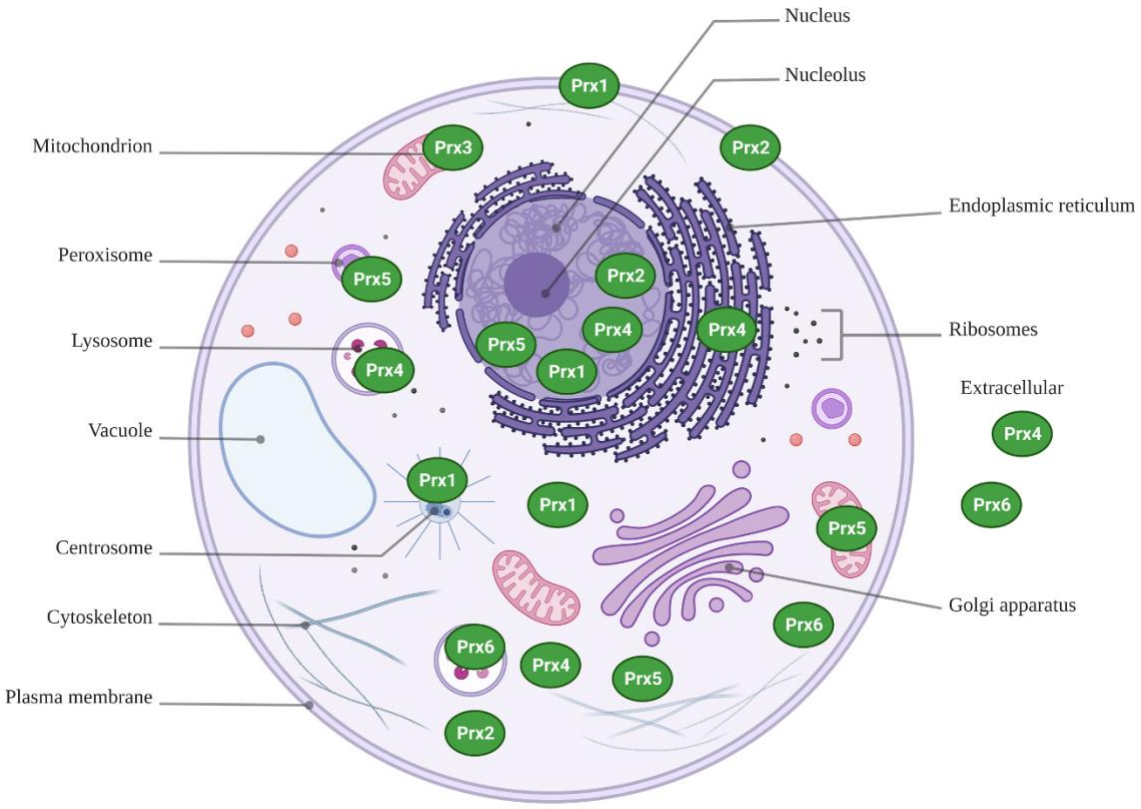

Figure 1.1. Subcellular localization of Prxs.
Single subunits are shown for simplicity.

1.3 Peroxidase Mechanism

In all six isoforms of Prxs, the C_PSH is oxidized to sulfenic acid (C_P-SOH) by peroxides and peroxynitrite (substrate shown as H_2O_2 in reactions below for simplicity). In 2-Cys Prxs, the resulting sulfenic acid forms disulfide bond with C_R-SH of another subunit which is then reduced preferably by Trx.

1) $\mathrm{Prx(CP-SH) + H2O2 \longrightarrow Prx(CP-SOH) + H2O}$

2) $\mathrm{Prx(CP-SOH) + Prx(CR-SH) \longrightarrow Prx(CP-S-S-CR)Prx + H2O}$

3) $\mathrm{Prx(CP-S-S-CR)Prx + (SH-)Trx(-SH)}$

$\mathrm{\longrightarrow Prx(CP-SH) + Prx(CR-SH) + Trx(S-S)}$

In Prx5, the C_P–SOH of Prx5 forms an intrasubunit disulfide with C_R–SH before reduction by Trx.

4) $\mathrm{Prx(CP-SOH) \longrightarrow Prx(CP-S-S-CR) + H2O}$

5) $\mathrm{Prx(CP-S-S-CR) + (SH-)Trx(-SH) \longrightarrow Prx(CP-SH) + Trx(S-S)}$

In Prx6, the C_P–SOH of Prx6 forms a heterodimeric disulfide with SH of π Glutathione-S-Transferase (πGST) before reduction by GSH.

6) $\mathrm{Prx(CP-SOH) + \pi GST(C-SH) \longrightarrow Prx(CP-S-S-C)\pi GST + H2O}$

7) $\mathrm{Prx(CP-S-S-C)\pi GST + GSH \longrightarrow Prx(CP-S-S)G + \pi GST(C-SH)}$

8) $\mathrm{Prx(CP-S-S)G + GSH \longrightarrow Prx(CP-SH) + GSSG}$

In the presence of high concentrations of peroxides, typical 2-Cys Prxs can become hyperoxidized and overoxidized instead of disulfide formation. Hyperoxidized 2-Cys Prxs can be reduced by the enzyme Sulfiredoxin in an ATP dependent manner. Mammalian Prx5 and Prx6 have been found to be more resistant to hyperoxidation, and they cannot be reduced by Srx [36].

9) $\mathrm{Prx(CP-SOH) + H2O2 \longrightarrow Prx(CP-SOOH) + H2O}$

10) $\mathrm{Prx(CP-SOOH) + ATP \xrightarrow{Srx} Prx(CP-SOH) + ADP}$

11) $\mathrm{Prx(CP-SOOH) + H2O2 \longrightarrow Prx(CP-SOOOH) + H2O}$

1.4 Prx4 Structure

Prx4 has approximately 68% homology with human Prx1 and Prx2, and 52% homology with Prx3 (Figure 1.2) [37-39]. As mentioned above, Prx4 is found on the X chromosome and the longest transcript contains 7 exons. Somatic Prx4 contains conventional exon 1 and exons 2-7 [40]. However, alternative splicing of Prx4 can occur

in testes (Figure 1.3). Prx4t in sexually mature testes contains alternative exon 1 along with exons 2-7 [41].

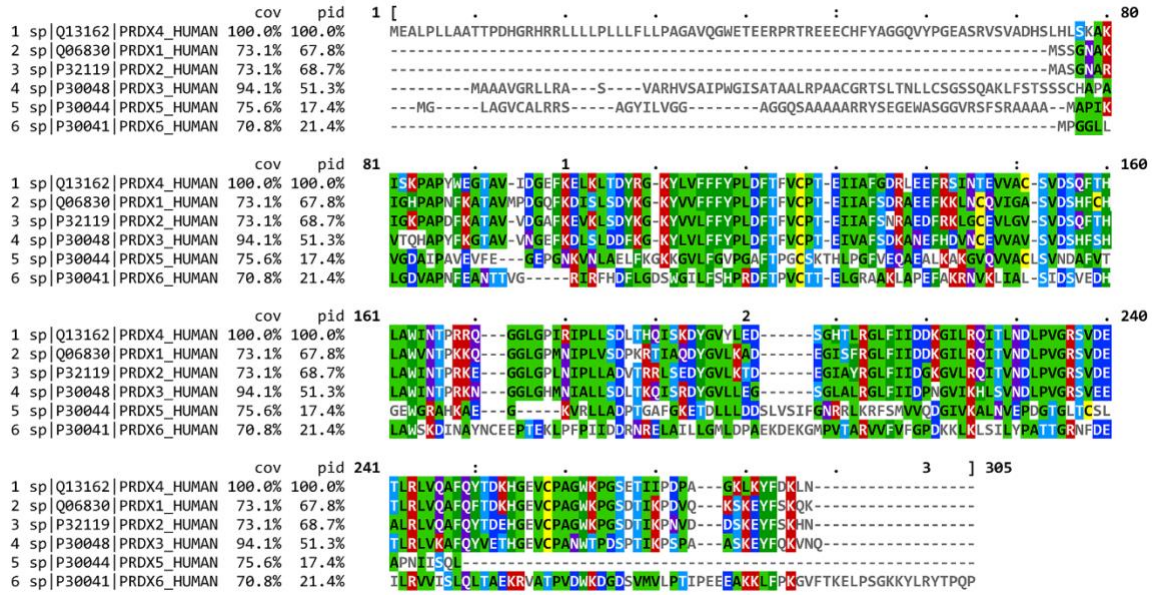

Figure 1.2. Multiple sequence alignment of human Prxs colored by consensus generated using MView.
Coverage and percentage identity values are indicated by cov and pid, respectively. Cysteines are highlighted with yellow color. For other residues, Red = positive.

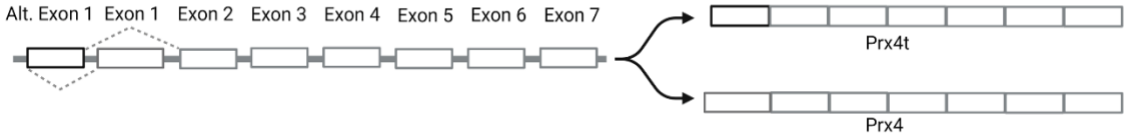

Figure 1.3. Schematic representation of alternative splicing of Prx4.
Systemic Prx4 contains exon 1, whereas Prx4t expressed in mature testes contains alternative exon 1.

Prx4 is localized mainly in the Endoplasmic Reticulum [28, 42]. It is also secreted into the extracellular matrix [28, 29, 43]. The unique extended N-terminal region in Prx4 allows for translocation of Prx4 across the ER membrane into the luminal space [42]. Since it lacks the N-terminal signal peptide, Prx4t is found in the cytosol. ER localization of Prx4

despite lacking the canonical ER retention 'KDEL' signal is due its interaction with PDI and ERp44. In HeLa cells, secretion due to overexpression of Prx4 could be suppressed by overexpression of ER proteins ERp44 and PDI [44]. Knockdown of ERGIC-53 in HeLa cells or treatment with 4-phenylbutyrate induces secretion of Prx4, further confirming the importance of ERp44 in its ER localization [45].

Human Prx4 has been crystallized in both oxidized and reduced states [46, 47]. In both states, Prx4 was crystallized as a decamer, composed of 5 dimers. Like other Prxs, each subunit contains the thioredoxin fold (ββαβαβαβαββαα). A dimer acts as a catalytic subunit. In the dimer, β1- and β8- strands of partner subunits interact with each other while a central twisted β-sheet is surrounded by α-helices. Cp is located in a2 helix in a pocket surrounded by β4- and β5- strands and α3- and α5- helices. Cr is located in a flexible loop between α5- and α6- helices. In the reduced state, there is a distance of 13 Å between the Cp of one subunit and Cr of another. Upon oxidation, there is local unfolding in α2- helix, facilitating repositioning of Cp for the formation of disulfide bond with Cr of partner subunit. Cao et al. suggest that the higher stability of Prx4 decamer compared to other Prxs could be attributed to Phe-122 displacing Pro-260 to maintain the hydrophobic interaction between subunits [47]. In addition, compared to other 2-Cys Prxs, Prx4 has a unique N-terminal sequence that is approximately 40 aa long. Wang et al. found that deletion of these N-terminal residues resulted in decreased stability of Prx4 decamers upon oxidation by H_2O_2 [46].

1.5 Prx4 Function

As mentioned above, Prxs are thiol-based peroxidases. Cysteine residues are utilized for redox purposes. Prx1-4 have two Cysteine residues that participate in catalysis:

reducing Cys (Cp) and resolving Cys (Cr). The N-terminal peroxidatic cysteine has pKa of 5-6, much lower than the normal Cys pKa of 8-9, because it is stabilized by neighboring arginine and threonine residues [19]. The low pKa makes it highly sensitive to the presence of ROS like H_2O_2. As shown in Figure 1.4, upon contact with peroxide, the thiol group of Cp in Prx4 is oxidized to sulfenic acid (Cys-SOH). The oxidized Prx4 forms a disulfide bond with Cr of another polypeptide resulting in a stable homodimer while H_2O_2 is reduced to water. This can be reduced by Thioredoxin (Trx), Glutathione (GSH), PDI or other ER oxidoreductases [29, 43, 48]. However, at higher concentrations of ROS, Prx4 gets further oxidized into sulfinic acid (Cys-SOOH) and sulfonic acid (Cys-SOOOH) leading to loss of enzyme activity [49]. Sulfinic acids can be reduced by Sulfiredoxin (Srx) in an ATP-dependent manner [50, 51]. Unlike other 2-cys Prxs, over-oxidized Prx4 can maintain stable decamers through hydrophobic interactions between subunits and disulfide bond between non-catalytic N-terminal cysteine residue [46, 47]. Later studies revealed that mutation of Cp and Cr alone or in combination prevents the formation of decamers [52]. The rate constant for H_2O_2 reduction of Prx4 is 2.2×10^7 $M^{-1}S^{-1}$ [46] which is comparable to that of Catalase and more than 5 orders of magnitude higher than that for reduction by GSH or Trx [53, 54]. This rate is also significantly higher than that of another ER antioxidant, GPx8 - 95 $M^{-1}S^{-1}$ [55].

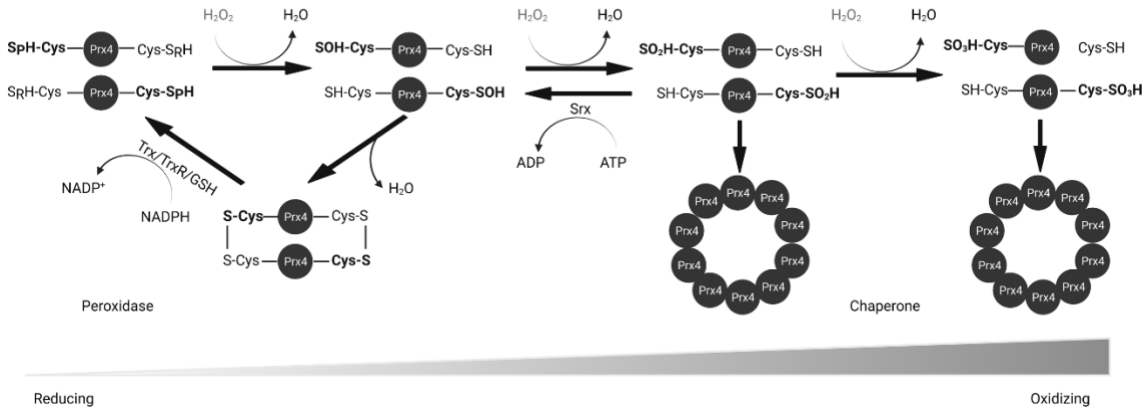

Figure 1.4. Reduction of H_2O_2 by Prx4.
Peroxidatic cysteine (Cys-SpH) is oxidized to sulfenic acid and either resolved and recycled with the help of Trx or GSH, or further oxidized into sulfinic and sulfonic acid forms. Srx reduces sulfinic acid. Prx4 loses peroxidase activity and gains chaperone activity with increasing oxidizing environment. Trx, thioredoxin; TrxR, thioredoxin reductase; GSH, glutathione; Srx, sulfiredoxin.

Oxidized Protein Disulfide Isomerase (PDI) family proteins introduce disulfide bond in nascent proteins in the ER [56]. ER oxidoreductin 1 (Ero1) re-oxidizes PDI using its cofactor Flavin Adenine Dinucleotide (FAD) and releases H_2O_2 as a byproduct [57]. For every disulfide bond introduced into nascent proteins, one molecule of H_2O_2 is produced [58]. Prx4 scavenges these H_2O_2 molecules and protects cells from oxidative stress. Prx4 also contributes to protein folding of plasma membrane proteins and secreted proteins, acting upstream of PDIs. The interaction of Prx4 with PDIs and other ER-associated proteins increases with its oxidation, likely through its recognition of Trx-domain within PDIs [52, 59]. Oxidized Prx4 engages in thiol-disulfide exchange with reduced PDIs, which results in restoration of activity for both (Figure 1.5) [48]. Loss of an Ero1 gene or Prx4 alone has no apparent phenotype in mice, but loss of both interferes with collagen synthesis and compromises the extracellular matrix [60]. Thus, Prx4 neutralizes

reactive oxygen species in its reduced state and promotes protein folding in its oxidized state. H_2O_2 and Srx act as an On-Off switch in regulating these activities [61].

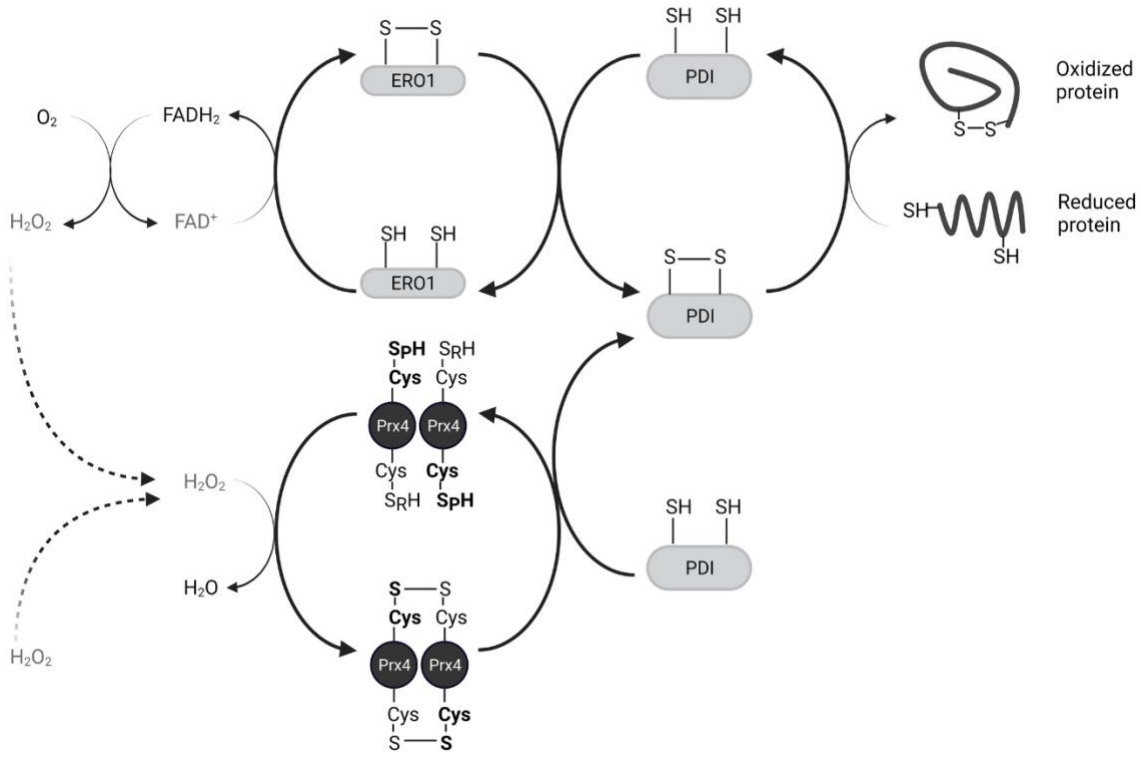

Figure 1.5. Prx4 mediates nascent peptide folding in the endoplasmic reticulum. Prx4 neutralizes H2O2 including those produced by Ero1. Oxidized Prx4 transfers disulfides to protein disulfide isomerases which catalyze the formation of disulfide bonds in nascent proteins. Only the catalytic dimer of Prx4 is shown for simplicity. Ero1, ER oxidoreductin 1; PDI, protein disulfide isomerase.

The mechanism of Prx4 secretion or the function of secreted Prx4 are not well understood. Okado-Matsumoto et al. have previously shown that Prx4 can be secreted in both reduced and oxidized forms [29]. Since the reduced form of extracellular Prx4 binds to heparin and human umbilical vein endothelial cells in a manner similar to another extracellular antioxidant SOD3, the authors suggest extracellular Prx4 also protects tissues against antioxidant injury. Additionally, acute exercise is known to affect redox balance in skeletal muscle [62, 63] while muscle cells and immune cells have been shown to secrete redox proteins in response to increase in H_2O_2 [64, 65]. Wadley et al. reported a significant

increase in plasma Prx4 levels after high intensity exercise [66]. These studies suggest a role for Prx4 in scavenging ROS in the extracellular space. Furthermore, as described in more detail below, secreted Prx4 also likely plays a role in regulating inflammation via NF-κB signaling.

1.6 Prx4 in Reproductive System

As shown in Figure 1.3, Prx4 mouse gene can be alternatively spliced. This alternatively spliced Prx4 (Prx4t) expression has been detected in human testis, epididymis and spermatozoa [67]. Since it lacks the signal peptide, it cannot enter the ER lumen but is found in the cytosol [41].

Prx4 also has protective role against oxidative stress in testis [68-70]. Sasagawa et al. and Matsuki et al. first suggested the involvement of Prx4 in maturation of spermatids in rats [71, 72]. Iuchi et al. generated Prx4 knockout mice and found that the male knockout mice had decreased testicular size at ages 6 weeks, 8 weeks and 15 weeks compared to the wild type. The testicular sections of Prx4 knockout mice also showed stronger staining for DNA fragmentation, and for the common markers of oxidative stress HNE, 8-OHdG, and TBARS. However, the normal fertility appeared unharmed: Litter sizes produced by pairing male Prx4 knockout mice and female WT mice did not differ significantly compared to those produced by male Prx4 WT and female WT mice. In addition, by in vitro fertilization test, the authors found that there was no significant difference in the number of embryos formed by sperm from Prx4 WT or Prx4 knockout mice with oocytes from female WT mice [68]. Tasaki et al. later confirmed the protective role of testicular Prx4 against oxidative stress. HEK293T cells transfected with testis specific Prx4 had

lower ROS levels compared to empty vector control cells, both with and without treatment with H_2O_2 and UV irradiation [69].

However, a study by Homma and colleagues has indicated that Prx4 and Prx4t are not important for fertility in male mice [73]. Mice lacking Prx4t alone and those lacking both Prx4 and Prx4t (DKO) had similar sperm count, testis to body weight ratios and normal sized litters when paired with WT female mice as WT pairs. Similarly, there was no difference in heat induced ER stress between WT and DKO mice testis. However, a different study reported that there was higher levels of 8-OHdG and higher rate of apoptosis of spermatogenic cells in Prx4KO mice than WT mice after heat treatment [74].

There have been other studies that suggest Prx4 promotes fertility. Prx4 protein expression is higher in the first-trimester placenta and lower in full term placenta [75]. Prx4 has been suggested to be a predictive marker for in vitro fertilization and embryo transfer outcomes [76]. The study found that Prx4 expression levels was significantly higher in the follicular fluid of pregnant women group than non-pregnant group on the day of oocyte retrieval. There was a positive correlation between Prx4 levels and fertilization rate and good quality embryo rate. The authors found that high Prx4 expression corresponds to a higher chance of clinical pregnancy. However, no significant difference was reported in the Prx4 levels in the follicular fluid of women with endometriosis vs those without endometriosis [77]. Lower level of serum Prx4 was detected in pregnant women with preeclampsia than in those without this disease, suggesting a protective role of Prx4 against high blood pressure [78].

Analysis of ovaries from young (4-5 years old) and old (18-20 years old) cynomolgus monkeys revealed a differential expression of Prx4 [79]. There was decreased

expression of Prx4 transcripts in older group's granulosa cells compared to the younger group. Higher expression of Prx4 has also been reported in middle aged mice than in pubescent or aged groups [80]. The authors found that this observation was also true for humans as young women had higher expression of Prx4 in the ovaries than premenopausal women. The group also discovered that Prx4 protects against ovarian ageing in mice [81]. In D-galactose induced model, where intraperitoneal injection of D-gal is performed at 150 mg/kg/day for 6 weeks, they found that compared to WT, Prx4KO mice had lower ovarian weight, more strongly disrupted estrous cycle (hypothalamic-pituitary-ovary axis), higher number of atretic follicles, higher number of apoptotic granulosa cells, increased expression of 8-OHdG, NTY and 4-HNE in ovarian interstitial cells, increased expression of ovarian senescence related protein P16 in granulosa cells and oocytes, and elevated levels of SOD-2, ATF-4, CHOP, activated caspase-12 and BAX. Thus, these studies suggest that Prx4 plays a critical role in protecting male and female reproductive system, but further mechanistic studies are necessary to clarify the importance of Prx4 in aging and reproduction.

1.7 Prx4 in Inflammatory Diseases

1.7.1 Diabetes and Nonalcoholic Fatty Liver Disease (NAFLD)

Yamada et al. have generated human Prx4 transgenic mice and summarized the protective role of Prx4 in various chronic inflammatory diseases [82]. In brief, they found that overexpression of hPrx4 protected the mice against Streptozotocin-induced type 1 diabetes mellitus (DM), progression of hypercholesterolemia-induced atherosclerosis, high fructose diet and streptozotocin- induced Type 2 DM and NAFLD as well as methionine- and choline-deficient high-fat diet- induced NAFLD by suppressing oxidative damage,

inflammation and apoptosis. However, two independent studies have described higher levels of serum Prx4 in patients with prediabetes and type 2 DM than in healthy volunteers [83, 84]. It is not yet clear what the function of elevated serum Prx4 levels might be in relation to these diseases. In another study, stable knockdown of Prx4 in MIN6 β-cells increased the susceptibility of proinsulin misfolding, especially after oxidative stress [85]. Conversely, transfection of Prx4 plasmid promoted insulin folding. The authors also report that human islets from patients with Type 2 DM contain higher fraction of overoxidized Prx4 (Prx4-SO_3) than samples from normal individuals, suggesting a possible role for glucose in regulation of Prx4.

Knockout of Prx4 or SOD1 alone did not contribute significantly to the development of liver failure in mice [86]. However, the combined silencing of Prx4 and Superoxide Dismutase 1 (SOD1) significantly exacerbated the effects. There was an increase in hyperoxidation of Prx 1-3, and an upregulation of ER chaperone Grp78 and ER stress response protein CHOP in the whole liver lysates of double knockout mice, indicating the importance of Prx4 in protection against oxidative stress and ER stress.

1.7.2 Cardiovascular Diseases

Loss of Prx4 is associated with cardiac stress in the absence of QSOX1 [87]. The authors of this study found that QSOX1 participates in early protective response to acute cardiac stress. Under normal conditions, Prx4 and Ero-1α were found to be upregulated in the hearts of QSOX1 knock out mice. Induction of acute stress by intraperitoneal injections of isoproterenol resulted in decrease of Prx4 levels and increase in inflammation (increased galectin-3, CD68+ cells) and oxidative stress within 3 days of injection [87]. Prx4 also has a more direct relationship with galectin-3. Galectin-3 downregulates Prx4 in human cardiac

fibroblasts [88]. Galectin-3 is induced in tissue injury such as heart failure, and it is known to promote fibrosis and inflammation. Human cardiac fibroblasts stimulated with Galectin-3 had decreased Prx4 protein levels [88]. The study showed that knockdown of Galectin-3 *in vitro* with siRNA for 24h resulted in upregulation of Prx4 protein. Similarly, Prx4 was upregulated in hearts of Galectin-3 knockout mice compared to WT mice. In spontaneously hypertensive rats which present enhanced cardiac Galectin-3, its pharmacological inhibition increased cardiac Prx4 levels and decreased oxidative stress. No association was detected between serum Galectin-3 levels and serum Prx4 levels in samples from Aortic Stenosis (AS) patients. In immunohistochemical analysis of myocardial biopsies of AS patients, Prx4 expression was lower in AS patients compared to control. In addition, an inverse correlation was detected between Prx4 mRNA and Galectin-3 protein levels [88]. A later study found that cardiotoxicity caused by the chemotherapeutic drug Doxorubicin could be reduced by upregulating Prx4 through Galectin-3 inhibition [89]. Thus, Prx4 has a protective role in heart tissue.

1.7.3 Cerebral Ischemia and Alzheimer's Disease

Ischemic stroke is a common cause of death and disability. Rowe et al. discovered that human umbilical cord blood cell (HUCBC) treatment of oligodendrocytes in a non-contact co-culture model protected the cells from oxygen glucose deprivation (OGD) [90]. Subsequent microarray analysis revealed HUCBC treatment following OGD had induced Prx4 and another antioxidant, Metallothionein 3, in the oligodendrocytes. The group also found that co-treatment of oligodendrocytes with inhibitor of Akt during OGD suppressed the increase in Prx4. The protective effect of HUCBC following OGD could be reversed by Akt inhibitor or Prx4- neutralizing antibody. Similarly, another study found that Prxs

are highly expressed in mesenchymal stromal cells (MSCs) [91]. The authors of this study reported MSC cells with stable expression of CCR2 to be promising for promoting neurological recovery after acute ischemic stroke. They propose that Prx4 secreted by MSCs had an important role in preserving the blood brain barrier in this process. Silencing Prx4 in MSC-CCR2 cells increased their ROS levels, disrupted tight junction, and decreased the length of blood brain barrier marker Glut1 in brain slices, effectively reversing the effect of CCR2 expression. Thus, extracellular Prx4 has a protective role in ischemia, and it should provide an additional strategy for improving cell therapy.

Prx4 expression was detected in ependymal layer, choroid plexus, astrocytes and neurons, but it was not detected in microglia and oligodendrocytes in normal adult mouse brain [24]. In analysis of postmortem brains of Alzheimer's disease (AD) patients, Prx4 protein levels were found to be decreased [92]. The authors suggest the high oxidative stress as a result of this downregulation could potentially lead to concurrent phosphorylation of AMPK and mTOR in AD [92]. Prx4 was found to have protective effect against amyloid beta oligomer (AβO)- and glutamate- mediated stress *in vitro* [93]. Treatment of mouse hippocampal neuronal HT-22 cells with 5μM of AβO upregulated Prx4 expression in a time dependent manner [93]. Pretreatment of cells with tauroursodeoxycholic acid (TUDCA) or N-acetyl cysteine (NAC) disrupted this increase. The study also noted that HT-22 cells stably overexpressing Prx4 had lower ROS levels and lower ER stress compared to cells targeted with siRNAs against Prx4. Prx4 overexpression also decreased AβO-induced intracellular Ca^{2+} uptake and protected against apoptotic cell death. In a different study, overexpression of Prx4 in HT-22 cells reduced glutamate-induced apoptosis by inhibiting ROS formation, Ca^{2+} influx and ER

stress [94]. β-amyloid, known to contribute to neuron degeneration, is derived from the amyloid precursor protein (APP). Triple knockdown of APP family genes APP, APLP1 and APLP2 in HEK293T cells resulted in a significant downregulation of Prx4 protein (but not mRNA) levels [95]. Together these studies suggest Prx4 plays a beneficial role against AD.

1.7.4 Colitis

Two-dimensional gel electrophoresis and mass spectrometric analyses of colon tissue samples showed that Prx4 was upregulated (while Prx3 and Prx6 were downregulated) in ulcerative colitis patients compared to healthy controls [96]. This suggests Prx4 could be utilized as a potential diagnostic marker for inflammatory bowel disease. However, this pro-inflammatory association of Prx4 contrasts with other data reporting anti-inflammatory role. Takagi et al. report high expression of Prx4 in the epithelial cells of the colon [97]. Treatment of mice with 2.5% Dextran sulfate sodium (DSS) in drinking water for 7 days resulted in significantly shorter colon length in Prx4 knockout mice than WT mice. Prx4 KO mice had greater epithelial damage and higher infiltration of neutrophils as well as elevated expression of inflammatory cytokines including TNF-α and IFN-γ. After DSS treatment, the Prx4 KO mice had increased epithelial permeability than WT mice, expanded ER, increase expression of CHOP and elevated cleaved caspase 3. Without DSS treatment, there was no significant difference in collagen IV between WT and KO mice. After treatment, it increased in both groups, but compared to WT, increased less in KO. These KO mice had less collagen fibers in the intercellular space than WT. Finally, Prx4 KO mice had greater induction of fibrosis related

proteins α-SMA and TGF-β than WT mice after DSS treatment. Thus, Prx4 protected mice against DSS-induced inflammation in this study [97].

1.7.5 Rheumatism and Other Inflammatory Conditions

A protective role for Prx4 has been suggested in osteoarthritis (OA). Overexpression of Prx4 in rat primary chondrocytes in an OA model decreased IL-1β induced ROS production and apoptosis- factors which are known to contribute to cartilage degeneration [98]. This could also be partially reversed by treatment with Akt inhibitor AZD5363, suggesting Prx4 utilizes PI3K/Akt pathway. Interestingly, two-dimensional gel electrophoresis and mass spectrometric analyses of synovial tissue samples showed that Prx4 was upregulated in rheumatoid arthritis (RA) patients compared to osteoarthritis (OA) and ankylosing spondylitis (AS) [99]. Using enzyme-linked immunosorbent assay (ELISA), the authors also detected higher Prx4 in plasma from early stage RA patients compared to healthy control, suggesting Prx4 could be used as a diagnostic marker. The function of Prx4 in the initiation of RA is not understood. The upregulation of Prx4 in RA synovial tissue was confirmed by a later study [100]. The authors also found that knockdown of Prx4 in primary fibroblast-like synoviocytes, an important cell type in synovial tissue, decreased phosphorylated PI3K and Akt and suppressed cell proliferation, migration and invasion *in vitro*. These effects could be reverted by Akt inhibitor MK-2206. Thus, Prx4 is a potential therapeutic target in arthritis.

It has been reported that expression of Prx4 protein is lower in alveolar macrophages of patients with the development of silicosis [101]. This suggests a role for Prx4 in suppression of inflammation in the lungs. The authors also suggest monitoring the markers of oxidative stress as prognostic and predictive factors for silicosis.

Prx4 expression is increased at mRNA and protein levels during LPS-induced differentiation of B cells into plasma cells [102]. However, Prx4 is not essential for this differentiation, as Prx4 knockout cells also differentiated normally.

In a wound healing model, overexpression of Prx4 promoted skin wound healing in adult and aged mice by reducing oxidative stress and neutrophils and by increasing macrophage infiltration and growth factor levels [103].

1.8 Signaling Pathways Regulated by Prx4 in Inflammation

1.8.1 NF-κB

Transcription factor NF-κB is a key regulator of inflammation that has been implicated in the initiation of various cancers [104-106]. In general, intracellular Prx4 appears to suppress NF-κB while extracellular Prx4 activates NF-κB.

Jin et al. discovered that cytosolic Prx4, which they called AOE372, negatively regulated NF-κB activation [107]. Overexpression of Prx4 in HeLa cells significantly suppressed HIV-1 Tat-, Tumor necrosis factor (TNF)- and 12-*O*-tetradecanoylphorbol-13-acetate (TPA)- dependent activation of NF-κB. NF-κB dependent reporter assays showed that Prx1 and Prx4 inhibited NF-κB synergistically. The authors suggested that Prx4 could affect phosphorylation of IκB-α as a potential mechanism.

In HEK293 cells with stable expression of immune receptor NOD2, treatment with microbial product muramyl dipeptide (MDP) upregulated Prx4 expression [108]. Interestingly, the authors also found that loss of Prx4 in HEK293 cells enhanced NF-κB activation upon treatment with MDP, suggesting Prx4 negatively regulates NF-κB signaling.

In large yellow croaker *Pseudosciaena crocea*, bacterial infection upregulated Prx4 in the spleen [109]. When the fish were injected with Prx4-siRNA before bacterial challenge, NF-κB binding activity in the spleen increased, mRNA levels of TNF-α and CC chemokine increased, while IL-10 decreased. Opposite results were seen were fish with injected with recombinant Prx4. Thus, the result indicates that in P. crocea, Prx4 negatively regulates the activity of NF-κB, downregulates pro-inflammatory cytokines and upregulates anti-inflammatory cytokines in response to bacterial infection. The negative regulation of NF-κB by Prx4 in P. Crocea was later confirmed in another study [110].

In *Drosophila* model, flies overexpressing Prx4 at high levels (over 5-fold) exhibited upregulation in the mRNA expression of AttD, Dipt and Mtk (some of the targets of *Drosophila* NF-κB), as well as upregulation of TotA which is a downstream target of the JAK/STAT pathway [111]. However, injection of Prx4 into the body cavity of Drosophila did not yield significant changes in mRNA levels of AttD, Dipt and Mtk (it did upregulate TotA). Hence, the authors suggest that only intracellular Prx4 is involved in the activation of immune response.

In contrast, Haridas and colleagues reported that secreted Prx4 activated NF-κB in human cell lines [43]. They confirmed the secretion of Prx4 from Jurkat and HL-60 cells into conditioned medium. Treatment of human myeloid cells U-937 with Prx4 for 30 minutes showed Prx4 activated NF-κB in a dose-dependent and time-dependent manner. NF-κB activation peaked at 4 hours post-treatment which coincided with the complete degradation of IκB-α. Prx4 treatment also increased NF-κB dependent luciferase activity by seven-fold. Zhao et al. studied the pro-inflammatory properties of Peroxiredoxins in mouse macrophages *in vitro* [112]. 24-hour treatment of RAW264.7 cells with different

concentrations of recombinant mouse Prx4 ranging from 1nM to 50nM had no effect on cell viability. However, at the higher concentrations of 20nM and 50nM, Prx4 induced a significant increase in NO levels in the conditioned medium in a dose dependent manner. Finally, a 24-hour treatment with 20nM Prx4 significantly increased TLR4 expression and the nuclear translocation of NF-κB p65 subunit. These data suggest that extracellular Prx4 could have pro-inflammatory effect through TLR4/ NF-κB signaling activation.

1.8.2 Inflammasome

Inflammasomes are protein complexes assembled by the innate immune system to regulate inflammatory response. Inflammasomes trigger maturation of proinflammatory cytokines IL-1β and IL-18 through activation of caspase-1 [113]. Prxs have been increasingly associated with regulation of inflammasomes. Activation of inflammasomes NLRP3, NLRC4 or AIM2 in murine macrophages *in vitro* caused secretion of Prx1, Prx2, Prx5 and Prx6 [114]. Downregulation of Prx1 was suggested to transcriptionally inhibit NLRP3 inflammasome expression in intestinal inflammation [115]. Serum Prx1 was found to promote inflammation in acute liver injury through NLRP3 inflammasome signaling [116]. Knockdown of Prx3 in liver aggravated acetaminophen-induced liver injury and this was associated with increased markers of NLRP3 inflammasome activation [117]. Curcumin analogue, AI-44, prevented activation of procaspase 1 by promoting its interaction with Prx1 [118]. Similarly, loss of phospholipase A2 activity in Prx6 in primary endothelial cells protected against LPS-induced upregulation of NLRP3 [119].

Lipinski et al. report that Prx4 limits caspase-1 activation and restricts inflammasome-mediated signaling by extracellular vesicles [120]. The authors found that when challenged with sub-lethal dose of LPS intraperitoneally, Prx4-null mice had

increased weight loss, increased serum TNF-α, IL-1β, CXCL1 and delayed restoration of weight than WT mice. This could be prevented by treatment with an interlukin-1-receptor antagonist. In mice lacking Prx4 in myeloid cells, the results found in whole body knockout was replicated suggesting a crucial role of myeloid cells in Prx4-mediated protection. *In vitro*, oxidized Prx4 decamer complex directly inhibited caspase-1 activity through interacting with redox sensitive C397 of caspase-1. Their studies also show inflammasome-activated cells secreting Prx4 in extracellular vesicles along with components of inflammasome. Presence of Prx4 in extracellular vesicles caused lower pro-inflammatory response in recipient cells and mice. Thus, Prx4 negatively regulates caspase-1 and IL-1β activation to lower the inflammatory response.

1.8.3 Other inflammatory pathways

Cyclooxygenase-2 (COX-2) catalyzes a critical step in the synthesis of prostaglandins and other prostanoids, and it is a target of non-steroidal anti-inflammatory drugs (NSAIDs) [121]. In hyperosmotic medium, which was used as an *in vitro* model for studying dry eye disease, the expression of COX-2 was upregulated, while Prx4 and SOD1 were downregulated in human corneal epithelial cells [122, 123]. However, treatment with the small molecule L-carnitine, or with Pterostilbene, a natural component of blueberries, restored the expression of these enzymes back to the levels seen in isosmotic condition [122, 123]. Thus, suppression of inflammation combined with maintenance of Prx4 and other anti-oxidants seems vital to the treatment of dry-eye disease.

Although no causal relationship has been reported between Prx4 and Interleukin 6 (IL-6), there appears to be a negative correlation. TNF-α, IL-1β, IL-6 are all upregulated in human corneal epithelial cells under hyperosmotic conditions. Treatment with

Pterostilbene reduces their expression while Prx4 is upregulated [122]. Similarly, in the goldfish animal model, exposure of the fish to 10ng/L of the organotin Triphenyltin (TPT) significantly lowered the mRNA levels of antioxidants including Prx4 while increasing the secretion of TNF-α, IL-1β, IL-6 in the serum [124]. Finally, in both acute and chronic treatments with DSS, pro-inflammatory cytokines TNF-α, IFN-γ and IL-6 were downregulated at mRNA level while Prx4 mRNA and protein were significantly upregulated in colon of Prx6 knockout mice compared to Wild type mice [125]. Thus, intracellular Prx4 has a negative correlation with IL-6. However, extracellular Prx4 activates IL-6. Recombinant mouse Prx4 induced secretion of TNF-α and IL-6 upon addition to murine macrophages RAW264.7 [112].

In kuruma shrimp (*M. japonicus*), bacterial infection upregulated shrimp Prx4 at transcript and protein levels [126]. Knockdown of Prx4 with dsRNA injection increased bacterial number in shrimp and decreased overall survival. Mechanistic studies showed that nuclear translocation and phosphorylation of STAT increased upon infection in control group but was suppressed in Prx4-depleted group. STAT-activation could also be blocked by injection of Prx4 antibody prior to bacterial challenge, suggesting extracellular Prx4 was responsible for STAT activation. Similarly, treatment with purified shrimp Prx4 activated STAT whereas mutant Prx4 modified on both catalytic cysteines failed to do so. The authors also report that extracellular Prx4 acted through the receptor Domeless to activate JAK/STAT as knockdown of this receptor blocked nuclear translocation of STAT [126]. Thus, Prx4 contributes to antibacterial immunity of the shrimp through JAK/STAT pathway.

1.9 Prx4 in Cancer

Prx4 has been found to be upregulated in majority of cancers. Below, we briefly discuss roles of Prx4 in major cancer types and their tumor microenvironment (Figure 1.6).

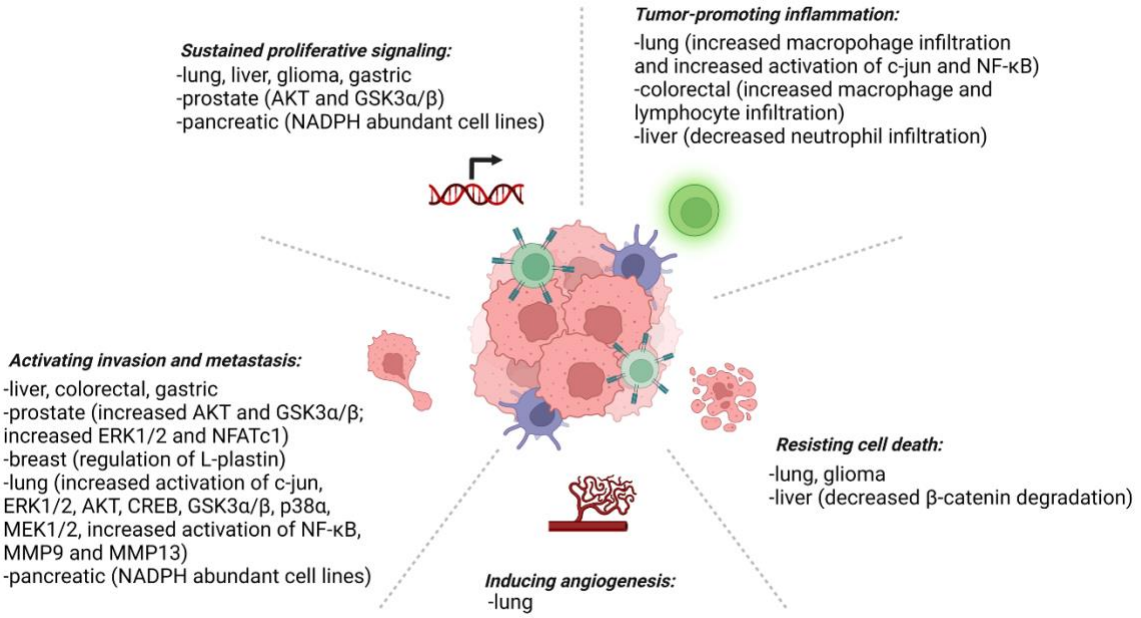

Figure 1.6. Prx4 promotes the hallmarks of cancer in different cancer types. Known aberrant signaling pathways and markers are shown in parentheses.

1.9.1 Prostate Cancer

Prx4 has been found to be pro-tumorigenic in prostate cancer. Studies have reported that there is an upregulation of Prx4 in human prostate cancers [127, 128]. Prx4 upregulation enhances proliferation of prostate cancer cell lines DU145 and LNCaP *in vitro* [127]. Incidentally, they also discovered Prx4 overexpression to correlate negatively with TMPRSS2-ERG gene fusion, a highly common genomic alteration present in prostate cancer patients. In a different study, Prx4 overexpression in prostate cancer was associated with increase in tumor stage, increase in Gleason sum score and increase in age at prostatectomy [128]. Knockdown of Prx4 in prostate cancer cell line PC3 to reduce Prx4 secretion repressed the ability of cancer cells to induce osteoclastogenesis *in vitro* and

osteolysis *in vivo* [129]. The authors have suggested that Prx4 deficiency might interfere with ERK1/2 signaling pathway and NFATc1 nuclear translocation. In addition, Prx4 has been found to be upregulated in prostate cancer and other cancers that commonly metastasize to bone [130]. One possible mechanism for Prx4 upregulation is through Androgen Receptor signaling. Treatment of LNCaP cell line with synthetic androgen R1881 led to dose-dependent increase in Prx4 expression [131]. Depletion of Prx4 in LNCaP and DU145 cell lines decreased cell proliferation, migration and invasion likely through decreased activation of AKT and GSK3 signaling pathways. Prx4 depletion also sensitized the cancer cells to radiation *in vitro* and in mouse xenograft model [131].

1.9.2 Breast Cancer

Prx4 is overexpressed in breast cancer samples compared to normal tissues [132, 133]. Immunohistochemical staining revealed that Prx4 is overexpressed in Triple negative breast cancer (TNBC) cases compared to the non-TNBC cases [134]. TNBC group had lower oxidative stress, as measured by 8-Hydroxydeoxyguanosine (8-OHdG) staining, and poor breast-cancer specific survival. Another study confirmed using the UALCAN database that Prx4 expression at the transcript level was highest in Triple Negative breast cancer group, followed by Her-2 positive group [135]. This upregulation of Prx4 was positively correlated with shorter disease-free survival and poor overall survival. Similar to prostate cancer, breast cancer cells also utilize secreted Prx4 to mediate osteoclastogenesis. Knockdown of Prx4 in MDA-MB-231 cells significantly reduced osteoclast formation *in vitro* [129]. In addition, their bioinformatics analysis revealed that patients with lower Prx4 expression in primary tumor were less likely to develop metastasis at 5 years compared to those with higher Prx4 expression. Tiedemann et al. have suggested

that Prx4 influences L-plastin expression, with both proteins involved in mediating breast-cancer induced osteolysis *in vivo* [130]. When MDA-MB-231 cells lacking both L-plastin and Prx4 were injected into CD-1 immunodeficient mice, complete loss of osteolysis was observed. Prx4 also contains single-nucleotide polymorphisms (SNPs) associated with clearance of docetaxel [136]. Finally, exposure of cell line MDA-MB-231 to increasing concentrations of docetaxel followed by Whole exome sequencing at 5 different stages revealed that there was a copy number loss of a number of genes on X chromosome, including Prx4 at stage 2/3 [137]. Thus, Prx4 is a novel therapeutic target for the treatment of breast cancer.

1.9.3 Lung Cancer

In general, Prx4 has been found to be pro-tumorigenic in lung cancer. Prx4 is the primary substrate of Srx in lung cancer cells [138]. Knockdown of Srx or Prx4 represses anchorage independent colony formation and cell invasion of A549 and H226 cells [138, 139]. Accordingly, disruption of Srx-Prx4 axis reduces tumor growth and metastasis *in vivo* in mouse models. Furthermore, knockdown of Prx4 affects a large number of kinase signaling pathways including c-Jun, ERK1/2, AKT, CREB, GSK3α/ß, p38α, and MEK1/2 among others.

Hwang et al. reported that strong Prx4 expression in stage II non-small cell lung cancer (NSCLC) patients correlated with short disease-free survival in squamous cell carcinoma (SCC) subgroup but not in adenocarcinoma (LUAD) subgroup [140]. 1g/kg urethane i.p. injection of non-transgenic control and human Prx4 expressing transgenic mice for 16 weeks resulted in significantly more and bigger tumors in the transgenic group [141]. This was attributed to the suppressed apoptosis and enhanced proliferation in the

tumors in transgenic group. The authors also found that the hPrx4 expressing group had higher microvascular permeability, macrophage infiltration, MMP9, MMP13 and IL-1β production, and significantly lower oxidative stress. In NSCLC cell lines A549 and H460, irradiation upregulated TRIAP1 and several antioxidants including Prx4 [142]. Knockdown of TRIAP1 sensitized these cells to radiation as the induction of Prx4 and other antioxidants was disrupted. Thus, Prx4 promotes chemically-induced tumorigenesis and radioresistance in NSCLC.

However, anti-tumorigenic role of Prx4 in lung cancer has been found in LUAD. Shioya et al. reported that weak Prx4 expression correlated positively with poor differentiation and high invasiveness of tumors in stage I LUAD [143]. A later study of stage I LUAD found that weak Prx4 expression correlated positively with Wild Type (WT) status of EGFR [144]. The authors have suggested that the combination of weak expression of Prx4 with high MIB-1 labelling index and/or WT status of EGFR may be a useful tool to predict poor disease-free survival in early-stage LUAD [143, 144].

1.9.4 Colorectal Cancer

Prx4 has an oncogenic role in colorectal cancer (CRC). The analysis of CRC patient specimens showed that Prx4 mRNA and protein expression were significantly higher in CRC samples compared to adjacent normal tissue [145]. The study also found a significant positive correlation between Prx4 protein expression in CRC tissues and the depth of invasion, Lymph node metastasis, tumor stage and shorter survival; however, univariate and multivariate analyses revealed that Prx4 was not an independent unfavorable prognostic factor for the survival of CRC patients. Li et al. found through hierarchical cluster analysis using data from cDNA microarray and subsequent quantitative PCR that

Prx4 was expressed at a significantly higher levels in primary CRC tumors with liver metastasis than in tumors without metastasis [146]. Prx4 was one of 18 proteins differentially expressed between tissue samples of stage I and stage IV colorectal cancer [147]. Prx4 upregulation in advanced stages of CRC was identified using two-dimensional gel electrophoresis and mass spectrometry and validated in tissue microarray. Knockdown of Prx4 in DLD-1 cells induced G1/S arrest and reduced migration and invasion *in vitro*. Western blot showed that Prx4 knockdown led to decreased expression of Twist1/2 and Cyclin D1. Subcutaneous injection of control and Prx4 knockdown DLD-1 cells resulted in smaller tumors in the knockdown group. Prx4 depleted tumors had reduced protein levels of PCNA, N-Cadherin, β-catenin and MMP-9. Finally, the authors found that treatment of DLD-1 with inhibitors of Protein Kinase Cα, RhoA GTPase, ERK1/2 or EGFR increased trimethylation of H3K4 of Prx4 promoter [147]. Thus, this study suggests EGFR induced Prx4 promotes metastasis of CRC.

Study by Ouyang et al. has suggested that Curcumin, a polyphenolic compound with anti-inflammatory properties, protects against late-onset diarrhea side-effect of the chemotherapeutic agent CPT-11 [148]. Curcumin treatment of mice *in vivo* and IEC-6 cells *in vitro* reversed the suppression of Prx4 by CPT-11 as detected by Western Blot analysis. Similarly, treatment of colorectal cancer cell line LOVO with curcumin alone or in combination with CPT-11 significantly enhanced Prx4 protein expression [149]. In addition, treatment of HT-29 cells with portoamides (which have anti-proliferative activity on certain cancer cell lines) also increased the expression of Prx4 protein [150]. Thus, Prx4 is a promising therapeutic target for CRC prevention or treatment.

1.9.5 Esophageal Carcinoma and Gastric Cancer

Kobayashi and colleagues have reported higher levels of auto-antibodies against Prx4 in serum of esophageal squamous cell carcinoma and gastric cancer patients compared to healthy donors [151]. Thus, Prx4 antibodies could serve as a potential marker for these cancers. In gastric cancer, it was shown that Prx4 is overexpressed in tissue specimens, and higher expression of Prx4 is associated with shorter survival [152]. Knockdown of Prx4 in AGS and MKN28 cell lines decreased cell proliferation, migration and invasion. The authors also found that Prx4 knockdown decreased the expression of EMT transcription factors Snail and Slug. In esophageal carcinoma, Prx4 has been identified to interact with one of the proteins highly upregulated in this cancer AGR2 [153]. AGR2 is an ER chaperone known to promote tumor growth and migration in esophageal carcinoma [154]. Identification of this interaction could provide a new strategy for the development of therapeutics.

1.9.6 Liver Cancer

Prx4 knockout mice had significantly higher incidence of Diethylnitrosamone (DEN)- induced hepatocellular carcinoma (HCC) than wild type or human Prx4 transgenic mice [155]. After DEN treatment, transgenic mice had lower infiltrated neutrophils, less 8-OHdG positive hepatocytes, lower thiobarbituric acid reactive substances (TBARS), and lower serum levels of aspartate aminotransferase and alanine aminotransferase than WT. IHC staining of human HCC tissues revealed that tumors with low Prx4 expression had more hepatic and portal vein invasion, higher 8-OHdG level, and were more aggressive [155]. Low Prx4 group also had a significantly reduced overall survival than high-Prx4 group. *In vitro*, knockdown of Prx4 in PLC/PRF/5 and HepG2 cell lines using siRNAs

enhanced ROS levels and decreased cell proliferation. The knockdown-cells also had higher rate of apoptosis and autophagy. Thus, the study indicates that Prx4 inhibits HCC initiation but may have dual role in the progression of HCC [155].

A later study reported that Prx4 is oncogenic in HCC. Knockdown of Prx4 significantly reduced both anchorage dependent and anchorage independent colony formation of HCC cells [156]. SMMC-7721 shPrx4 cells resulted in significantly smaller xenograft tumors than shNT cells while Prx4 overexpression cells resulted in significantly bigger tumors than vector control cells. Tail-vein injection in nude mice followed by bioluminescence measurement revealed that shPrx4 cells had significantly lower lung metastasis. HCC cells in suspension culture were found to have lower Prx4 expression than those in adherent condition [156]. They also had higher cleaved caspase 3 in suspension which is exacerbated by knockdown of Prx4. Conversely, overexpression of Prx4 promoted the survival of HCC cells in suspension. Prx4 overexpression in HCC cells increased expression of total β-catenin protein. Active β-catenin protein also increased though to a lower extent. However, no change was seen in β-catenin mRNA levels. Subsequent analysis revealed that Prx4 interacts directly with ubiquitin ligase β-TrCP thus inhibiting ubiquitination of β-catenin. In anchorage-independent condition, knockdown of β-catenin decreased the growth of Prx4 overexpression cells and increased their susceptibility to anoikis [156]. Similarly, overexpression of β-catenin increased the growth and survival of Prx4 knockdown cells. The authors suggest Prx4 upregulation increases the recruitment of β-catenin to ID2 promoter. ID2 acts downstream of Prx4 to mediate the oncogenic activity. Finally, the long non-coding RNA TP53TG1 which is known to suppress HCC promotes

the ubiquitination and degradation of Prx4 [157]. Thus, targeting Prx4 is a promising therapeutic option for treating HCC.

1.9.7 Glioma

Prx4 expression is upregulated in human and mouse Glioblastoma multiforme (GBM) [158]. Silencing Prx4 expression *in vitro* in GBM neurospheres reduced cell viability and increased ROS production, DNA damage, and apoptosis. Furthermore, Prx4 knockdown decreased radiation resistance *in vitro*. Combination of Prx4 silencing and irradiation was significantly more effective in killing GBM cells and suppressing colony formation than irradiation alone [158]. In an orthotopic transplantation model, it was found that knockdown of Prx4 increased survival of recipient mice by 35% [158]. The knockdown groups had significantly reduced cell proliferation in infiltrating cells as measured by Ki67 staining and significantly higher DNA damage and apoptosis in tumor sections as measured by P-H2AX and cleaved caspase 3 staining than control groups.

Kim et al. reported in 2014 that Prx4 mRNA is significantly upregulated in mouse high grade-glioma (HGG) cultures [159]. Piperlongumine treatment of HGG cells increased ROS levels and suppressed cell growth, mimicking the effects of Prx4 knockdown. The authors found that after piperlongumine treatment, there was an increase in hyperoxidized form of Prx4 and a corresponding decrease in H_2O_2 degradation activity. Furthermore, they also noticed higher levels of ER stress after treatment which could again be attributed to Prx4 inactivation. Knockdown of Prx4 *in vitro* increased mRNA expression of ER stress and UPR markers as well as ER stress response genes. Analysis of REMBRANDT database revealed that patients with intermediate levels of Prx4 in their

gliomas survive significantly longer than those with upregulation of Prx4 [159]. These studies suggest Prx4 is a promising target for treating astrocytoma and glioblastoma.

1.9.8 Melanoma of the Skin

Hintsala et al. report an inverse association between age and Prx4 expression in primary tumors [160]. Higher expression of Prx4 in sweat gland cells and cytoplasmic Prx4 expression in endothelial cells were associated with better survival. In Analysis of 111 melanoma patient samples, expression of nuclear Prx1 was found to decrease in different cell types including pigment cells, keratinocytes and endothelial cells compared to benign and dysplastic samples [160]. The same study found that fibroblasts in melanoma-patent derived tissues had lower expression of cytoplasmic Prx1 and nuclear Prx2. This study suggests Prxs could be used for prognosis and as therapeutic targets for treating melanoma.

1.9.9 Non-Hodgkin Lymphoma and Leukemia

Upregulation of Prx3 and Prx4 transcripts correlates with poor prognosis for Diffused large B-cell lymphoma patients [161]. The role of these proteins in initiation of progression of this cancer have not been studied.

Prx4 transcript and protein are downregulated in Acute Promyelocytic Leukemia (APL) relative to AML samples, presumably due to increased levels of H3K27me3 at the transcription start site of Prx4 as indicated by Chromatin immunoprecipitation [162]. The molecular mechanism of how the decrease in Prx4 expression might contribute to APL is not understood. In addition, Prx1 is found to be upregulated in activated natural killer cells *in vitro* [163]. Further studies are warranted to elucidate the function of Prxs in NK cell function.

1.9.10 Oral Squamous Cell Carcinoma (OSCC)

Prx4 was one of the four antioxidants found to be upregulated in tumor samples of OSCC patients compared to adjacent normal tissue [164]. The authors suggest these genes are potential candidates for biomarkers. In addition, Prx1 was also upregulated in mouse xenograft tumors of OSCC cell line SCC15 [165]. Additional studies are needed to understand the functions of Prx1 and Prx4 in OSCC.

1.9.11 Pancreatic Cancer

High expression of Prx4 is associated with liver metastases and lower survival of pancreatic cancer patients [166]. Orthotopic implantation of human cancer cell lines in mice pancreas confirmed that loss of Prx4 increased the disease-free survival. Treatment of pancreatic cancer cell lines with 6-aminonicotamide to reduce NADPH levels reversed the decrease in cell proliferation seen upon Prx4 depletion. Therefore, targeting Prx4 has the potential of being beneficial to pancreatic cancer patients.

1.10 Other Prxs in Major Cancers

Other Prxs besides Prx4 are also frequently dysregulated in cancer and are being increasingly associated with cancer initiation and metastasis. Experimental data using in vitro and in vivo models has shown the redox- dependent and independent roles of Prxs in oncology. Below, we have summarized recent progresses in other Prxs in major cancers.

1.10.1 Prxs Promote Carcinogenesis

Prx1 is positively associated with colitis and colon cancer. Two-dimensional agarose gel electrophoresis (2-DE) followed by mass spectrometry analysis of proteins isolated from biopsies (sigmoid colon) of two patients with active ulcerative colitis (UC),

two patients with inactive ulcerative colitis, and four healthy subjects showed that Prx1 is upregulated in active UC compared to inactive UC and healthy controls [167]. Oxidized Prx1 protein levels were higher in healthy and inactive UC groups while reduced Prx1 level was higher in the active UC group. Immunohistochemical (IHC) staining of patient samples confirmed that Prx1 increased with increasing inflammation in mucosal crypts [167]. Furthermore, IHC staining of Prx1 in 22 normal mucosae, six UC-associated low-grade dysplasias, five high-grade dysplasias, and five UC-associated carcinomas detected increasing Prx1 expression in dysplasia and carcinoma [167]. Further studies are warranted to establish a causal relationship between Prx1 and colon tumorigenesis in inflammation-associated sporadic colorectal cancer (CRC) as well as hereditary CRC models.

In breast cancer, loss of Prx1 due to reduced zinc (Zn) intake is linked to tumor formation [168]. Bostanci et al. treated offspring of nulliparous mice fed control (ZA, 30 mg Zn/kg) or a marginal Zn diet (ZD, 15 mg Zn/kg) with corn oil or 7,12-dimethylbenz(a)anthracene (DMBA, 1 mg/wk) for 4 weeks. Mice fed ZD had shorter tumor latency and greater incidence of non-palpable tumors. Mechanistic studies showed reduced protein levels of Prx1 and p53 and higher oxidative DNA damage in mammary tissue of mice fed ZD diet. The authors propose that Zn deficiency compromises the antioxidant capacity of mammary cells leading to higher oxidative stress and carcinogenesis [168]. This points to the need to delineate the role of diet components such as Zn in transcriptional and translational regulation of Prxs in normal physiology and cancers. In addition, Prx1 inhibits cancer-associated fibroblast-like phenotype in breast cancer [169]. Primary mammary fibroblasts (MFs) isolated from Prx1 knockout mice had increased α-SMA, collagen, and Vimentin compared to Prx1 wildtype MFs. Mechanistic

studies revealed that Prx1 knockdown MFs had increased oxidation of PTEN and phosphorylation of JNK when treated with H_2O_2. JNK1 binds to reduced Prx1 but not to overoxidized Prx1. Thus, Prx1 prevents corrupt activation of MFs [169].

Prx2 enhances intestinal tumorigenesis induced by *APC* mutation [170]. Prx2 homozygous knockout mice developed significantly fewer small intestine and colon tumors and had longer survival compared to Prx2 heterozygous and Prx2 wildtype groups in an $APC^{Min/+}$ mouse model. Prx2 knockdown increased H_2O_2 accumulation and decreased total β-catenin protein levels in APC-mutant HT-29 and SW480 cells. β-catenin reduction could be blocked by inhibition of proteasomes and GSK3β. Immunoprecipitation (IP) assay revealed that Prx2 increased Axin1 complexes by blocking PARylation/ubiquitination of Axin1 [170]. In an in vitro PARP assay, the authors found that Prx2 loss impaired tankyrase activity in HT-29 and SW480 cell lines. In summary, Prx2 promotes intestinal tumorigenesis by inhibiting β-catenin degradation.

In a urethane-induced lung cancer model, human Prx4-expressing transgenic mice developed larger tumors than non-transgenic control mice [141]. IHC staining of extracted tumors showed increased cell proliferation, decreased oxidative DNA damage and apoptosis, and increased microvascular permeability and macrophage infiltration in Prx4 overexpressing tumors. Western blot analysis of tumor tissues showed increased p-c-Jun and p-p65 in Prx4-overexpression tumors, suggesting the involvement of NF-κB and AP-1 pathways [141]. Similarly, we have recently shown that Prx4 knockout FVB/N mice developed a reduced number and size of tumors compared to wildtype FVB/N mice in azoxymethane/dextran sulfate sodium (AOM/DSS)-induced colorectal cancer and urethane-induced non-small cell lung cancer (NSCLC) [171, 172]. Loss of Prx4 reduced

tumor cell proliferation in the lung cancer model and increased tumor cell death in the colorectal cancer model. Our studies also report novel functions of Prx4 in promoting immune infiltration into the tumors as well as regulating cytokine secretion from the immune cells [171, 172]. Thus, Prx4 promotes tumor formation in lung cancer and colorectal cancer.

Prx6 also promotes lung tumorigenesis in animal models [173]. Presenilin 2 (PS2) N141I transgenic mice developed significantly lower spontaneous lung cancer compared to wildtype transgenic mice. The authors found that mutant PS2 transgenic mice tumors had over 500 times lower Prx6 expression compared to wildtype [173]. Accordingly, both peroxidase and phospholipase activities were lowered in mutant PS2 transgenic mice compared to their wildtype transgenic counterpart. IHC staining of Prx6 in human lung cancer tissue array showed overexpression of Prx6 in tumors compared to normal tissues. In addition, the authors discovered a 50% increase in PLA_2 activity in cancer tissues compared to normal tissues. In IP assay, Prx6 and PS2 co-localization was increased in PS2 mutant skin fibroblasts AG09908 cells compared to non-mutated epithelial cells A431 cells [173]. Immunofluorescence analysis proved that this co-localization could be reversed by treatment of γ-secretase inhibitor L685,458. Prx6 and PS2 colocalization was increased in urethane-induced lung tumors isolated from mutant PS2 transgenic mice compared to wildtype. IP analysis of A549 and NCIH460 also demonstrated that compared to wildtype PS2, the mutant PS2 had a higher affinity for Prx6 [173]. Transfection of mutant PS2 plasmid into A549 and H460 cells inhibited Prx6 expression and cell viability and increased PLA_2 cleavage and γ-secretase activity compared to wildtype PS2

transfection or vector transfection. Thus, PS2 mutation inhibits the PLA_2 activity of Prx6 to suppress lung tumor development [173].

1.10.2 Prxs in Cancer Progression

1.10.2.1 Prx1

In lung cancer, Prx1 protects cells against apoptosis and promotes invasion in vitro. Knockdown of Prx1 in A549 cells upregulated E-cadherin at the protein level and suppressed TGF-β-induced cell migration [174]. Using a luciferase activity assay, it was shown that catalytic Cys51 of Prx1 was critical in regulation of E-cadherin expression. The mechanism of how Prx1 peroxidase activity is used to regulate E-cadherin is not understood. In a different study, Prx1 overexpression increased anchorage-dependent colony formation and Matrigel invasion of A549 cells [139]. In A549 cells, inhibition of Prx1 with the small molecule AMRI-59 caused apoptosis [175]. AMRI-59 treatment activated both mitochondria- and apoptosis signal-regulated kinase-1-mediated signaling pathways, resulting in cell death. This could be prevented by Prx1 overexpression or N-acetyl cysteine (NAC) pretreatment. AMRI-59 was later discovered to act as a radiosensitizer in non-small cell lung cancer cells [176]. In a clonogenic assay of H460 and H1299, pre-treatment with AMRI-59 increased sensitivity of these cells to irradiation. Western blot analysis showed an increase in cleaved caspase 3 upon combined treatment of ionizing radiation (IR) and AMRI-59, and cell survivability could be rescued by pan-caspase inhibitor z-Vad-Fmk. Similarly, combined treatment of IR and AMRI-59 induced ROS production (measured using DCFDA assay) and oxidative DNA damage (measured using γH2AX immunofluorescence staining), both of which could be rescued by NAC [176]. Subcutaneous injection of these NSCLC cell lines in BALB/c nu mice followed by

various modes of treatments showed the combination of IR and AMRI-59 to be the most effective approach. Western blot analysis of cells in vitro showed that the combined effect of IR and AMRI-59 could be further increased by CREB-1 inhibitor [176]. Thus, inhibition of Prx1 is a novel approach to overcome radioresistance in NSCLC.

Prx1 protects hepatoma cells against apoptosis in vitro [177]. Knockdown of Prx1 in the HCC cell line decreased cell proliferation and increased apoptosis. This was associated with upregulation of Bax protein level and activation of mitochondrial fission as indicated by elevated Drp1, Fis1, and Dyn2 protein levels. Prx1 also contributes to epithelial–mesenchymal transition (EMT) in head and neck squamous cell carcinoma (HNSCC): Long non-coding RNA LINC00460, which enhances HNSCC cell proliferation and metastasis, physically interacts with Prx1 and facilitates Prx1 entry into the nucleus [178]. Prx1, in turn promotes the transcription of LINC00460, forming a positive feedback loop. In addition, overexpression of Prx1 upregulated Zeb1, Zeb2, Vimentin, and N-cadherin at mRNA and protein levels. Using quantitative real-time polymerase chain reaction (qRT-PCR) of paired HNSCC and adjacent normal tissues, the authors also demonstrated that high levels of LINC00460 and Prx1 expression were positively associated with lymph node metastasis and tumor size in HNSCC patients [178].

Several studies have shown that Prx1 promotes prostate cancer survival and migration. Prx1 was identified to interact with Tumor protein D52 (TDP52) in the LNCaP cell line via GST pull down assay and 2-D mass spectrometry [179]. Increasing TDP52 induction by doxycycline in LNCaP and PC3 cells caused an increase in Prx1 levels, suggesting that TDP52 causes dimerization of Prx1. When these cell lines stably expressing TPD52 were exposed to increasing concentrations of H_2O_2 (from 0 μM to 100 μM), tandem

affinity purification of TPD52 showed an increase in the fraction of Prx1 purified. This indicates that Prx1 interaction with TPD52 increases with oxidative stress. Knockdown of either Prx1 or TDP52 caused comparable reduction in cell proliferation and cell migration of LNCaP and PC3 cells [179]. Prx1 also promotes prostate cancer growth by activating androgen receptor (AR) signaling [180]. Overexpression of TXNDC9, which can also be induced by tunicamycin, increased AR protein levels in LNCaP, VCaP, and C4-2B cell lines. GST pull down assay followed by mass spectrometry identified Prx1 and MDM2 as two of the major interacting proteins of TXNDC9 in LNCaP and VCaP cell lines. Knockdown of Prx1 reduced, while overexpression of Prx1 enhanced, AR protein levels in the presence of tunicamycin. In addition, knockdown of TXNDC9 reduced the expression of prostate-specific antigen (PSA) in LNCaP cells, and this could be reversed by overexpression of Prx1 under tunicamycin treatment [180]. Transfection of increasing amounts of Flag-Prx1 plasmid into LNCaP and C4-2B cells followed by western blot analysis showed that the binding between MDM2 and AR decreased steadily in the presence of tunicamycin. The authors suggest that Prx1 competing with MDM2 to bind with AR may facilitate MDM2-mediated degradation of TXNDC9. Combination of ConoidinA (which inhibits Prx1) and Enzalutamide (which inhibits AR) reduced the cell viability of C4-2B cells more significantly when compared with single treatments [180]. Thus, combined inhibition of Prx1 and AR or disruption of Prx1–TDP52 interaction might represent a promising treatment strategy for prostate cancer treatment.

Prx1 also promotes colorectal cancer progression. IHC staining of Prx1 in 60 colorectal cancer patient tissues showed positive Prx1 expression in 70% of the samples [181]. Prx1 expression was associated with microvascular density (measured using CD34

staining), tumor grade, metastasis, and shorter survival of patients. Wound healing and transwell Matrigel invasion assays demonstrated that Prx1 knockdown in HCT116 decreased migration and invasion, while Prx1 overexpression in HT-29 increased these phenotypes in vitro [181]. Three-dimensional co-culture of human umbilical vein endothelial cell (HUVEC) with CRC cell lines showed that tube formation decreased in Prx1-depleted cell lines and increased in Prx1 overexpression cell lines. Finally, MMP2, MMP9, and VEGF were downregulated in Prx1 knockdown cells and upregulated in overexpression cells as detected by western blot analysis, further suggesting that Prx1 promotes CRC angiogenesis and metastasis [181]. Qu et al. studied the role of potential tumor suppressor miR-431-5p in colorectal cancer [182]. CRC tissues and cell lines had lower miR-431-5p expression than adjacent normal tissues and normal epithelial cell line. Prx1 was identified as a potential target through bioinformatics analysis and confirmed in vitro. After co-culture, human umbilical cord mesenchymal stem cell (hUCMSC)-derived exosomes inhibited miR-431-5p increased cell proliferation, migration, and invasion in LoVo cells compared with negative control-inhibitor-exosome treatment. This effect was not observed in Prx1 knockdown cells, further confirming that miR-431-5p exerts tumor suppressive functions through Prx1 [182]. Prx1 also promotes degradation of pro-apoptotic protein NOXA to increase CRC survival [183]. Western blot analysis of apoptosis regulators showed a significant increase of NOXA in HCT116 Prx1 knockdown cells and a decrease of NOXA in SW480 Prx1 overexpression cells. In cycloheximide assay, NOXA had longer half-life in shPrx1 cells. MG132 treatment followed by co-immunoprecipitation revealed lower ubiquitination of NOXA in shPrx1 cells, suggesting Prx1 promotes ubiquitin-mediated degradation of NOXA. Depletion of Prx1 in HCT116 reduced the

neddylation of CUL5 (which activates CRL5 to ubiquitinate NOXA). In anti-CUL5 immunoprecipitation, knockdown of Prx1 reduced the amount of UBE2F, suggesting Prx1 enables their interaction [183]. Knockdown of Prx1 sensitized HCT116 cells to apoptosis induced by etoposide, and overexpression of Prx1 increased resistance of SW480 cells against etoposide. Time-dependent increase in CUL5 neddylation was observed in HCT116 upon etoposide treatment, but this effect was not seen in Prx1 knockdown cells. This indicates that cancer cells utilize Prx1-mediated CUL5 neddylation to survive against chemotherapeutics [183]. Thus, Prx1 supports angiogenesis and survival of CRC cells.

Prx1 has been reported to promote breast cancer proliferation and survival through its peroxidase function. In breast cancer cell lines MCF-7 and ZR-75-1, depletion of Prx1 decreased cell proliferation and anchorage-dependent colony formation [184]. Implantation of control and Prx1 knockout MCF-7 cells into the mammary fat pad of nude mice resulted in significantly slower tumor growth rate in the knockout group. As expected, Prx1-depleted cells were more sensitive to glucose oxidase-induced cell death. Prx2-SO_3 and Prx4-SO_3 levels were significantly higher in Prx1 knockout cells compared to control after glucose oxidase treatment, suggesting Prx1 protects these 2-Cys Prxs from oxidation in breast cancer. Interestingly, glucose oxidase and another prooxidant agent, sodium L-ascorbate also reduced the viability of breast cancer cell lines T47D, MDA-MB-231, HCC 1806, and SK-BR-3, but not of non-malignant cell line MCF-10A [184]. Other studies have also shown that Prx1 protects breast cancer cells against oxidative stress-induced cell death. Prx1 depletion increased sensitivity of triple-negative breast cancer cell lines MDA-MD-231 and HCC1806 to ascorbate and menadione [185]. Deacetylation and inhibition of Prx1 by SIRT2, a protein deacetylase, sensitized breast cancer cells to prooxidants menadione

and arsenic trioxide [186]. Finally, loss of Prx1 also increases susceptibility of breast cancer cells to radiation [187]. Skoko et al. reported that Prx1 binds to and protects Rad51 cysteines from oxidation. Consequently, Prx1 knockdown sensitized MDA-MD-231 cells to irradiation-induced cell death by preventing Rad51-mediated homologous recombination DNA repair.

While Prx1 supports growth and survival of breast cancer cells, Prx1 expression in stromal cells of the breast tumor microenvironment is associated with inhibition of cancer progression. Loss of Prx1 prompts collagen remodeling known to promote breast cancer development [188]. Knockdown of Prx1 in mammary fibroblasts followed by injection into mammary fat of BALB/c mice resulted in an enrichment of intratumoral collagen in the shPrx1 group. In vitro studies indicated that Prx1-depleted mammary fibroblasts had higher α collagen, β collagen, and β/α collagen ratio [188]. Conditioned media derived from MDA-MB-231 cells caused Y194 phosphorylation of Prx1 (known to inactivate peroxidase activity), and this could be reversed by co-treatment with Src inhibitor PP1. shPrx1 mammary fibroblasts had increased secretion of lysyl oxidase (LOX). Per IP assay of LOX in HEK293T cells, endogenous Prx1 interacts with LOX, but this interaction was decreased when Prx1 was phosphorylated, resulting in increased extracellular LOX accumulation and collagen remodeling [188]. Another study suggested that Prx1 mediates tumor suppressor activity of cytoskeletal protein transgelin-2 (TAGLN2) [189]. Knockdown of TAGLN2 in MDA-MB-231 increased cell migration in vitro and increased lung metastasis in a tail-vein injection mouse model. IP of TAGLN2 in MDA-MB-231 lysates followed by mass spectrometry analysis showed that TAGLN2 binds to Prx1. Knockdown of TAGLN2 in MDA-MB-231 caused downregulation of Prx1 protein. Accordingly, DCFDA assay

demonstrated that TAGLN2 knockdown resulted in higher ROS production [189]. Thus, interaction of Prx1 with LOX and TAGLN2 plays anti-tumorigenic role. The direct or indirect mechanism of how TAGLN2 upregulates Prx1 needs to be examined. Furthermore, the importance of peroxidase function in Prx1 in its interaction with TAGLN2 remains to be seen.

Prx1 also inhibits pro-tumorigenic activation of macrophages in breast cancer [190]. Wang and Liu et al. discovered that lysosome-associated membrane protein type 2a (LAMP2a) is upregulated in tumor-associated macrophages (TAMs) by tumor cells. Depletion of LAMP2a in macrophages reduced tumor growth in vitro and in vivo. IP of LAMP2a in bone marrow-derived macrophages treated with tumor supernatant revealed that LAMP2a binds to Prx1 [190]. Knockdown of Prx1 reversed the effects of LAMP2a knockdown in mouse hematopoietic stem cells in vitro. The authors suggest increased oxidative stress (measured using H_2O_2 accumulation) caused by knockdown of LAMP2a in bone marrow-derived macrophages likely causes pro-inflammatory activation in macrophages [190]. Finally, Prx1 protects natural killer cells from oxidative stress in the breast cancer microenvironment [191]. The authors performed bioinformatics analysis of non-stimulated human primary T cells, B cells, and Natural Killer (NK) cells and found that Prx1 transcript was significantly lower in NK cells. This was confirmed by qRT-PCR and western blot analysis in vitro. Priming NK cells with cytokine IL-15 protected cells from glucose oxidase-induced cytotoxicity via upregulation of Prx1. Stable overexpression of Prx1 in primary NK cells and NK-92 cell line further improved cell viability under oxidative stress. Intra-tumoral transplantation of PD-L1-CAR NK cells overexpressing Prx1 in NSG mice showed increased survival and proliferation of Prx1 overexpression cells

compared to control cells [191]. Thus, overexpression of Prx1 might be a useful approach to improve CAR NK-based immunotherapy in breast cancer.

1.10.2.2 Prx2

Prx2 promotes progression of non-small cell lung cancer (NSCLC). Western blot analysis showed that the expression of Prx2 in NSCLC cell lines is higher than in normal bronchial epithelial cells (BEAS-2b) [192]. Knockdown of Prx2 in A549 cells reduced cell proliferation, migration, and invasion. Subcutaneous injection of Prx2 knockdown A549 cells resulted in slower tumor growth compared to control cells. IHC staining of extracted tumors revealed a decrease in cell proliferation in the shPrx2 group. Tail-vein injection of A549 cells resulted in fewer metastatic nodules in Prx2 knockdown group compared to control, and this was associated with higher E-cadherin and lower Vimentin and Slug expression [192]. Jing et al. have reported similar findings in A549 and H1299 cell lines. They also discovered that loss of Prx2 reduced the phosphorylation of AKT and mTOR [193]. In addition, Prx2 promoted the stemness of drug-resistant cancer stem cells. Knockdown of Prx2 reduced colony formation and sphere formation, increased ROS (DCFDA assay) and apoptosis, and reduced migration and invasion of gefitinib-resistant A549 (A549/GR) $CD133^+$ cells [194]. The authors validated that microRNA miR-122 targets Prx2 and showed that overexpression of miR-122 also suppressed proliferation, migration, and invasion of A549/GR $CD133^+$ cells. In mechanistic studies, the authors used western blot analysis to show that miR-122-mediated downregulation of Prx2 resulted in reduced activation of the Hedgehog, Notch, and Wnt/β-Catenin signaling pathways in A549 cells [194]. Finally, loss of Prx2 activity resulted in death of lung cancer cells. S-nitrosoglutathione (GSNO) nitrosylates Prx2 on Cys51 and Cys172, resulting in H_2O_2

accumulation and apoptosis in A549 and NCI-H1299 cells [195]. GSNO-induced H_2O_2 increased phosphorylation of AMPK and inhibited deacetylation activity of SIRT1, leading to cell death. Thus, Prx2 aids survival and malignancy of NSCLC through a variety of pathways.

Prx2 increases growth and progression of CRC. Knockdown of Prx2 using shRNAs reduced proliferation of HCT116 and LoVo cell lines [196]. Flow cytometry analysis proved that Prx2 knockdown caused increased cell cycle arrest in G2/M phase in HCT116 and G1 phase in LoVo cells. There was no difference in p53 mRNA levels after Prx2 knockdown, but cycloheximide treatment showed an increased half-life of p53 in shPrx2 cell lines [196]. The authors discovered through IP and mass spectrometry that ribosomal protein RPL4 binds to Prx2. Ubiquitination assays were used to confirm RPL4 interaction with MDM2 and show that Prx2 increases ubiquitination of p53. Subcutaneous injection of control and shPrx2 cell lines resulted in higher tumor growth and larger tumor volume in the control group. IHC analysis showed shPrx2 tumors had higher expression of p53 [196]. Thus, Prx2 causes colorectal cancer growth in vitro, likely by facilitating degradation of p53.

Loss of Prx2 sensitizes CRC stem cells to chemotherapy [197]. IHC staining of 19 CRC patient tissues showed that Prx2 expression was significantly higher in $CD133^+/CD44^+$ tissues than in $CD133^-/CD44^-$ tissues. In spheroids of $CD133^+/CD44^+$ cells isolated from HCT116 and HT-29, the authors found higher expression of Prx2 compared to spheroids of $CD133^-/CD44^-$ cells. Western blot analysis showed significant downregulation of stemness-related proteins Oct4, Nanog, and Sox2 in $CD133^+/CD44^+$ cells isolated from HCT116 and HT-29 shPrx2 cell lines compared to those from control

cell lines [197]. shPrx2 knockdown $CD133^+/CD44^+$ cells had lower migration and invasion in vitro compared to control stem cells. Orthotopic implantation of these two groups of cells in the cecal wall of nude mice resulted in significantly reduced liver metastasis in the shPrx2 group. The authors also found that shPrx2 $CD133^+/CD44^+$ cells had increased E-cadherin and decreased N-cadherin, Vimentin, Twist, and nuclear β-catenin than control $CD133^+/CD44^+$ cells [197]. Treatment of control or Prx2 knockdown $CD133^+/CD44^+$ cells with 500 μg/mL 5-fluororuracil or 100 μM oxaliplatin for 24 h showed increased cell death in the knockdown group as measured by annexin V flow cytometry analysis. DCFDA assay illustrated that chemotherapeutics induced significantly higher ROS in the Prx2 knockdown group. This was accompanied by increased DNA damage in shPrx2 CSC group cells than control CSCs as measured using alkaline comet assay [197]. Similar experimental findings were reported by Wang et al. [198]. The authors sorted $CD133^+$ and $CD133^-$ cells from SW620, HT-29, and HCT116 and found by western blot analysis that Prx2 expression was higher in $CD133^+$ cells in all three groups. Knockdown of Prx2 using shRNA reduced sphere formation of these cell lines by decreasing the mRNA and protein expression of CD44, CD133, and Nanog. Flow cytometry analysis showed that Prx2 depleted $CD133^+$ cells were more prone to apoptosis by 5-FU [198]. $CD133^+$ cells were isolated from control and HCT116 shPrx2 cell lines and injected into nude mice subcutaneously. Compared to the control group, the shPrx2 group had significantly smaller tumors at endpoint of the study, suggesting Prx2 contributes to tumorigenicity of colon cancer cells. The authors found by western blot that in HT-29 $CD133^+$ cells, knockdown of Prx2 decreased and overexpression of Prx2 increased the expression of SMO and Gli1

proteins, suggesting Prx2 might regulate cancer stem cell properties via Hedgehog/Gli1 pathway [198].

Other studies have also shown that Prx2 depletion sensitizes CRC cells to ionizing radiation and chemotherapy [199-202]. Prx2 was silenced using siRNA in HCT116, Caco2, and T84 cell lines and clonogenic survival assay was performed after exposure to different doses of radiation [199]. Silencing Prx2 sensitized these cell lines to radiation. Oxaliplatin treatment before radiation was more effective in killing the shPrx2 cell line compared to control. HCT116, HCT116 shControl, and HCT116 shPrx2 cells were subcutaneously injected into flanks of nude mice, which were irradiated with 2 Gy four days after inoculation. Six days post-radiation, shPrx2 radiation group had significantly smaller tumors compared to day 1, while this effect was not seen in the other two groups [199]. Similar findings were reported by Xu et al. Annexin V staining showed increased apoptosis in HT-29 and HCT116 shPrx2 cell lines after 5-FU treatment [202]. Intraperitoneal injection of HCT116 control and shPrx2 cell lines into flanks of nude mice followed by no treatment or 5-FU treatment showed that the shPrx2 + 5-FU group had the longest survival. In addition, IHC staining of 49 patient specimens indicated that cyclophilin A (CypA) and Prx2 were upregulated in patients that did not respond to FOLFOX compared to patients that did respond [200]. The authors discovered through mass spectrometry that CypA interacts with Prx2. CypA overexpression decreased ROS levels in RKO cells which could be partly rescued by knockdown of Prx2, indicating that Prx2 promotes reduction of CypA. Overexpression of CypA increased resistance of RKO cells to 5-FU and oxaliplatin and this could be reversed by knockdown of Prx2 [200]. Similarly, overexpression of miR-200b-3p, which targets Prx2, sensitized LoVo cells to apoptosis by oxaliplatin, and this

could be partly rescued by overexpression of Prx2 [201]. In a subcutaneous xenograft model, miR-200b-3p overexpression in LoVo cells inhibited tumor growth whereas silencing miR-200b-3p in SW480 promoted tumor growth. Implantation of extracted subcutaneous tumors into the cecum of nude mice showed that miR-200b-3p overexpression tumors developed significantly fewer metastatic nodules than control mice [201]. Thus, degradation of Prx2 reduces metastasis and enhances sensitivity of chemotherapeutics in CRC.

Loss of Prx2 also sensitized HCT116 cells to antimalarial drug dihydroartemisinic (DHA) [203]. DHA treatment (15 μM) of HCT116 reduced Prx2 expression at mRNA and protein levels at 12 h and 24 h. DHA-induced ROS was confirmed by DCFDA staining in RKO and HCT116. DHA also induced ER stress-related proteins ATF4 and p-eIF2α in a time- and concentration-dependent manner. Prx2 knockdown further increased the sensitivity of HCT116 cells to DHA. Prx2 knockdown also enhanced the activation of JNK and p38 signaling pathways by DHA [203]. Combined treatment with oxaliplatin and DHA synergistically increased apoptosis in HCT116 and RKO cells. Furthermore, Prx2 was demonstrated to protect cells against DNA damage in checkpoint kinase 2 (CHEK2) null CRC [204]. The CHEK2 gene is involved in maintaining chromosomal stability and in homologous recombination repair. The authors treated CHEK2 null HCT116 cells with siRNA against Prx2 and found that combined loss of CHEK2 and Prx2 was lethal to the majority of HCT116 cells. Similarly, N-carbamoyl alanine (NCA, an inhibitor of Prx2) treatment of CHEK2 null HCT116 cells also reduced the viability of cells [204]. DCFDA assay showed increased ROS levels in HCT116 and CHEK2 null HCT116 cells with NCA treatment. However, NCA treatment caused more DNA damage in CHEK2 null HCT116

cells (as indicated by γ-H2AX staining) than in WT HCT116 cells. Accordingly, immunofluorescence staining showed higher increase of cleaved caspase 3 in CHEK2 null HCT116 cells than WT HCT116 upon NCA treatment [204]. This suggests that Prx2 plays an important role in preventing oxidative-stress induced DNA damage in the absence of tumor suppressor CHEK2 in CRC.

Prx2 promotes vasculogenic mimicry formation in CRC [205]. Vasculogenic mimicry refers to the vascular-like structures formed by cancer cells for blood supply independent of endothelial cells. IHC staining of Prx2 in 70 CRC patient tissues revealed that 70% of the tissues were positive for Prx2. Authors also performed double staining of CD34 and periodic acid–Schiff as markers for vasculogenic mimicry (VM). Pearson correlation analysis showed a positive correlation between Prx2 and VM formation [205]. Stable siPrx2 HCT116 cells were established, and recombinant VEGF was added to 3D culture of HCT116 cells to induce VM formation in vitro. siPrx2 cells had significantly fewer tubular structures than control cells. siPrx2 cells also had lower levels of p-VEGFR2 protein compared to control cells, suggesting Prx2 promotes VM formation by activating VEGFR2 [205]. Knockdown of Prx2 reduced the cell invasion of HCT116 caused by VEGF chemoattractant in Matrigel invasion assay. Thus, Prx2 supports the growth of aggressive tumors through VM formation.

Prx2 loss inhibits autophagy in CRC [206]. Analysis of RNA-Seq data of HT-29 and SW480 control and siPrx2 cell lines followed by KEGG (Kyoto Encyclopedia of Genes and Genomes) analysis indicated enrichment of the FOXO pathway. Knockdown of Prx2 resulted in an increase of p21 and p27 proteins in western blot analysis. shPrx2 cells had lower LC3B-GFP staining than non-targeting control cells [206]. Western blot analysis

was used to show reduced LC3B II/LC3B I ratio and Beclin 1, and increased Sqstm1/p62 in Prx2 knockdown cells compared to control. This indicates that Prx2 inhibits autophagosome formation. Western blot analysis also showed reduced p-p38 in shPrx2 cells. Treatment with 1 μM dehydrocorydaline chloride (DHC, a p38 MAPK activator) for 24 h rescued p-p38 to some extent in Prx2 cells. In addition, DHC also caused a decrease in p21 proteins to similar levels as non-targeting controls. Subcutaneous injection of control and shPrx2 cells into nude mice resulted in smaller tumor formation in the shPrx2 group [206]. Another study reported that oxiconazole (Oxi), an antifungal compound derived from imidazole, downregulates Prx2 in CRC cells to initiate autophagy and inhibit autolysosome formation by downregulating Rab7a [207]. When nude mice were subcutaneously injected with HCT116 cells followed by control or Oxi treatment (50 mg/kg/day), the Oxi treatment group developed significantly smaller tumors. Annexin V staining showed increased apoptosis in HCT116 and RKO after Oxi treatment. Oxi treatment increased cellular ROS levels as measured by active oxygen analysis kit. This increase in ROS and apoptosis could be inhibited by co-treatment with N-acetyl cysteine, suggesting Oxi promotes ROS production to induce apoptosis [207]. The authors found through immunofluorescence staining that Oxi treatment increased autophagosome formation but not autolysosome formation in HCT116 and RKO cells. In Oxi-treated xenograft tissue, IHC showed stronger staining for LC3 than in control group. Co-treatment with 3-mA (an autophagy inhibitor) rescued the decrease in cell viability caused by Oxi [207]. Oxi treatment also decreased Prx2 expression in a dose-dependent manner. Accordingly, Prx2 was found to be depleted in an Oxi-treated mouse xenograft model. Western blot analysis was used to examine lysosome–autophagosome fusion proteins and

the authors found that Oxi decreased Rab7a expression. This could be partially reversed by Prx2 overexpression. Rab7a expression was also lower in the Oxi-treated mouse xenograft. Tandem monomeric mRFP-GFP tagged LC3 immunofluorescence assay in cells suggested that Oxi inhibits autolysosome formation through downregulation of Rab7a [207]. The role of Prx2 in CRC progression is summarized in Figure 1.7.

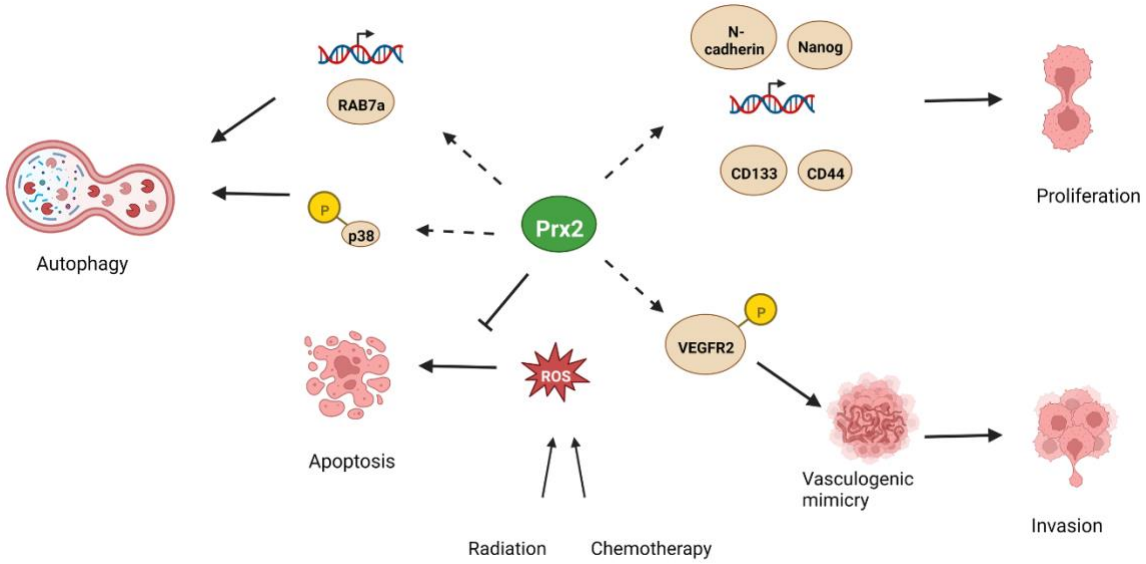

Figure 1.7. Prx2 promotes colorectal cancer progression.
Prx2 increases autophagic flux, cancer stem cell expansion, vasculogenic mimicry and inhibits ROS-induced apoptosis.

1.10.2.3 Prx3

Prx3 promotes survival and proliferation of lung adenocarcinoma cells in vitro. Prx3 was upregulated at mRNA and protein levels in 36 human lung adenocarcinoma (LUAD) samples compared to adjacent normal tissue [208]. Overexpression of tumor suppressor DACH1 resulted in downregulation of Prx3 transcript and protein in LUAD cell lines LTEP-α-2 and A549. DACH1-mediated downregulation of Prx3 resulted in reduced cell proliferation and anchorage-dependent colony formation in both cell lines. Similarly, downregulation of Prx3 increased susceptibility of NSCLC cells to radiation

[142]. Knockdown of oncogene TP53-regulated inhibitor of apoptosis 1 (TRIAP1) in A549 and H460 cells sensitized these cells to irradiation. TRIAP1 knockdown cells had increased apoptosis and decreased cell invasion upon irradiation compared to wildtype cells. Irradiation of A549 and H460 increased transcript and protein levels of TRIAP1 and impaired the radiation-induced increase of antioxidants including Prx3, Prx4, and Prx6 [142]. Downregulation of Prx3 also increased the susceptibility of NSCLC cells to thiosemicarbazones. Myers group have reported that tridentate iron chelator triapine (Tp) (3-aminopyridine-2-carboxaldehyde thiosemicarbazone) oxidizes Prx3 in lung cancer lines (A549, H23, and H1703) and A2780 ovarian cancer cells [209]. Cytotoxicity of Tp correlated with Prx3 oxidation in the clonogenic survival of lung cancer lines. Knockdown of Prx3 further sensitized A549 cells to Tp [209].

Downregulation of Prx3 reduces viability of breast cancer cells in vitro. Knockdown of B7-H4 (also called VTCN1) decreased cell viability of MCF-7 and T47D cells [210]. This was associated with depletion of Prx3. Silencing Prx3 using siRNA caused increased intracellular ROS and decreased cell viability similar to B7-H4 knockdown [210]. Thus, Prx3 likely protects breast cancer cells from oxidative stress-induced cell death.

Prx3 promotes stemness and survival of colon cancer cells [211]. qRT-PCR analysis showed increased Prx3 expression in $CD133^+$ CSCs freshly isolated from eight patients with colon cancer compared to non-cancer stem cells. mRNA levels of Prx3 and CD133 in CSCs isolated from patient tissues showed significant positive correlation. Prx3 knockdown resulted in a decrease in the size of the $CD133^+$ CSC population and sensitized the CSCs to 5-FU-induced cell death through mitochondrial dysfunction. Mice

subcutaneously injected with $CD133^+$ cells sorted from HT-29 shPrx3 showed reduced tumor volume and enhanced 5-FU-induced cell death compared with HT-29 shControl-injected mice [211]. Depletion of Prx3 resulted in a significant reduction in liver metastasis, colon metastasis, and local invasion in an orthotopic xenograft model produced by the injection of colon CSCs into the spleen and cecum of SCID mice. Chromatin immunoprecipitation assays showed that FOXM1 transcriptionally activates *CD133* and *Prx3* by binding to the promoter region of these genes. Overexpression of FOXM1 increased Prx3 and CD133 protein levels and expanded $CD133^+$ population [211]. Thus, Prx3 supports CRC stem cells.

1.10.2.4 Prx5

Prx5 promotes proliferation and EMT phenotype in gastric cancer cells [212]. Five-year survival data analyzed via the log-rank test indicated that overexpression of Prx5 was correlated with poor survival of gastric cancer patients. Expression of Prx5 significantly correlated with tumor size, lymph node invasion, and metastasis (TNM) stage [212]. Both proliferation and anchorage-dependent colony formation were higher in SNU-216 Prx5 overexpression cells than in parental SNU-216 cells. In western blot analysis, E-cadherin was decreased, while Snail and Slug were increased in Prx5 overexpression SNU-216 cells [212].

Prx5 also promotes survival and EMT in NSCLC. Administration of non-thermal plasma therapy using plasma-activated medium (PAM) induced apoptosis in cancer cells by increasing ROS levels [213]. PAM was developed by treating A549 cell culture medium with low temperature plasma at 16.4 kV for 0, 60, 120, or 180 s. Knockdown of Prx5 enhanced ROS production, cytotoxicity, and inhibition of migration in A549 cells caused

by PAM [214]. Western blot analysis showed that Prx5 knockdown in A549 reduced p-ERK and BCL2 and increased p-JNK and BAD proteins to promote apoptosis. Besides contributing to survival, Prx5 also promotes NSCLC growth and progression through its interaction with Nrf2 and Stat3. Prx5 could be pulled down using anti-Nrf2 antibody and vice versa in NSCLC and non-tumor lung tissues and in H1229 and A549 cell lysates [215]. Knockdown of Prx5 decreased NQO1 protein levels in A549 and H1299 cells induced by H_2O_2 treatment. Similarly, knockdown of Prx5 or NQO1 reversed the increase in cell proliferation of A549 and H1299 cells induced by H_2O_2 treatment. In analysis of patient samples, the authors found strong correlation of Prx5 mRNA with Nrf2 and NQO1 [215]. Subcutaneous injection of A549 cells into flanks of nude mice followed by no treatment or intra-tumoral injection of Nrf2 or Prx5 shRNA led to a significantly reduced tumor growth in the shRNA treated group. Prx5 interaction with Stat3 was also reported by Xue research group. qRT-PCR of 121 paired NSCLC tumor and adjacent normal samples revealed that 65% of the samples contained Prx5 promoter demethylation, and Prx5 promoter demethylation was associated with higher TNM stage [216]. Overexpression of Stat3 in H1299 cells pre-treated with 100 μM H_2O_2 increased Prx5 protein level whereas knockdown of Stat3 decreased Prx5, suggesting that Stat3 is at least partially responsible for regulation of Prx5 expression. Overexpression of Prx5 in H1299 cells pre-treated with 100 μM H_2O_2 increased in vitro migration and invasion. This was associated with a decrease in E-cadherin and increases in Vimentin, Nrf2, and NQO1 as indicated by western blot [216]. Thus, Prx5 plays pro-tumorigenic role in NSCLC.

Prx5 promotes EMT phenotype in SW480 colon cancer cells [217]. Prx5 overexpression in SW480 cells increased cell proliferation, migration, and invasion rates

in vitro. In western blot analysis, Prx5 overexpressing cells had lower E-cadherin and higher Vimentin, Slug, and Snail [217]. Knockdown of Prx5 using siRNA reversed the increase in cell proliferation, migration, invasion, and E-cadherin expression seen upon Prx5 overexpression. Prx5 also protects colon cancer cells from ROS-induced apoptosis [218]. β-lapachone, a compound extracted from the South American lapacho tree, is known to have anti-cancer activity. The authors performed bioinformatics analysis using the GEPIA website to show that Prx5 was upregulated in colon cancer compared to normal tissue. Increasing concentrations of β-lapachone treatment for 24 h showed SW480 shPrx5 cells as more sensitive to this compound whereas SW480 HisPrx5 cells were more resistant compared to mock SW480 cells [218]. This was shown using a cell viability assay and annexin V staining. β-lapachone treatment decreased BCL2 (pro-apoptotic protein) expression in SW480 mock and shPrx5 cells. Dihydroethidium (DHE) staining indicated that β-lapachone treatment increased ROS levels in SW480 mock and shPrx5 cells [218]. In addition to ROS scavenging, Prx5 also regulates Wnt/ β-catenin pathway in response to β-lapachone. Per western blot analysis, the ratio of p-Gsk3-β/Gsk3-β was higher and p-β-catenin/ β-catenin was lower in Prx5-His cells than in mock and shPrx5 SW480 cells. The group also reported that Prx5 protects HCT116 and HT-29 cells from ROS-induced apoptosis [219]. Shikonin, a natural compound purified from the *Lithospermum erythrorhizon* plant, was previously reported to induce ROS in cancer cells. HCT116 and HT-29 cells were treated with increasing concentrations of Shikonin. JC-1 staining demonstrated that mitochondrial ROS increased in a dose-dependent manner. Similarly, DCFDA staining demonstrated a dose-dependent increase [219]. The authors found by western blot analysis that Shikonin did not affect expression of proteins Prx2, Prx3, and

Prx6, but Prx1 was increased and Prx5 was decreased with higher concentrations of Shikonin. Increasing concentrations of Shikonin resulted in a dose-dependent decrease of p-mTOR/mTOR ratio in HT-29 cells [219]. In MTT assay, HisPrx5 HT-29 cells had higher viability than control mock HT-29 cells with increasing Shikonin concentrations. This increased resistance to cell death was also confirmed by DHE staining and annexin V flow cytometry analysis. Finally, HisPrx5 overexpression prevented a decrease in p-mTOR/mTOR ratio upon Shikonin [219]. Thus, Prx5 plays a potential role in suppressing apoptosis in colon cancer.

1.10.2.5 Prx6

Prx6 promotes NSCLC growth and survival. Overexpression of Prx6 increased, and knockdown of Prx6 decreased, cell proliferation, invasion, and migration of A549 cells [220]. Western blot analysis indicated that Prx6 overexpression promotes EMT by downregulating E-cadherin and upregulating Vimentin, Twist, β-catenin, and c-Myc. In a subcutaneous A549 xenograft model, Prx6 overexpression increased tumor growth while Prx6 knockdown suppressed tumor growth [220]. A positive correlation between CD133 and Prx6 protein expression in NSCLC patient samples is reported [221]. Knockdown of Prx6 decreased the $CD133^{+}/ABCG2^{+}$ population in H1299 and A549 cells and decreased the sphere formation ability of these cancer stem-like cells. Knockdown of Prx6 also reduced the IC_{50} of cisplatin for H1299 and A549 CSCs by 50% [221]. Another study also reported a positive association between Prx6 and drug resistance. Two-dimensional gel electrophoresis of six pairs of pre-treatment fresh primary lung adenocarcinoma tumors with varied chemotherapy responses revealed that Prx6 was upregulated in chemo-resistant tumors [222]. Furthermore, Prx6 promotes growth of NSCLC. Withangulatin A (WA) is a

small molecule isolated from *Physalis angulata* var. *villosa* and is reported to reduce proliferation of cancer cells. Stable isotope labeling by amino acids in cell culture and activity-based protein profiling in H1975 cells identified Prx6 as a direct target of WA [223]. WA covalently binds to Prx6 to inhibit its function and increases the production of ROS as indicated by DCFDA assay in H1975 cells. Subcutaneous injection of wildtype and Prx6 knockout (Prx6 KO) H1975 cells resulted in significantly lower tumor volume in the Prx6 KO group. WA treatment had no significant effect on proliferation, GPx activity, and PLA_2 activity in H1975 Prx6 KO cells in vitro, or in growth of Prx6 KO tumors in vivo, confirming that WA acts through Prx6 [223].

Prx6 also contributes to the progression of CRC. IHC staining of Prx6 in a CRC patient tissue microarray showed that Prx6 was upregulated in node-positive CRC compared to node-negative CRC [224]. Stable knockdown of Prx6 reduced cell migration and invasion in HCT116 cells. Prx6 knockdown also caused downregulation of N-cadherin, CDK1, and Twist1 in HCT116. This was associated with reduced phosphorylation of PI3K, AKT, p38, and p50 as indicated by western blot [224]. Treatment of HCT116 with NAC, PI3K/AKT inhibitor wortmannin, and p38 MAPK inhibitor SB203580 resulted in a decreased trimethylation of histone H3 lysine 4 (H3K4me3) of Prx6 promoter [224]. This suggests a role for PI3K/AKT pathway in upregulation of Prx6 in CRC. The suggested roles of Prxs in cancer development and mechanisms are summarized in Table 1.2.

Table 1.2. Summary of Prxs in carcinogenesis and cancer progression.

Prxs	Cancers	Pro- or Anti-tumor	Mechanism/Pathway	References
Carcinogenesis				
Prx1	Colorectal	Pro-tumor	Increased inflammation	[167]
	Breast	Anti-tumor	Maintenance of redox homeostasis	[168]
Prx2	Intestinal	Pro-tumor	Stabilization of β-catenin in APC mutant cells	[170]
Prx4	Lung	Pro-tumor	Protection against oxidative stress-induced cell death and increased activation of NF-κB and AP-1 signaling	[141]
Prx6	Lung	Pro-tumor	Increased PLA2 activity	[173]
Progression				
Prx1	Lung	Pro-tumor	Downregulation of E-cadherin	[174]
		Pro-tumor	Protection against oxidative stress-induced cell death and inhibition of ASK1-JNK	[175, 176]
	Prostate	Pro-tumor	Protection against oxidative stress-induced cell death and cell death and interaction with TPD52	[179]
		Pro-tumor	Activation of AR signaling	[180]
	Colorectal	Pro-tumor	Cullin-5 neddylation-mediated NOXA degradation	[183]
	Breast	Pro-tumor	Prevention of Rad51 oxidation to promote homologous recombination	[187]
		Anti-tumor	Mediation of TAGLN2 activity	[189]
		Anti-tumor	Inhibition of LOX secretion and extracellular matrix remodeling	[188]
		Anti-tumor	Inhibition of pro-tumorigenic macrophage differentiation	[190]
		Anti-tumor	Inhibition of pro-tumorigenic fibroblast differentiation	[169]
		Anti-tumor	Increased survival of Natural killer cells	[191]
Prx2	Lung	Pro-tumor	Upregulation of Vimentin, Slug and activation of AKT/mTOR	[192, 193]
		Pro-tumor	Activation of Hedgehog, Notch, Wnt/β-catenin	[194]
		Pro-tumor	Maintenance of SIRT1 activity through inhibition of AMPK	[195]
	Colorectal	Pro-tumor	Degradation of p53	[196]
		Pro-tumor	Increased stemness, radioresistance and chemoresistance	[197-202]

Table 1.2 (continued)

		Pro-tumor	Protection against oxidative stress-induced cell death	[203, 204]
		Pro-tumor	Formation of vasculogenic mimicry	[205]
		Pro-tumor	Inhibition of autophagy	[206, 207]
Prx3	Lung	Pro-tumor	Radioresistance and chemoresistance	[142, 209]
	Breast	Pro-tumor	Protection against oxidative stress-induced cell death	[210]
	Colorectal	Pro-tumor	Increased stemness and chemoresistance	[211]
Prx4	Prostate	Pro-tumor	AR activation and radioresistance	[131]
	Prostate, Breast	Pro-tumor	Activation of ERK/NFATc1	[129]
	Lung	Pro-tumor	Activation of c-jun/AP-1	[139]
	Colorectal	Pro-tumor	Activation of EGFR, RhoA, PKCα, ERK	[147]
Prx5	Lung	Pro-tumor	Protection against oxidative stress-induced cell death	[214]
		Pro-tumor	Upregulation of Vimentin, Nrf2, NQO1	[215, 216]
	Colorectal	Pro-tumor	Upregulation of Vimentin, Slug	[217]
		Pro-tumor	Protection against oxidative stress-induced cell death	[218, 219]
Prx6	Lung	Pro-tumor	Upregulation of Vimentin, Twist, β-catenin	[220]
		Pro-tumor	Protection against oxidative stress-induced cell death	[223]
		Pro-tumor	Increased stemness and chemoresistance	[221, 222]
	Colorectal	Pro-tumor	Activation of PI3K/AKT and upregulation of N-cadherin	[224]

1.11 Research Objective

The aims of this study were to investigate the function of Prx4 in colorectal cancer initiation and progression.

In chapter three, we demonstrate using AOM/DSS model that loss of Prx4 provides resistance to inflammation-associated tumor formation. There was development of fewer and smaller colon tumors in Prx4 knockout mice compared to wildtype. Histopathological

analysis revealed that loss of Prx4 leads to increased cell death through lipid peroxidation and lower infiltration of inflammatory cells in the knockout tumors compared to wildtype.

In chapter four, we demonstrate that loss of Prx4 in human CRC cell lines decreases migration and invasion in vitro. In orthotopic implantation model, Prx4-depleted CRC cell lines had lower metastasis rate in vivo. Depletion of Prx4 upregulated DKK1 which is a known suppressor of colorectal tumor metastasis.

Our mechanistic studies of Prx4 in cancer development clearly show that Prx4 promotes both colorectal tumorigenesis and cancer progression. The results from this study provide a novel insight into the expression of Prx4 in tumor-infiltrating immune cells and the function of Prx4 in regulation of Wnt/β-catenin, NF-κB and focal adhesion signaling pathways. These findings could prove useful to develop effective strategies for the prevention and treatment of colorectal cancer in patients.

CHAPTER 2. MATERIALS AND METHODS

2.1 Mammalian Cell Culture

Authenticated human colon cancer cell lines HCT116, RKO, HT29, and GEO were obtained from the Cancer Cell Line Repository at Frederick National Laboratory for Cancer Research. McCoy's 5A medium (Corning, Corning, NY) supplemented with 10% Fetal bovine serum (FBS) (Gibco, Thermo Fisher Waltham, MA) was used to culture these cells. Human colon cancer cell lines SW620, SW480 and LoVo was commercially obtained from American Type Culture Collection (ATCC, Manassas, VA). Roswell Park Memorial Institute-1640 (RPMI-1640) medium (Corning) supplemented with 10% FBS (Gibco) was used to culture these cells. Penicillin-Streptomycin solution (HyClone, Logan UT) (where Penicillin is 100 units/mL, Streptomycin is 100 μg/mL) and 5 μg/mL Gentamicin (Gibco) were added to media before use. Cells were incubated in humidified atmosphere with 5% (v/v) CO_2 at 37°C.

MISSION ShRNA pLKO.1 based ShRNAs (Sigma-Aldrich, St Louis, MO), including a non-target shRNA control (ShNT) and specific shRNA against Prx4 were used for knockdown experiments as previously published [138]. p3xFlag-CMV Prx4 construct was used for overexpression. All plasmid constructs were confirmed by DNA sequencing. Lentiviral particles expressing shRNAs or Prx4-Flag were produced in HEK293T cells using the provider's plasmid packaging system and PolyJet Transfection reagent (SignaGen, Rockville, MD, cat. no. SL100688) following suggested transfection and virus production procedures. To establish stable knockdown or overexpression, HCT116, RKO and HT29 cells were infected with lentiviral particles. Cells were maintained in puromycin (Gibco) 1 μg/mL containing medium to establish stable cells. MISSION esiRNA targeting

human DKK1 (Sigma-Aldrich, cat no. EHU035311) were used for transient DKK1 knockdown at 400 ng/mL for 48 hours. esiRNA are small interfering RNA prepare using endoribonuclease. They are a heterogeneous mixture of siRNA that all target the same mRNA sequence. MISSION siRNA Universal Negative Control #1 was used as negative control at 400 ng/mL (Sigma-Aldrich, cat no. SIC001).

pGKWnt3a plasmids were transfected into HEK293T cells using Lipofectamine 3000 (Invitrogen cat no. L3000001) per manufacturer's protocol. Medium was changed after 12 hours to prevent toxicity. 48 hours later, conditioned medium was collected, centrifuged at 1000×g for 10 min, supernatant was collected and sterile filtered, and added to HCT116 cells at increasing concentrations.

2.2 Bioinformatics Analysis

Bioinformatics analysis was carried out using Genomic Data Commons Data Portal at National Cancer Institute (https://portal.gdc.cancer.gov/) and the University of Alabama at Birmingham Cancer (UALCAN) data analysis portal (http://ualcan.path.uab.edu/index.html) (12). These platforms use multiple sources of datasets from The Cancer Genome Atlas (TCGA) or published literature that contain data of DNA/RNA sequencing and microarray results from variety of patient specimens.

2.3 Quantitative Real Time PCR (qRT-PCR)

Total RNA was isolated from colon cancer cell lines HCT116, RKO and HT29 using RNeasy Mini kit (Qiagen, cat no. 74104). cDNA synthesis was performed using Superscript III Reverse Transcriptase kit (Invitrogen cat no. 18080044). Equal volume of cDNA was placed into 96 well plate with SYBR Green Master Mix (ThermoFisher, cat no. A25741) and following DKK1 and GAPDH primers. Each reaction was repeated in four

replicates and performed using LC480 (Roche, Basel, Switzerland). All values were averaged and normalized to the level of GAPDH.

DKK1-F: CCTTGAACTCGGTTCTCAATTCC
DKK1-R: CAATGGTCTGGTACTTATTCCCG
GAPDH-F: CAACGAATTTGGCTACAGCA
GAPDH-R: AGGGGTCTACATGGCAACTG.

2.4 Cell Proliferation, Adhesion and Migration Assays

For cell proliferation assay, cells were seeded in 96-well plates at 1000 cells/well. Cell number was measured using Cell Counting Kit- 8 (CCK-8) following the manufacturer's protocol (APExBIO, Boston, MA, cat no. K1018). Briefly, 10 μL of CCK-8 solution was added to each 100 μL medium containing well, placed in incubator for 2 hours and absorbance measured at 450nm in a multiplate reader (GloMax-Multi Detection System, Promega). For cell adhesion assay, 10,000 serum-starved cells were seeded onto fibronectin-coated wells (10 μg/mL) and allowed to adhere for 20 min. Medium was removed, cells were washed once with PBS gently and fresh medium was added. Cells were allowed to recover for 6 hours and the number of viable cells was counted using CellTiter-Glo (Promega cat no. G7570). Cell migration was measured using wound-healing assay and cell-movement tracking analysis. For wound healing, cells were seeded in 6 well plate and allowed to reach confluence. A scratch was made using p200 pipet tips. Cells were washed twice with phosphate-buffered saline (PBS) before culture medium was added. Photographs of cells were taken at indicated time points using Cytation5 (BioTek, Winooski, VT). ImageJ software was used to quantify the decrease in wound area. For cell-movement tracking, cells were seeded in collagen-coated chamber slides. After 24 hours,

time-lapse video was captured using Cytation5 at 3 frames per second for 10 hours. The movement of cells was quantified using Cell Tracker software as described previously.

2.5 Cell Invasion Assay and Invadopodia Formation Assay

Transwell Matrigel invasion assay was performed to measure cell invasion. Cells were trypsinized, resuspended in serum-free medium at 106/mL and added to upper chamber coated with 200 μg/mL Matrigel. 10% serum containing medium was added to the lower chamber as chemoattractant. Cells were allowed to invade for 48 hours. Cells were stained with 0.05% crystal violet solution. Cells on the upper side of the membrane were removed using cotton swabs. Invaded cells on the lower side of the membrane were imaged and quantified using ImageJ software. 3D invasion assay was performed following the manufacturer's protocol (Cultrex 3-D Spheroid Basement Membrane Extract Cell Invasion Assay, R&D Systems, cat no. 3500-096-K). Briefly, cells cultured to 80% confluence were resuspended in spheroid formation ECM and 50 μL of cell suspension was added per well in 96 well plate. After incubation in 37°C for 72 hours, 50 μL invasion matrix was added to each well. 100 μL cell culture medium containing 20% FBS + 10 μg/mL 12-O-tetradecanoylphorbol-13-acetate (TPA) were added. Pictures of spheroids were taken using Cytation5 for 3 days. For invadopodia formation assay, cells were seeded onto matrix containing gelatin and cultured for 24 hours in chamber slide, fixed with 3.7% paraformaldehyde and washed with PBS two times. Cells were permeabilized with 0.5% Triton-X-100 for 10 minutes, blocked with 5% normal goat serum blocking buffer for 1 hour, and incubated in Phalloidin-FITC (1:100, Invitrogen, cat no. F432) and Cortactin-Alexa Fluor 647 (1:100, Sigma-Aldrich, cat no. 05-180-AF647) primary antibodies at 1:100 for 1 hour each at room temperature. Cells were washed before mounting with

ProLong Gold Antifade mountant with DAPI (Invitrogen, cat no. P36935). Images were captured using confocal microscope (Nikon).

2.6 Mouse Genotyping

All schemes of mouse breeding and experimental protocols have been reviewed and approved by the University of Kentucky Institutional Animal Care and Use Committee (UK protocol 2016-2306). All procedures on mice were conducted following the Policy on Humane Care and Use of Laboratory Animals, and Guidelines of the Animal Care and Laboratory Animal Welfare (NIH). Mice, regardless of strain or genetic background, were all housed in standard cages in temperature-controlled environments under a 12-hour light/ 12-hour dark cycle with ad libitum access to standard chow (Teklad, Envigo, Indianapolis, IN, cat no. 2918) and water unless otherwise indicated. Original Srx-/- mice in C57BL/6 background was established by Planson et al. [225], and Prx4-/- mice in C57BL/6 background was established by Iuchi et al. [68]. Srx-/- or Prx4-/- mice in pure FVB/N background was further established by cross breeding with FVB/N mice for > 10 generations, and Srx-/- FVB/N mice were also used in the previous study [226].

For genotyping, genomic DNA was extracted from tail clips using genomic DNeasy Blood and Tissue Kit (Qiagen, Valencia, CA, cat no. 69504). Briefly, about 1 mm tip of mouse tail was lysed using tissue lysis buffer and proteinase K at 56C overnight. After adding ethanol, the mixture was loaded into a spin column, washed twice and DNA was eluted with nuclease free water. PCR-based genotyping was performed as reported previously (12). The following primers were used at 10 μM each to amplify 1 μL target DNA using OneTaq 2X Master Mix (NEB, cat no. M0482): Prx4 Wt-Forward 5′-GAAATATCC TGGACATATGCTTTAAGA-3′; Wt-Reverse, 5′-

AAGATCCCCTGGAACAGAAGTT A-3′; Prx4KO-Forward, 5′-ACTTCCGTTCCATGTTGAGC-3′; Prx4KO-Reverse, 5′-ACAAACAAACCCAACCCTGA-3’; Srx Wt forward 5’-GCCATTTCT CTGTCAGAA ATACTCT-3’; Srx Wt- Reverse 5’- GAGAACATATCCCATCTACAGCTTC- 3’. DNA was denatured at 95°C for 5 min, followed by 30 cycles of 95°C for 40 s, 58°C for 30 s, 72°C for 50s and a final extension at 72°C for 2 min. The PCR product was loaded into 1% agarose gel with 6X gel loading dye and SYBR green and visualized using UV imager.

2.7 AOM/DSS Protocol, Tumor Measurement and Histopathology Examination

The AOM/DSS protocol was performed as previously reported [227]. Briefly, mice at 8-week age, including Wild-type (Wt) (n=12), Prx4 null (n=14) and Srx null (n=17) were injected intraperitoneally with 10 mg/kg of AOM (azoxymethane, Sigma-Aldrich, cat no. A5486). DSS (Dextran sulfate sodium, Sigma-Aldrich, cat. no. D8906) was diluted to a concentration of 2% in autoclaved drinking water on the day of administration and supplied to mice 1 week and 8 weeks after AOM injection. At the 20th week after treatment, mice were humanely euthanized. Blood was collected in heparin-coated tubes, immediately centrifuged at 2000 g for 10 minutes at 4°C and isolated plasma was stored in -80°C. Mouse colon from the start of ascending to the anus were extracted and cleaned with phosphate-buffered saline. Tumor mass located within 1 cm of anus was counted as rectal tumors and all others were counted as colon tumors. Tumor numbers were recorded and dimensions were measured using a digital caliper. Tumor volume was calculated using the commonly accepted equation Volume = (length × width^2)/2 [228]. Tumor burden was obtained using the equation Burden = (tumor area/total colon area) where area equals the product of the length and the width [229]. After counting, samples of tumors were cut longitudinally to

be stored by snap-frozen in -80°C, or fixed in 4% paraformaldehyde and stored in 70% ethanol before proceeding with standard paraffin embedding, sectioning and H&E staining. For histology and pathology assessment, serial sections of tumors from each genotype were obtained. The first of the sequential slides was stained with hematoxylin and eosin (H&E) and examined by the board-certified gastrointestinal pathologist to determine tumor histopathology. For DSS only protocol, three groups of mice at 8-week age, including Wt (n=6) and Prx4 null (n=6) were administered normal water or 2% DSS in autoclaved drinking water for 7 days, humanely euthanized and samples were collected and processed as described above.

2.8 Immunohistochemistry and Immunofluorescence

Human tissue microarray slides CO1005a and CO246 with diagnosis and pathology information were commercially obtained (US Biomax, Rockville, MD). Immunohistochemistry (IHC) was performed using the Vectastain ABC-HRP Kit (Vector Laboratories, Burlingame, CA, cat no. PK-6101, PK-6102) and 3,3'- diaminobenzidine (DAB) substrate Kit (Vector Laboratories, cat no. SK-4100). Paraffin was first removed from tissue slides with two washes of xylene and sections were immersed in decreasing concentrations of ethanol. Antigen retrieval was performed using Citrate Buffer pH 6.0 (Sigma, cat no. C9999). Slides were incubated in freshly prepared 3% hydrogen peroxide-methanol solution for 10 min to block endogenous peroxidase activity. Tissues were blocked with normal animal serum for 1 hour and incubated with primary antibodies for 2 hours at room temperature in a humidity chamber. Antibodies used were Prx4 1:500 (Abcam cat no. 184167), Ki67 1:40 (Abcam, cat no. 16667), 8-oxoG 1:100 (Santa Cruz, cat no. 130914), F4/80 1:40 (Cell Signaling, cat no. 70076S), CD86 1:100 (Santa Cruz, cat

no. 28347), CD163 1:50 (Santa Cruz, cat no. 33715), CD138 1:100 (Santa Cruz, cat no. 12765), CD8 1:50 (Santa Cruz, cat no. 1177), CD4 1:100 (Cell Signaling, cat no. 90176T), CD19 1:100 (Cell Signaling, cat no. 25229T), PD-L1 1:100 (Cell Signaling, cat no. 13684S), PD-1 1:25 (Cell Signaling, cat no. 84651T). Samples were immersed in biotinylated secondary antibody for 1 hour and avidin-biotinylated enzyme solution for 30 min. DAB was used as chromogen and hematoxylin was used for counterstaining. Images of slides were taken using Aperio ScanScope XT (Vista, CA). Staining analysis was performed using HALO software (Indica Labs, Albuquerque, NM). For immunofluorescence staining, slides were de-paraffinized and antigen retrieval was performed as described above. Tissues were co-stained for markers of inflammatory cells and Prx4 sequentially. Primary antibodies used were CD86 1:100 (Santa Cruz), CD163 1:50 (Santa Cruz), CD138 1:100 (Santa Cruz) and Prx4 1:500 (Abcam). Fluorophore-conjugated secondary antibodies used were Alexa Fluor 488 and Alexa Fluor 594 (Invitrogen, cat no. A11005, A11017). Tissue slides were mounted with ProLong Gold Antifade mountant with DAPI (Invitrogen, cat no. P36935). Images were captured using Cytation5 (BioTek, Winooski, VT).

2.9 *In Situ* Apoptosis Assay

Mouse colon apoptosis assay was performed using terminal deoxynucleotidyl transferase-mediated dUTP nick end labelling (TUNEL) assay. The TACS2TdT-DAB in situ apoptosis detection kit was commercially obtained and assay was performed per manufacturer instructions (R&D Systems, Minneapolis, MN, cat no. 4810-30-K). Briefly, de-paraffinization and antigen retrieval were performed as described above. Tissues were incubated in Proteinase K for 30 min at room temperature followed by treatment with 3%

hydrogen peroxide for 5 min. Tissues were covered with labelling reaction mix for 1 hour at 37°C, streptavidin-HRP solution for 10 min and immersed in DAB. Samples were then counterstained with hematoxylin, dehydrated and mounted before visualization and analysis.

2.10 Tumor Lipid Peroxidation Measurement

Tumors isolated from mice colon were snap-frozen and embedded in the optimal cutting temperature medium (Sakura, Torrance, CA, cat no. 4583). Cryosectioning was performed to obtain sections 5 μm in thickness (Leica Biosystems, Wetzlar, Germany, CM1860). Sections were stained with 2 μM C11 BODIPY 581/591 at 37°C for 20 min (Invitrogen, cat no. D3861). Sections were fixed with paraformaldehyde for 10 minutes before mounting with ProLong Gold Antifade mountant with DAPI (Invitrogen). Images were taken using Cytation5 (BioTek).

2.11 Proteome Profiler Mouse Cytokine Array and Mouse Chemokine Array

The antibody-based array kits, which are capable of simultaneously measuring the levels of 25 chemokines and 111 cytokines in duplicates on the same membrane was commercially obtained (R&D Systems, cat no. ARY020, ARY028). The membranes were first blocked for 1 hour at room temperature. 33.3 μl of plasma from 3 mice in each group were mixed. Membranes were incubated in diluted 100 μL plasma sample and detection antibody overnight at 4°C. Streptavidin-HRP solution was applied for 30 min at room temperature and signal was detected using Amersham ECL Select Western Blotting Detection Reagent. Amersham Imager 680 was used to visualize the spots. The intensity of each spot representing the individual cytokine and chemokine was determined using

ImageJ software. The relative spot intensity was obtained by normalizing with the intensity of the internal positive control on each membrane.

2.12 Western Blot

Fresh colon tumors or tissues collected from Wt, $Prx4^{-/-}$ and $Srx^{-/-}Prx4^{-/-}$ mice or human colon cancer cells were lysed using radioimmunoprecipitation (RIPA) lysis buffer system (Santa Cruz, cat no. sc-24948). Western blot was performed using a standard protocol. Briefly, proteins were electrophoresed on SurePage gel (GenScript, Piscataway, NJ, cat no. M00654) and transferred to polyvinylidene difluoride membrane. Membranes were blocked for 1 hour in 5% non-fat dry milk in tris-buffered solution (TBS), using TBS, incubated in primary antibody overnight at 4°C, washed and incubated in horseradish peroxidase-conjugated secondary antibody for 1 hour. After final wash, signal was detected using Amersham ECL Select Western Blotting Detection Reagent (Cytiva, Marlborough, MA, cat no. RPN2235) and visualized by Amersham Imager 680 (GE Healthcare). Primary antibodies used were: Prx4 1:10,000 (Abcam, Cambridge, UK, cat no. 184167), Srx 1:1000 (Proteintech, Rosemont, IL, cat no. 14273-1-AP), β-actin 1:5000 (Sigma-Aldrich, St Louis, MO, cat no. A2228), DKK1 1:5000 (Proteintech, Rosemont, IL, cat no. 21112-1-AP), β-catenin 1:2500 (BD Transduction lab, San Jose, CA, cat no. 610153), BSA 1:4000 (Santa Cruz Biotechnology, Dallas, TX, cat no. sc-32816), LRP6 1:2000 (ABclonal Technology, Wuhan, China, cat no. A13325), phospho-LRP6 (Ser1490) 1:1000 (Cell Signaling Technology, Danvers, MA, cat no. 2568), p65 1:1000 (Cell Signaling Technology, cat no. 8242), phospho-p65 (Ser536) 1:1000 (Cell Signaling Technology, cat no. 3033), Focal adhesion Kinase 1:1000 (ABclonal Technology, cat no. A0024) and phospho-FAK (Tyr397) 1:500 (ABclonal Technology, cat no. AP0302).

2.13 Orthotopic Implantation Model

Orthotopic implantation in severe combined immunodeficiency (SCID) mice was performed as described previously [230]. Briefly, HCT116 shNT and shPrx4 cells were trypsinized and resuspended at 10^6 / 50 μL PBS and 50 μL was implanted into cecum of NOD.Cg-Prkdcscid Il2rgtm1Wjl/SzJ mice (Jackson Laboratory) under anesthesia. Four weeks after injection, mice were humanely euthanized and cecum, liver and lungs were extracted. Mouse tissues were fixed in 4% paraformaldehyde, washed in PBS and stored in 70% ethanol before proceeding with standard paraffin embedding, sectioning and H&E staining. The protocol for mouse experiment was reviewed and approved by the Institutional Animal Care and Use Committee (IACUC) of University of Kentucky. All animal procedures were conducted following the Policy on Humane Care and Use of Laboratory Animals, and Guidelines of the Animal Care and Laboratory Animal Welfare (NIH). Mice were housed in specific pathogen-free conditions in temperature-controlled environments under a 12-hour light/ 12-hour dark cycle with ad libitum access to food and water.

2.14 RNA Sequencing and Related Analysis

Total RNA was isolated from three 100 mm dishes each of HCT116 shNT and shPrx4 cell lines (RNeasy mini kit, Qiagen). mRNA sequencing was done using DNBSEQ platform (BGI Yantian District, Shenzhen, China). Differentially expressed genes were identified by Partek Flow GSA algorithm (Partek, St. Louis, MO). mRNA expression data was subsequently analyzed using Gene Set Enrichment Analysis software (version 4.2.2) at 1000 permutations of gene sets to identify pathways differentially enriched in shPrx4

cells. Leading edge analysis of gene sets enriched in shPrx4 cells with nominal p-value less than 0.1 was performed.

2.15 Statistical Analysis

Quantitative data are presented as means ± standard deviation (SD). Data were analyzed with Student's t-test (unless otherwise indicated) using GraphPad Prism 9. For calculation of the p value, parameters of two-tailed, 95% confidence interval were used for all analyses. A p value of less than 0.05 is considered statistically significant.

CHAPTER 3. PEROXIREDOXIN IV PROMOTES AZOXYMETHANE/DEXTRAN SULFATE SODIUM INDUCED COLORECTAL CANCER FORMATION

3.1 Introduction

Colorectal cancer (CRC) is the third most common cancer and the third leading cause of cancer deaths in the US and worldwide [231]. Risks for CRC development in human include chronic inflammation (such as ulcerative colitis and Crohn's disease), hereditary disorders (such as familial adenomatous polyposis and Lynch syndrome), as well as lifestyle related factors (such as obesity, alcohol and tobacco usages). While progress has been made in the early detection of CRC in human, a significant amount of work remains to be done to improve the long-term survival rate of patients. In fact, there is an increasing incidence of CRC in young adults below the age of 50 while mortality in elders remains high [232]. Further understanding of the pathogenesis of CRC and development of more effective therapeutic strategies are in urgent need.

Among all mechanisms of cancer development, oxidative stress has been widely recognized as one of the major cellular cues that contribute intrinsically to occurrence of cell transformation, tumorigenesis, promotion and progression to malignancy. High levels of reactive oxygen species (ROS) and reactive nitrogen species (RNS) causes damages to DNA, lipids as well as proteins by altering their structure and/or changing of their biological function [233]. Therefore, cells have evolutionarily developed various mechanisms of defense including expression of intracellular antioxidants to scavenge reactive species. Among them, Peroxiredoxin IV (Prx4) is a member of the family of peroxidase that contains active thiol group to reduce hydrogen peroxide, alkyl hydroperoxide and peroxynitrite with high levels of selectivity and sensitivity [30, 51]. Within the cell, Prx4 is found primarily in the endoplasmic reticulum (ER) where its

peroxidase activity is essential for the maintenance of cellular redox balance and homeostasis. It also protects cells from ER stress which involves a process of oxidative protein folding through exchanging disulphide bond with members of the protein disulphide isomerase family [234]. Under normal physiological condition, the oxidation-reduction cycles of Prx4 and its substrate are accomplished through the coordination of thioredoxin, glutathione and thioredoxin reductase. Upon oxidative stress conditions, excessive ROS cause the hyperoxidation of the catalytic cysteine of Prxs, leading to the loss of enzymatic activity and even apoptotic cell death in normal cells [49]. However, cancer cells can survive oxidative stress through the upregulation of Prxs and/or expression of another redox enzyme, Sulfiredoxin (Srx), which is exclusively dedicated to revitalize hyperoxidized two-Cysteine Prxs through an ATP-dependent oxidation-reduction cycle [235, 236].

In our previous series of studies, we found that Srx preferentially interacts with Prx4 due to its intrinsically higher binding affinity, and the Srx-Prx4 axis contributes to the activation of oncogenic signaling pathways in different types of human cancer [138, 139, 235]. Unlike the ubiquitously expressed Prxs in normal tissues, Srx is not expressed in normal or cancer adjacent normal colon tissues but is highly abundant in colorectal carcinomas. In mice, depletion of Srx does not generate any detrimental effect since Srx knockout ($Srx^{-/-}$) mice are viable and have no defects in early development or adult life under laboratory conditions [225]. Interestingly, our previous studies show that $Srx^{-/-}$ mice are more resistant to tumorigenesis in either skin or colon carcinogenesis model induced by a complete protocol of carcinogen plus tumor promoter, i.e., 7,12-dimethylbenz[α]anthracene/12-O-tetradecanoylphorbol-13-acetate (DMBA/TPA) and

azoxymethane/dextran sulfate sodium (AOM/DSS), respectively [226, 237]. Therefore, the next series of logical questions to ask are whether such effects of Srx are dependent on the presence of Prx4. To answer these questions, we established strains of Prx4 knockout ($Prx4^{-/-}$) and $Srx^{-/-}Prx4^{-/-}$ double knockout mice, and these mice were subjected to AOM/DSS protocol to induce colorectal tumors. We found that $Prx4^{-/-}$ mice developed fewer and smaller tumors than wildtype littermates. There was no significant different between wildtype and double knockout group. Series of strategies including pathohistological, immunochemical, and serological methods were used to determine how the loss of Prx4 affects the development of colorectal tumors in this model. Our mechanistic understanding of the Srx-Prx4 axis in tumorigenesis may provide novel insights to develop effective strategies for the prevention and treatment of colorectal cancer in patients.

3.2 Results

3.2.1 Establishment of Prx4 knockout and Srx-Prx4 double knockout mice in FVB/N background

The susceptibility of mice to carcinogen-induced tumorigenesis varies due to difference in genetic background [238]. Prx4 whole-body knockout mice was originally established in C57BL/6N background by deletion of exon 1 [68]. Targeting vector was constructed using *Prx4* genomic DNA cloned from b129/SVJ mouse genomic library, neomycin cassette flanked by loxP sequences were inserted in intron 1, an additional loxP sequence was inserted upstream of exon 1 and the vector was transfected into embryonic stem cells. Following homologous recombination, embryonic stem cells were injected into blastocysts. Sperm collected from the resulting male mice was injected into unfertilized

eggs and implanted into uterus of pseudopregnant C57BL/6 female mice. The resulting *Prx4*$^{flox/+}$ female mice were mated with male cre transgenic mice to generate *Prx4*$^{-/y}$ male or *Prx4*$^{+/-}$ female mice [68]. Similar to the normal phenotype of Srx whole-body knockout, loss of Prx4 in mice also does not cause any defects in both embryo development and adult life under laboratory conditions [225]. Examination of proteins from colon tissues of wildtype and Prx4 knockout mice by immunoblotting showed that the protein expression of antioxidants SOD1, SOD2, GPx1, GPx2 and Catalase were comparable between the groups [97]. In addition, the expression of other members of the Prx family also remained unchanged [97]. To minimize the complexity of data interpretation due to genetic variations in different mouse strains, we established Prx4 Prx$^{-/-}$ in FVB/N background. Prx4$^{-/-}$ were bred with Srx$^{-/-}$ mice to generate Srx-Prx4 double knockout mice. All knockout mice have been cross bred with pure inbred, FVB/N wildtype for multiple generations (≥ 10) at the same breeding facility under the same feeding, drinking and resting scheme. Regardless of strain background, we found that all Prx4 knockout mice are completely normal and fertile under laboratory conditions. The genomic loss of exons in Prx4 and Srx was verified by genotyping using PCR with the combination of target-specific primers (Figure 3.1A). Using previously validated anti-Prx4 and IHC staining method [131, 235], we examined the expression of Srx and Prx4 in mouse intestinal tract. We found that Prx4 positive staining is ubiquitously present in the mucosa, submucosa and muscularis layers of mouse colon (Figure 3.1B). In particular, strong positive staining is mainly found in epithelial cells of the crypt in mouse colon (Figure 3.1B). In contrast, the staining of Srx is very weak in all tissue layers of wild-type mouse colon, and the only weakly positive staining is found in microvilli, which is most likely due to non-specific binding of the

antibody as similar pattern of staining was also found in knockouts (see Figure 3.1B). Moreover, we examined the presence of Prx4 protein in the intestinal tract of wildtype mice by Western blotting. We found that Prx4 is present in the whole extracts of jejunum, colon and rectum (Figure 3.1C). From these experiments, we found that Prx4 is ubiquitously present in the intestinal tract of wildtype mice and knockout of exon 1 leads to the absence of Prx4 in $Prx4^{-/-}$ mice.

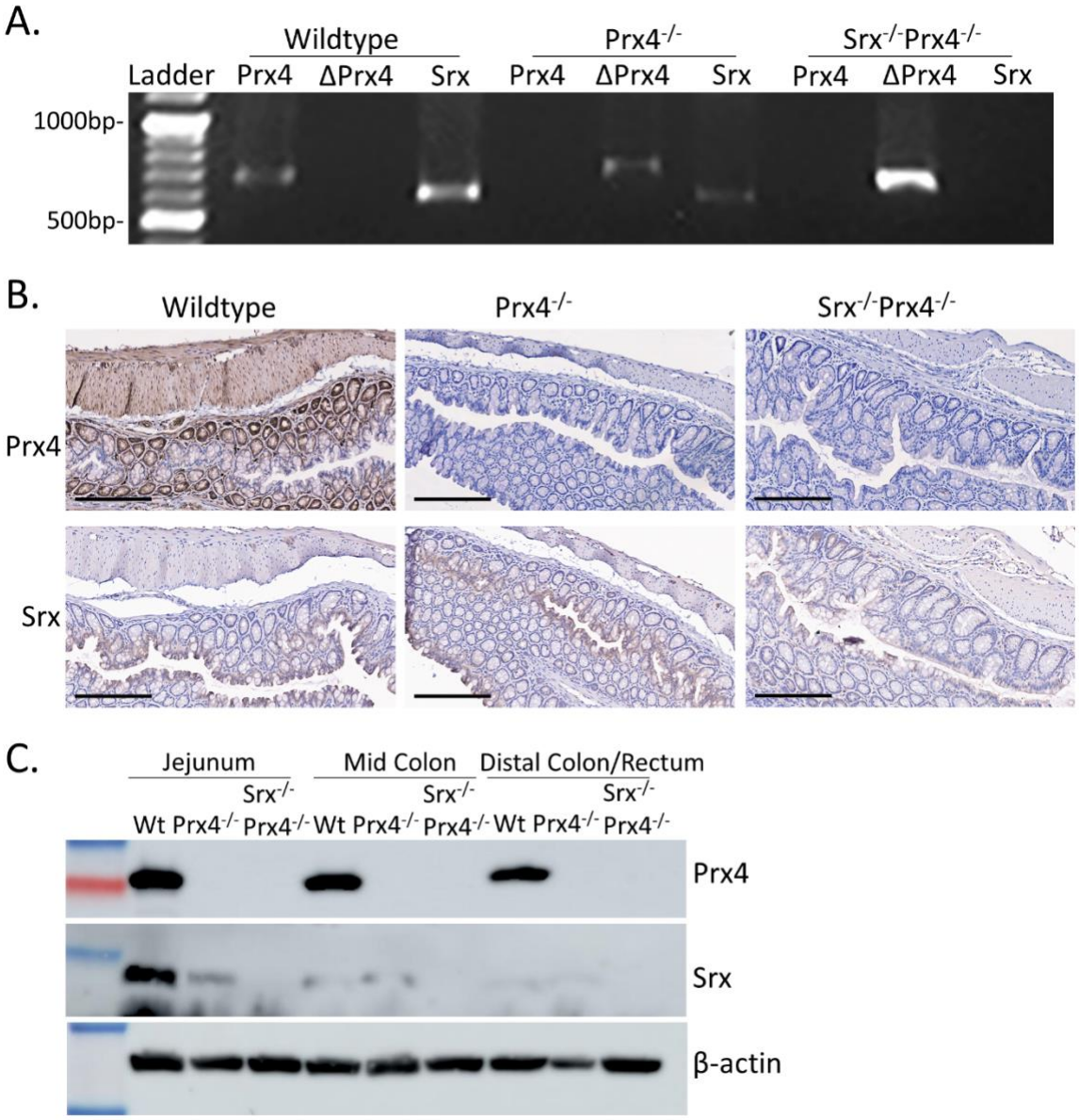

Figure 3.1. Genotyping of Prx4 null (Prx4-/-) and Srx-Prx4 null (Srx-/- Prx4-/-) FVB mice.

(A) Genotyping was performed using a PCR-based amplification of Prx4 exon 1 sequence in genomic DNA of mouse tail. (B) Immunohistochemistry (IHC) detection of Prx4 (upper panel) and Srx (lower panel) in wildtype, Prx4 knockout and Srx-Prx4 knockout mouse colon. Bar = 200 μm. (C) Immunoblotting of Prx4 and Srx in wildtype, Prx4 knockout and SrxPrx4 knockout mice tissues jejunum, mid colon and distal colon/rectum.

3.2.2 Gross tumor analysis reveals that $Prx4^{-/-}$ and $Srx^{-/-}Prx4^{-/-}$ mice are resistant to AOM/DSS-induced colorectal tumorigenesis.

To study the role of Prx4 in the development of colorectal tumor in vivo, we used a well-established AOM/DSS protocol to induce colitis-associated tumorigenesis in wildtype and knockout mice (Figure 3.2A). A total of 43 mice, including 12 wildtype (4 male and 8 female), 14 Prx4 knockout (5 male and 9 female) and 17 Srx-Prx4 double knockout mice (10 male and 7 female) were used in this study. All mice were initiated with a single dose of AOM through intraperitoneal injection and followed by two rounds of administration of DSS in drinking water, and euthanized 20-weeks after AOM injection. Visual examinations reveal that all colons extracted from wildtype mice have multiple, large tumors that are often aggregated to form big mass in the middle colon, and the rectum is also obviously enlarged with tumors (representative image shown in Figure 3.2B, whole images in Figure 3.3). In contrast, colons extracted from $Prx4^{-/-}$ and $Srx^{-/-}Prx4^{-/-}$ mice bear fewer tumors with smaller size in the middle colon, and much reduced size or absence of rectal tumors (representative images shown in Figure 3.2B, Figure 3.3). We counted the number and measured the size of all tumors formed both in the middle colon and the rectum, and all data were quantitatively analyzed and compared for statistical significance between groups. Compared with wildtype, mice with $Prx4^{-/-}$ and $Srx^{-/-}Prx4^{-/-}$ show significantly lower rates in colon tumor incidence (Figure 3.2C), multiplicity (Figure 3.2D), volume (Figure 3.2E) and burden (Figure 3.2F). Similar findings are also obtained when the incidence, multiplicity, volume and burdens of rectal tumors were compared between wildtype and knockout, double knockout mice (Figure 3.2G–J). This data indicates that loss of Prx4 alone is sufficient to cause resistance to AOM/DSS-induced colorectal tumorigenesis.

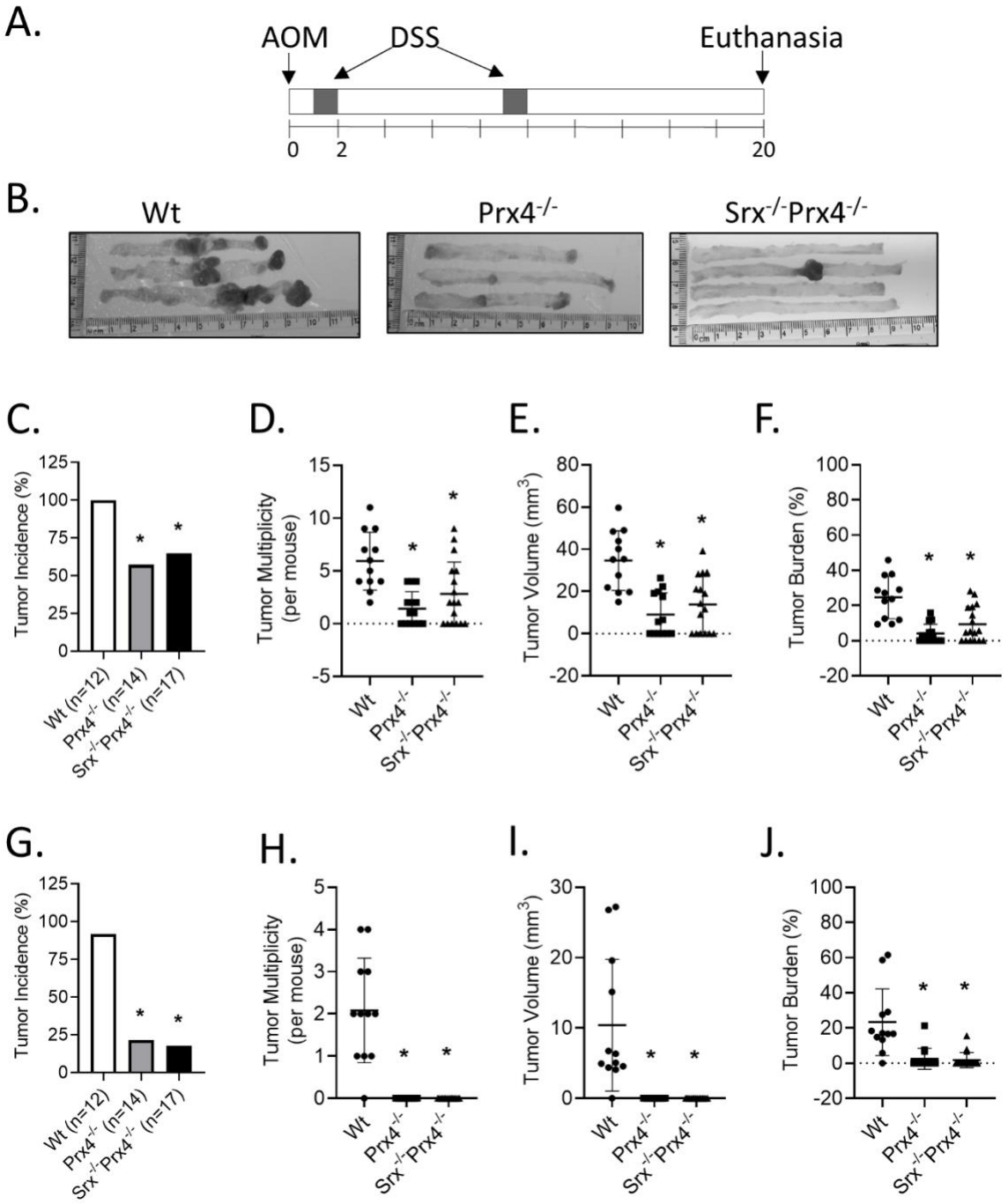

Figure 3.2 Prx4 knockout and SrxPrx4 knockout mice are resistant to AOM/DSS-induced carcinogenesis.

(A) Schematic presentation of the AOM/DSS protocol. (B) Representative gross images of extracted colons. The average in Wt, Prx4 KO and SrxPrx4 KO mice of mid colon tumors. (C-F) incidence, multiplicity, volume and tumor burden percent and of distal colon rectum tumors (G-J) incidence, multiplicity, volume and tumor burden percent respectively. Compared with Wt group, *$p<0.05$ (one way ANOVA).

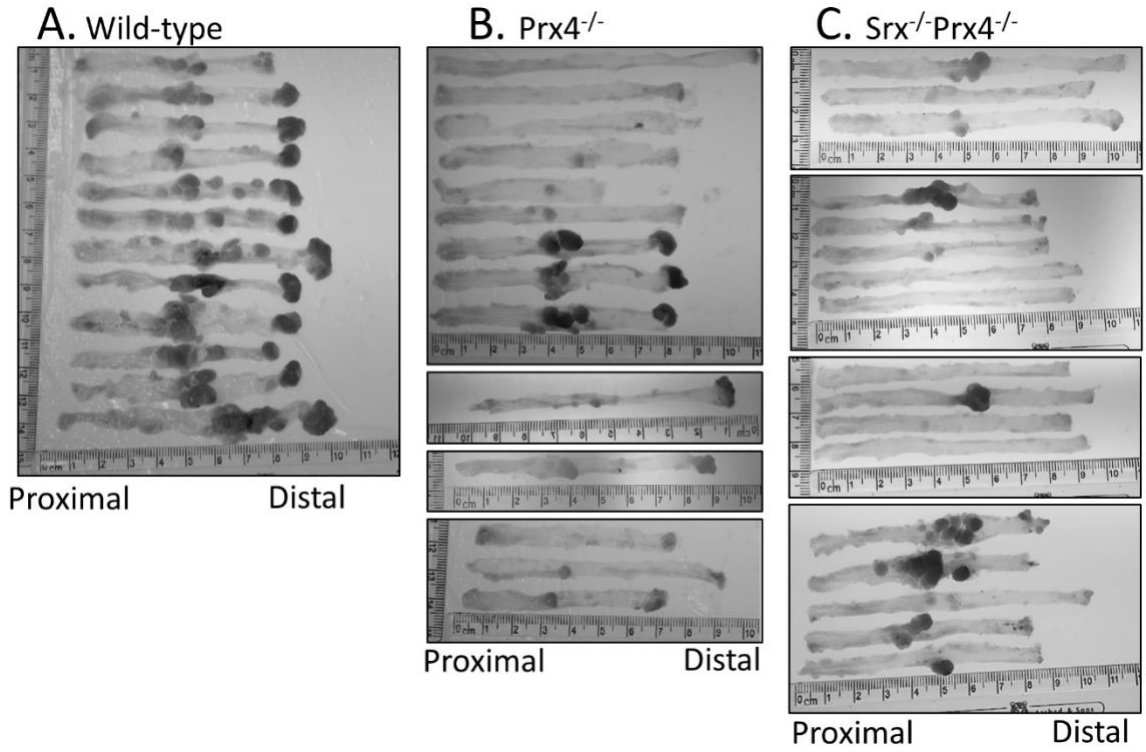

Figure 3.3 Gross images of colons extracted from AOM/DSS treated mice.
(A) Wildtype, (B) Prx4 knockout and (C) Srx-Prx4 knockout.

3.2.3 Prx4 is highly expressed in AOM/DSS-induced colon tumors as well as infiltrated macrophages and plasma cells in wildtype mice.

To understand why the loss of Prx4 leads to resistance against colon tumorigenesis, we performed hematoxylin and eosin (H&E) staining and immunohistochemical examination of colon tumors extracted from wildtype and Prx4 null mice. H&E staining shows that wildtype tumors present as poorly differentiated with disrupted aberrant crypts and abundant infiltration of inflammatory cells, while Prx4 null tumors characterize as more differentiated crypts surrounded with fewer inflammatory cells (Figure 3.4A). The levels of Prx4 in wildtype tumors are also significantly increased compared to normal colon (Figures 3.4B compared to 3.1B). In the IHC staining of Prx4 in wildtype tumors, we noticed that not only tumor cells but also some stromal cells in the tumor microenvironment

had strong staining for Prx4 (Figure 3.4B). Bioinformatics analysis of RNA-sequencing data using Gene Immunological Genome Project database suggested that macrophages and plasma cells have high expression levels of Prx4 (Figure 3.5) [239]. To confirm this in tumors, we performed double immunofluorescence staining for Prx4 plus markers of these cell types in tumors from wildtype mice. Macrophages can undergo a spectrum of activation states in response to different stimuli and are generally divided into two categories: M1-like macrophages that are involved in pro-inflammatory response, and M2-like macrophages that are involved in anti-inflammatory responses. In the context of tumor microenvironment, M1 macrophages are considered anti-tumorigenic while M2 macrophages are considered immunosuppressive and pro-tumorigenic [240]. We used antibodies against CD86 as a specific marker for M1 macrophages (Figure 3.4C) and against CD163 as a specific marker for M2 macrophages (Figure 3.4D). Tumor infiltrating B lymphocytes play important role in tumor malignancy and immunity as reported through either their pro-tumorigenic or anti-tumorigenic capabilities. [241]. Plasma cells are terminally differentiated mature B lymphocytes. We used antibodies against CD138 as a marker for plasma cells (Figure 3.4E). The inflammatory cell markers CD86, CD163 and CD138 were stained with green fluorescence while Prx4 was stained with red fluorescence in wildtype tumor (Figure 3.4C–E). We found that such co-staining frequently merged into yellow fluorescence, confirming that Prx4 is expressed in subsets of macrophages and plasma cells (Figure 3.4C–E). Together, this data suggests that Prx4 is highly expressed in tumor cells as well as tumor-infiltrating macrophages and plasma cells.

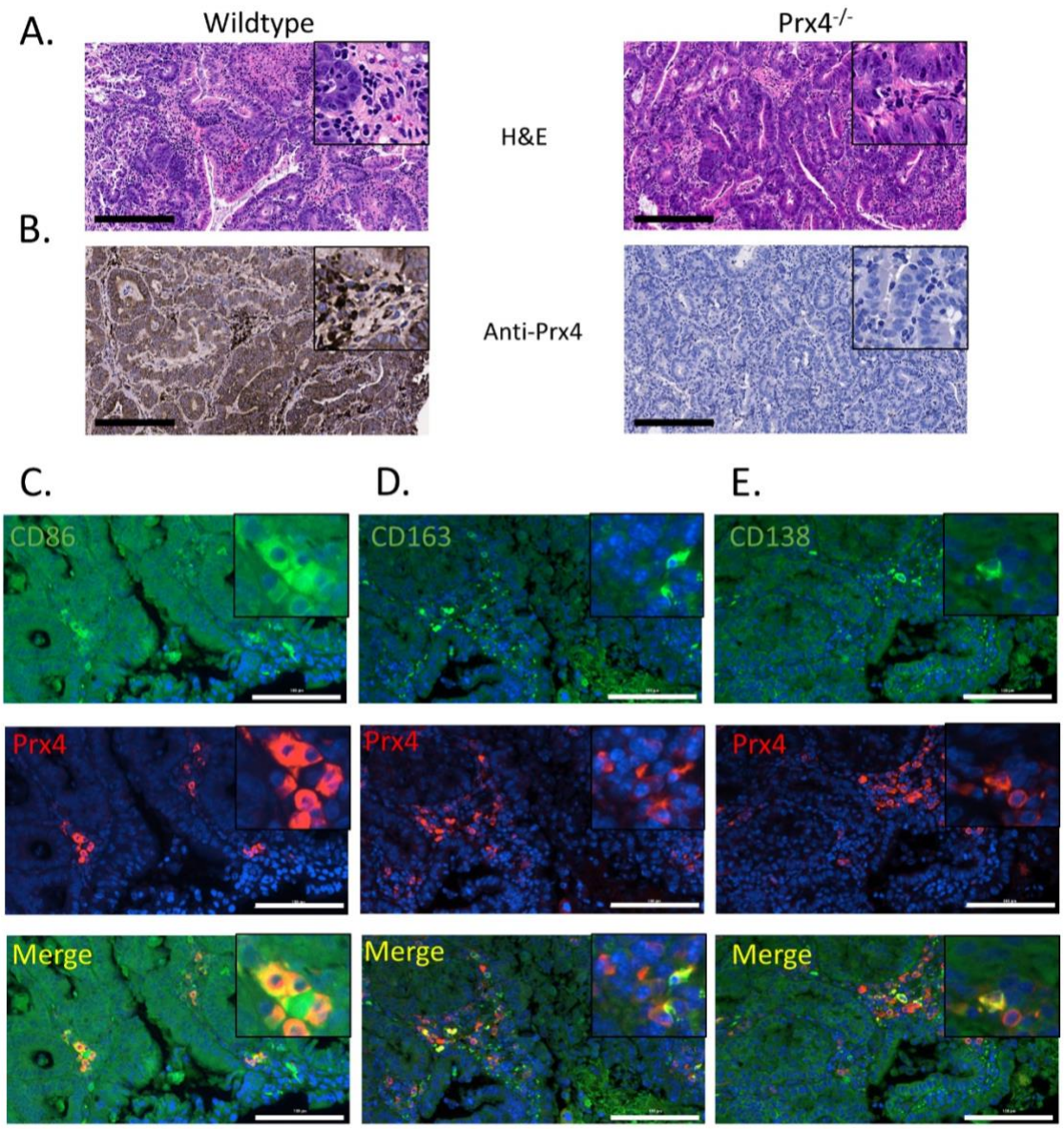

Figure 3.4 Prx4 is expressed in tumor-infiltrating immune cells.

(A) Representative H&E staining of AOM/DSS-induced tumors extracted from Wt and Prx4-/- mouse. (B) Representative IHC staining of Prx4 in Wt tumor shows high expression of Prx4 in tumor cells as well as stromal cells, while Prx4 is not expressed in tumors from Prx4-/- mice. Bar = 200 μm. Double immunofluorescence staining of Prx4 with (C) M1 macrophage marker CD86, (D) M2 macrophage marker CD163 and (E) plasma cell marker CD138 in Wt tumors. Framed inserts indicate higher magnification. Bar = 100 μm.

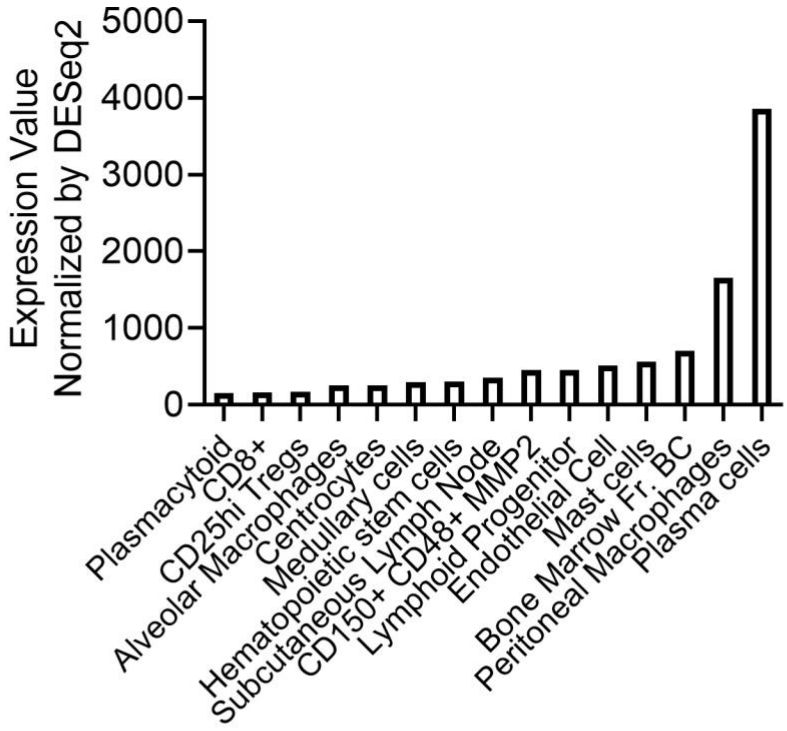

Population Full Name	Population Sorting Description
Splenic Plasmacytoid	sorted on CD45lo CD11b+
Spleenic CD8+	sorted on CD45+ MHCII+ CD11c+ CD8+ CD4-
Splenic CD25hi Tregs	sorted on CD4+CD8-TCRbhiCD62LhiCD44loCD25hiDump-
Alveolar Macrophages	sorted on CD45+ CD11c+ SiglecF+
Splenic Germinal Center Centrocytes	sorted on CD19+B220+IgD-Fas+CD38-CXCR4lo CD86hi
Thymic Medullary Epithelial cells, MHCIIhi	sorted on CD45-Ly51loMHC-IIhiEPCAMhi
Bone Marrow 34- LTHSC/Bone Marrow 34-Long Term hematopoietic stem cells	sorted on Lin-Sca1+ckit+CD135-CD150+CD48-CD34-
Subcutaneous Lymph Node	sorted on CD45- CD31- PDPN- ITGA7+
Bone Marrow CD150+ CD48+ MMP2	
Bone Marrow Common Lymphoid Progenitor	sorted on LIN-CD93+CD117+IL7Ra+CD45R-
Subcutaneous Lymph Node Lymphatic Endothelial Cell	sorted on CD45- CD31+ PDPN+
Peritoneal Mast cells	
Bone Marrow Fr. BC (Pro-B)	sorted on CD93+IgM-CD19+CD43+HSA+
Peritoneal Macrophages	sorted on F4/80+ICAM2+CD5-CD19-CD43-
Splenic Plasma cells	6 week old C57BL/6J BLIMP1-GFP mice sorted on GFPhi CD138+ MHCIIlo (dump: NK1.1- TCRb- Gr1- CD11b-)

Figure 3.5 Bioinformatics analysis of RNA sequencing dataset using Immgen.
High expression of Prx4 is shown in peritoneal macrophages and splenic plasma cells of 6 week old C57BL/6J mice.

3.2.4 Loss of Prx4 leads to decreased inflammatory cell infiltration into tumors

Inflammation is known to contribute to tumorigenesis [242]. Since we observed strong expression of Prx4 in tumor-infiltrating immune cells, we speculated that the decrease in tumor burden in Prx4 knockout group was linked to decrease in inflammation. Therefore, we next examined immune cell infiltration in tumors of wildtype and $Prx4^{-/-}$ mice. Macrophages are one of the most abundant immune cells in the tumor microenvironment [243]. Using the AOM/DSS induced colon tumorigenesis model, previously we found that there is significantly decreased macrophage infiltration in tumors of $Srx^{-/-}$ mice compared to those of wildtype [226]. To examine whether this is also true in $Prx4^{-/-}$ tumors, we stained tumor slides with specific antibody to macrophage marker F4/80. Indeed, there are significantly fewer F4/80 positive cells in tumors from Prx4 null mice than those of wildtype mice (Figure 3.6A,B). We also used antibodies against CD86 as a specific marker for M1 macrophages (Figure 3.6C,D) and against CD163 as a specific marker for M2 macrophages (Figure 3.6E,F). We found that the presence of both M1 and M2 macrophages are significantly lower in $Prx4^{-/-}$ tumors compared to wildtype tumors.

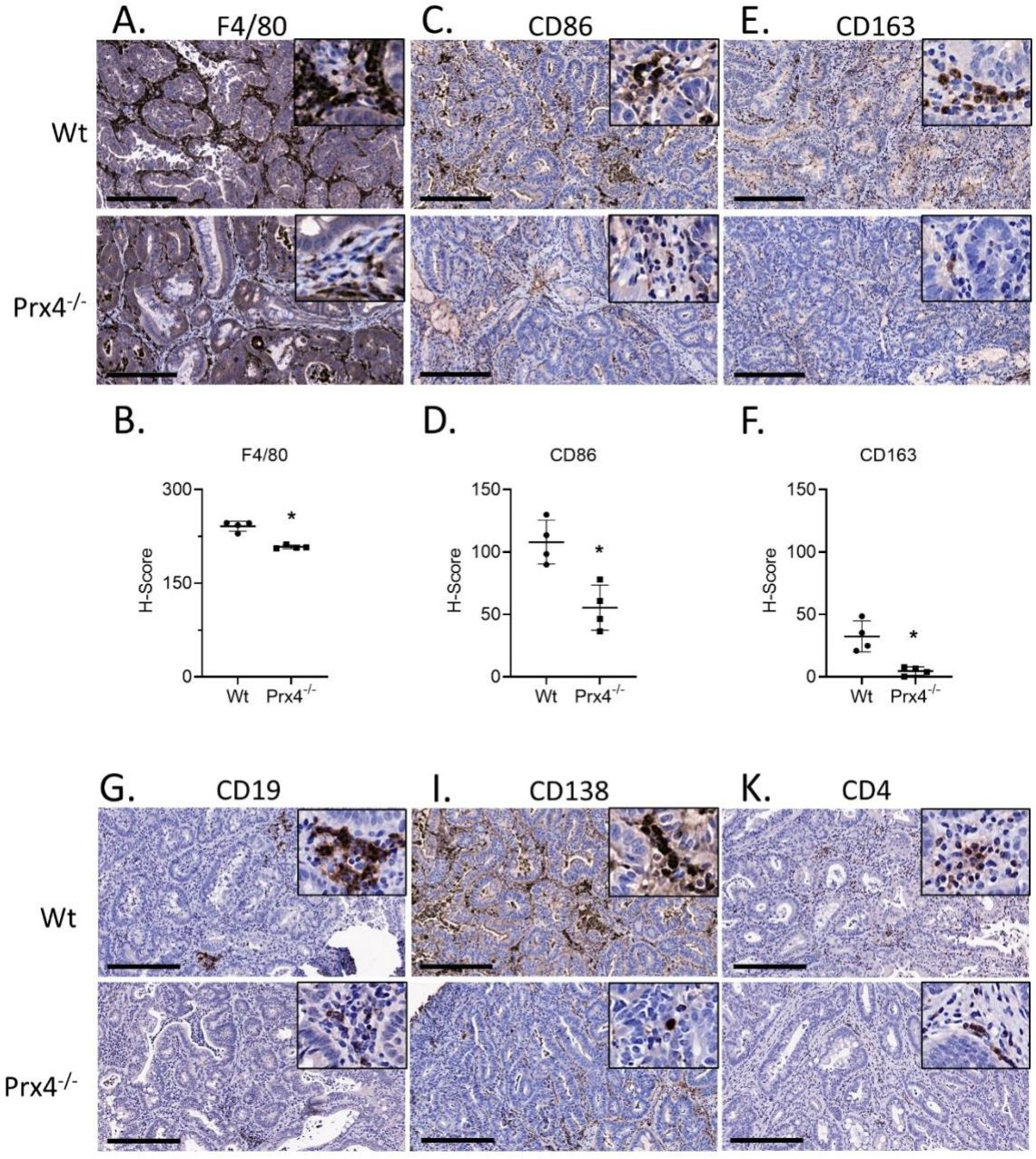
A.
F4/80
C.
CD86
E.
CD163
Wt
Prx4-/-
B.
F4/80
H-Score
300
150
0
Wt
Prx4-/-
D.
CD86
150
100
50
0
F.
CD163
G.
CD19
I.
CD138
K.
CD4

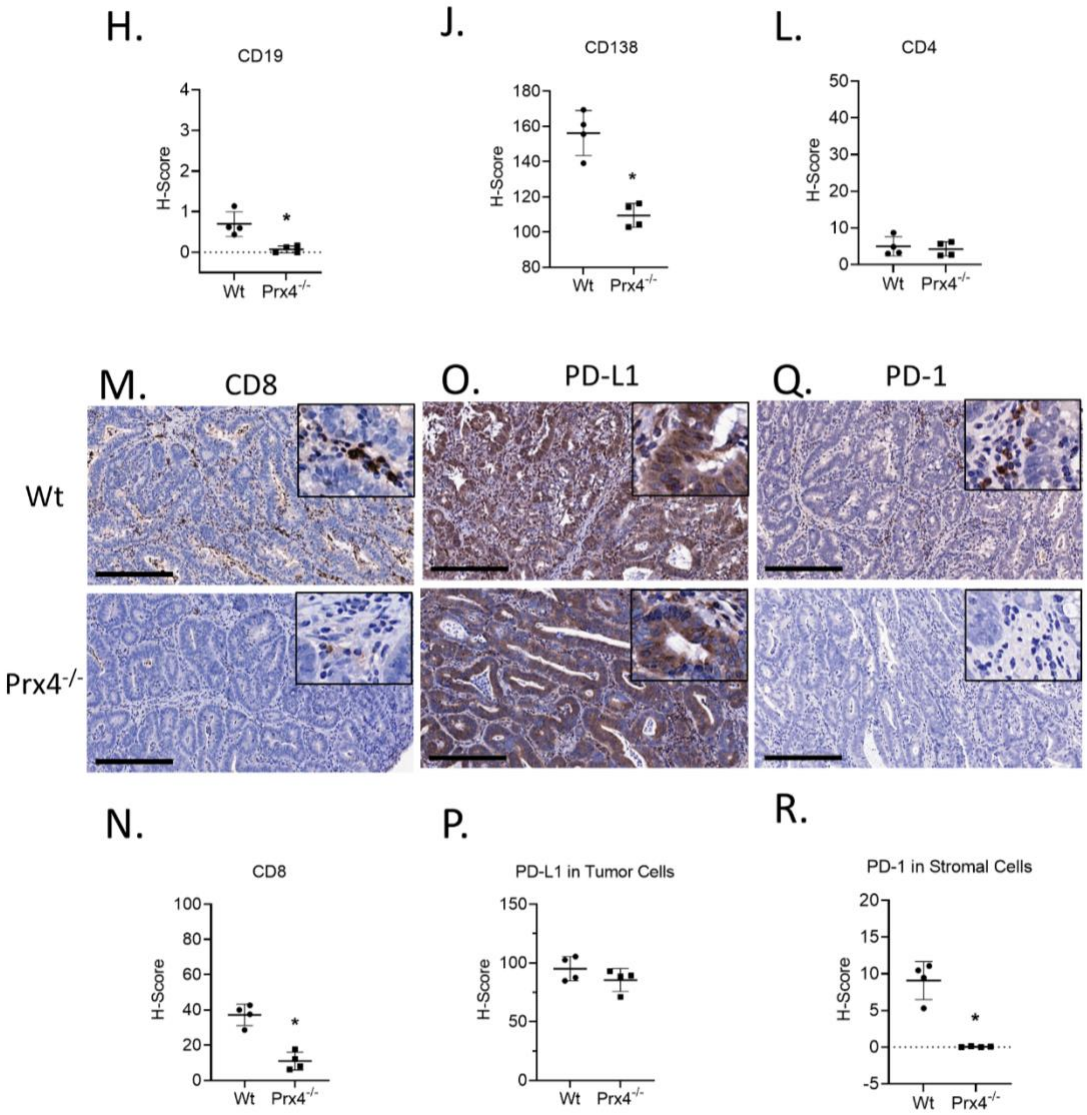

Figure 3.6 Prx4 knockout tumors have lower myeloid and lymphocyte infiltration compared to Wt.

(A and B) Representative images of murine macrophage marker F/480 stained wildtype and Prx4 knockout tumors. H-score= histochemical score. (C and D) IHC of M1 macrophage marker CD86 shows lower staining in Prx4 KO tumor. (E and F) IHC of M2 macrophage marker CD163 shows lower staining in Prx4 KO tumor compared to Wt. (G and H) Decreased naïve B cell infiltration in Prx4 KO tumors as indicated by staining of CD19. (I and J) IHC of CD138 indicates lower in-filtration of differentiated plasma cells in Prx4 KO tumors. (K and L) Similar levels of CD4+ staining was found between Wt and Prx4 KO tumors. (M and N) IHC staining of CD8 shows de-creased recruitment of cytotoxic T cells in Prx4 KO tumors. (O and P) IHC of PD-L1 in tumor sections shows comparable staining. (Q and R) IHC detection of PD-1 in wildtype and Prx4 KO tumor sections. Compared with Wt group, *$p<0.05$ (Student's t-test). Bar = 200 μm.

In addition to macrophages, next we compared the presence of lymphocytes in AOM/DSS induced colon tumors. The markers used for B lymphocytes were CD19 for naïve B cells (Figure 3.6G,H) and CD138 for terminally-differentiated plasma cells (Figure 3.6I,J). We detected lower presence of both cell types in Prx4 knockout tumors compared to those of wildtype. T cells are another key component of the colorectal tumor microenvironment and essential for immunotherapy [244]. T cells are broadly classified into two groups based on the lineage markers CD4 and CD8. $CD4^+$ T cells (helper T cells) secrete cytokines to enhance or suppress pro-inflammatory response [245]. $CD8^+$ T cells (cytotoxic T cells) can kill pathogen-infected or malignant cells [246]. We used these cell surface markers to stain the tumors and found that there was no significant difference in infiltration of $CD4^+$ cells between the groups (Figure 3.6K,L). However, $CD8^+$ staining was significantly lower in Prx4 knockout tumors than in wildtype (Figure 3.6M,N). Together, these data indicate that loss of Prx4 decreases infiltration of macrophages, B cells and cytotoxic T cells into the tumor microenvironment.

Programmed cell death protein 1 (PD-1) is a transmembrane protein expressed in T cells, B cells, monocytes and dendritic cells [247]. Programmed death ligand 1 (PD-L1) is a transmembrane protein, expressed in immune cells as well as a variety of nonhematopoietic cells, that binds to PD-1. PD-L1 ligation with PD-1 is important for immune homeostasis and to prevent autoimmunity. However, tumor cells also upregulate PD-L1 to escape immune surveillance [248]. Since we observed a decrease in immune cell population in the $Prx4^{-/-}$ tumors, we next asked if PD-1 and PD-L1 expression were also affected in the tumors. PD-L1 was found to be highly expressed in tumor cells and its levels were similar between the groups (Figure 3.6O,P). In contrast, positive staining of PD-1 was

mainly found in infiltrated inflammatory cells from tumors of wildtype mice, while significantly reduced number and levels of PD-1 are observed in tumors from Prx4 null mice (Figure 3.6Q,R). This observation is consistent with the decrease of immune cell infiltration in Prx4 null tumors. Taken together, these data indicate that the absence of Prx4 leads to significant changes of tumor microenvironment characterized by reduction of macrophages, T lymphocytes and plasma cell infiltration.

3.2.5 Loss of Prx4 leads to increased rates of apoptosis and lipid oxidation

We then examined tumors for markers of cell proliferation and cell death. Nuclear protein Ki67 was used as a marker for cell proliferation. There was no significant difference in the percentage of Ki67 positive tumor cells between the groups (Figure 3.7A,B). Terminal deoxynucleotidyl transferase-mediated dUTP nick end labelling (TUNEL) assay, which detects DNA fragmentation, was used to measure apoptosis in mouse tumors. TUNEL-positive cells were significantly increased in tumors from Prx4-/- mice than those from wildtype mice (Figure 3.7C,D). This suggests that lower tumor incidence, multiplicity and volume in Prx4 knockout group is a consequence of increased apoptosis in Prx4-/- tumors. Because Prx4 functions as scavenger of hydrogen peroxides, alkyl hydroperoxide and peroxynitrite and protects cells from oxidative stress, we next asked if loss of Prx4 led to higher oxidative stress in the tumors. Oxidative DNA lesion 8-oxoguanine (8-oxoG) was used as a marker of oxidative DNA damage. We found that 8-oxoG (Figure 3.7E,F) immunoreactivity was not significantly different between the groups. Since Prx4 is primarily distributed in the endoplasmic reticulum and extracellular matrix and since Prx1 and Prx2 are still present in the nucleus, it is possible that loss of Prx4 does not affect DNA damage. To examine lipid peroxidation, snap-frozen tumors were cryosectioned and

stained with BODIPY 581/591 C11, a fluorescent fatty acid analogue, before fixation. In this assay, there is a shift of the fluorescence emission peak from ~590 nm (red fluorescence) to ~510 nm (green fluorescence) upon oxidation of the polyunsaturated butadienyl portion of the dye. Fluorescence microscopy examination of the stained tumors showed that Prx4 knockout tumors had significantly higher green fluorescence, indicating higher lipid peroxidation in Prx4 knockout tumors compared to wildtype (Figure 3.7G,H). Thus, loss of Prx4 did not increase oxidative DNA damage but did increase lipid peroxidation and apoptosis in Prx4-/- tumors.

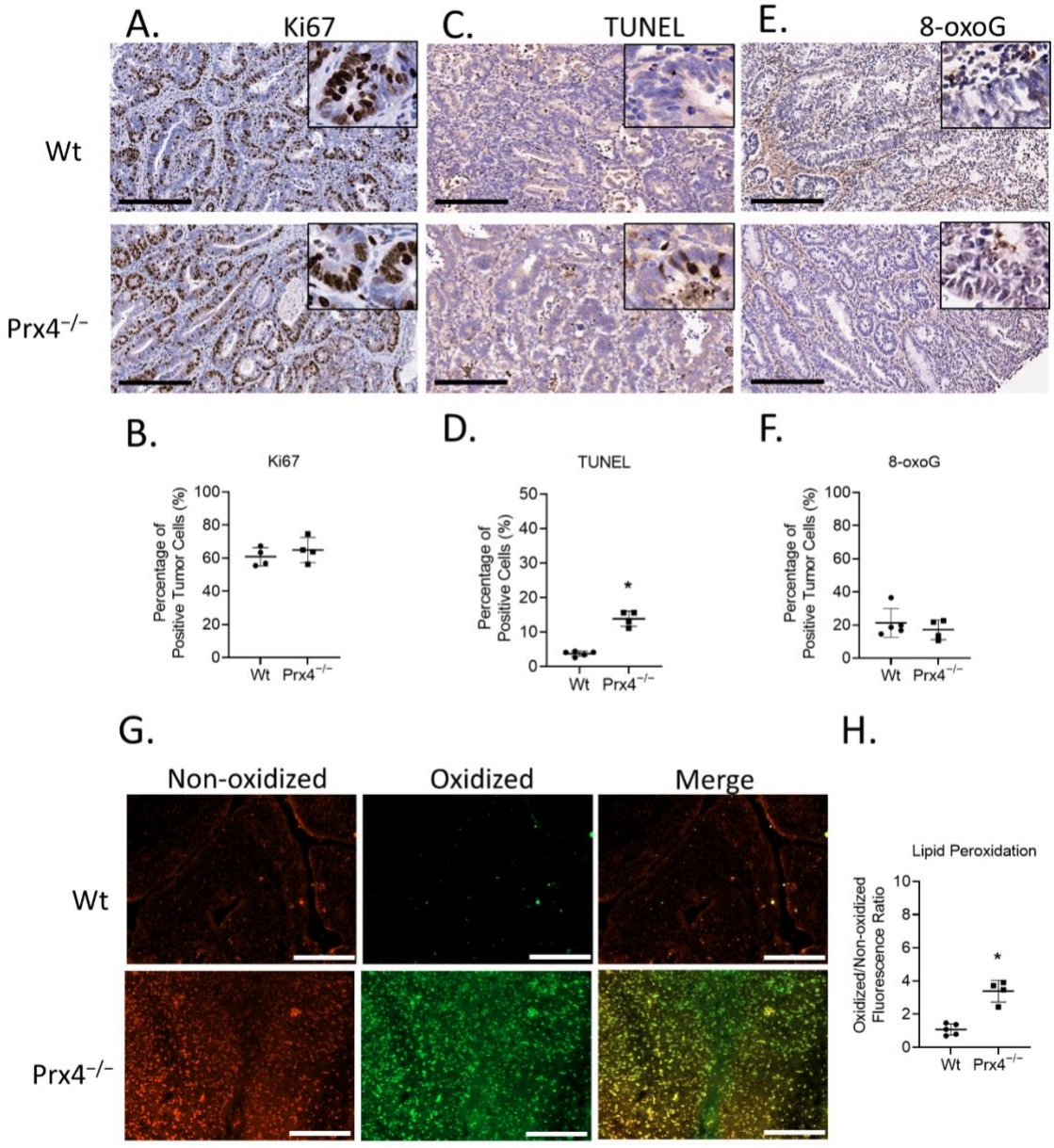

Figure 3.7 Prx4 knockout tumors have higher apoptosis and lipid peroxidation than Wt. (A and B) Similar levels of Ki67 staining were found between Wt and Prx4 knockout tumors. (C and D) TUNEL as-say indicates increased rate of apoptosis in Prx4 KO tumors. (E and F) Nuclear 8-oxoguanine, a marker of oxidative DNA damage, stained at similar levels in the Wt, Prx4 KO groups. Bar = 200 μm. (G and H) C11- BODIPY 581/591 staining of tumor sections to measure lipid peroxidation. Bar = 100 μm. Compared with Wt group, *p<0.05 (Student's t-test).

3.2.6 Loss of Prx4 disrupts cytokine-mediated signaling

To understand the mechanisms of how Prx4 might regulate inflammation, we next treated wildtype and Prx4 knockout mice with 2% DSS for seven days. We characterized the circulating cytokine and chemokine levels of wildtype and $Prx4^{-/-}$ groups using proteome profiler array (R&D Systems). Layout of arrays and names of chemokines and cytokines are shown in Figure 3.8. For each group, plasma was collected after no treatment (basal), DSS treatment, or AOM/DSS treatment. Plasma from three mice in each group were mixed and incubated in membranes containing capture antibodies. Array signals were imaged and quantified using ImageJ. We found that loss of Prx4 affected secretion of a variety of pro-inflammatory as well as anti-inflammatory cytokines as indicated by difference in spot size and intensity (Figure 3.9A,B). Proteins with significant fold change compared to corresponding wildtype group are shown in Figure 3.9C. Namely, untreated $Prx4^{-/-}$ mice had higher levels of Epidermal Growth factor (EGF) and Matrix Metallopeptidase 9 (MMP-9) than untreated wildtype mice. Endoglin, Fetuin A, Insulin Like Growth Factor Binding Protein 1 (IGFBP-1), Macrophage Colony-Stimulating factor (M-CSF) and Serpin F1 were upregulated in Prx4 knockout group after DSS compared to wildtype, while Platelet-Derived Growth Factor (PDGF)-BB was downregulated. Finally, at the end of AOM/DSS treatment, Interferon-Inducible T-Cell Alpha Chemoattractant (I-TAC), Keratinocyte-Derived Chemokine (KC) and EGF were higher and IGFBP-1 was lower in $Prx4^{-/-}$ group relative to wildtype. Thus, these data suggest that Prx4 plays a critical role in regulating inflammation via cytokines.

A.

	1	2	3	4	5	6	7	8	9	10	11	12	13	14	15	16	17	18	19	20
A	Reference																		Reference	
B			6Ckine		BLC		C10		C5/C5a		CCL28		Chemerin		CTACK		CXCL16			
C			Eotaxin		Fractalkine		IL-16		IP-10		I-TAC		JE		KC		LIX			
D			MCP-2		MCP-5		MDC		MIG		MIP-1α/β		MIP-1γ		MIP-2		RANTES			
E			SDF-1		Adipsin		Gp130		HSP60		Control (-)									
F	Reference																			

B.

	1	2	3	4	5	6	7	8	9	10	11	12	13	14	15	16	17	18	19	20	21	22	23	24
A	Reference		Acrp30		Amphiregulin		Angpt1		Angpt2		Angptl3		BAFF		C1q R1		CCL2		CCL3/CCL4		CCL5		Reference	
B			CCL6		CCL11		CCL12		CCL17		CCL19		CCL20		CCL21		CCL22		CD14		CD40			
C			CD160		Chemerin		Chitinase 3-like 1		CD142		C5/C5a		Complement Factor D		CRP		CX3CL1		CXCL1		CXCL2			
D	CXCL9		CXCL10		CXCL11		CXCL13		CXCL16		Cystatin C		DKK-1		CD26		EGF		Endoglin		Endostatin		Fetuin A	
E	FGF acidic		FGF-21		Flt-3 Ligand		Gas 6		G-CSF		GDF-15		GM-CSF		HGF		ICAM-1/CD54		IFN-γ		IGFBP-1		IGFBP-2	
F	IGFBP-3		IGFBP-5		IGFBP-6		IL-1α/IL-1F1		IL-1β/IL-1F2		IL-1ra/IL-1F3		IL-2		IL-3		IL-4		IL-5		IL-6		IL-7	
G	IL-10		IL-11		IL-12 p40		IL-13		IL-15		IL-17A		IL-22		IL-23		IL-27 p28		IL-28A/B		IL-33		LDL R	
H	Leptin		LIF		Lipocalin-2		LIX		M-CSF		MMP-2		MMP-3		MMP-9		Myeloperoxidase		Osteopontin		TNFRSF11B		PD-ECGF	
I	PDGF-BB		Pentraxin 2		Pentraxin 3		Periostin		Pref-1		Proliferin		PCSK9		RAGE		RBP4		Reg3G		Resistin			
J	Reference		E-Selectin		P-Selectin		Serpin E1		Serpin F1		Thrombopoietin		TIM-1		TNF-α		VCAM-1		VEGF		WISP-1		Control (-)	

Figure 3.8 Layout of proteome profiler.
Mouse chemokine (A) and cytokine (B) arrays adapted from manufacturer's datasheet.

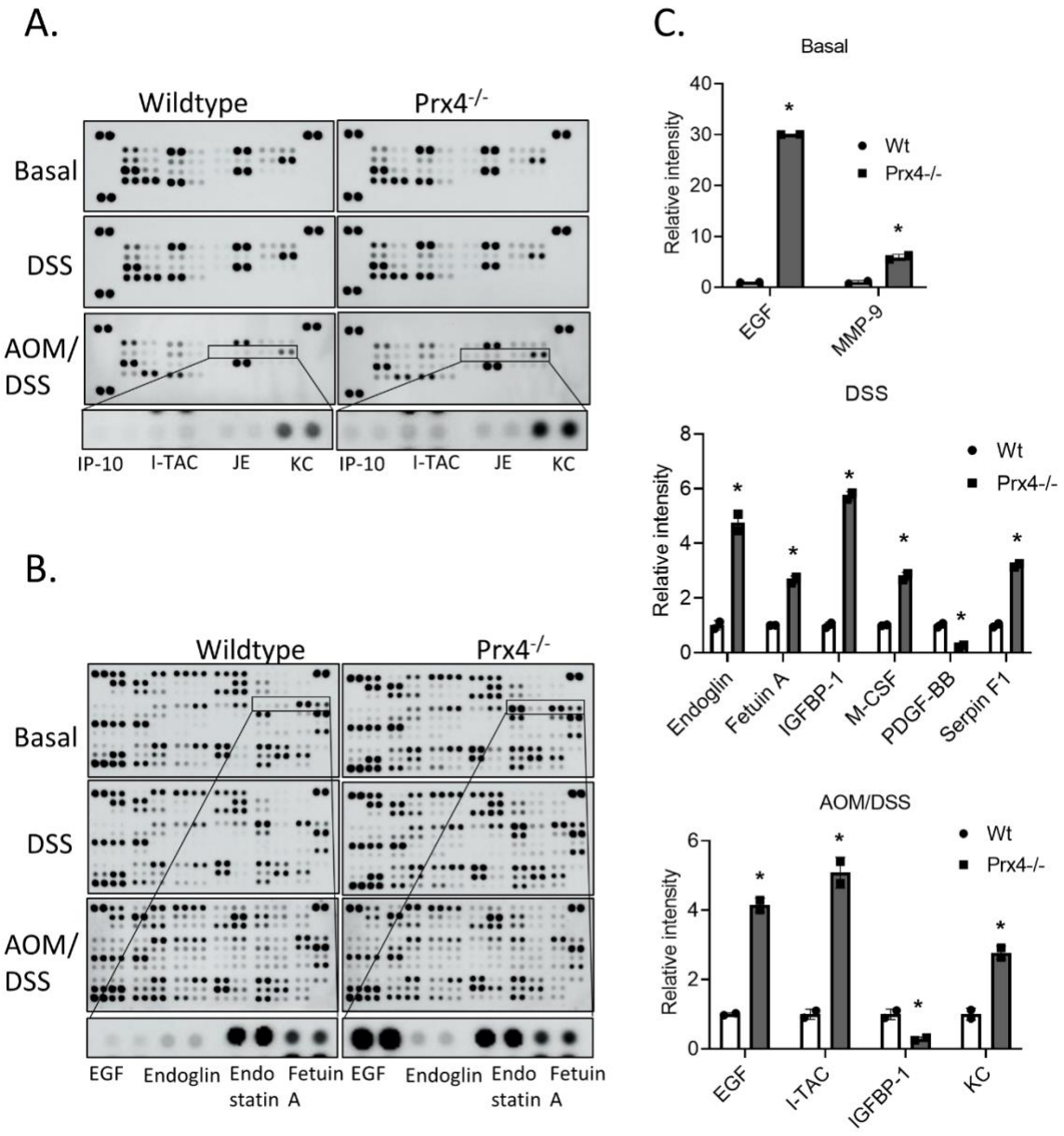

Figure 3.9 Loss of Prx4 affects chemokine- and cytokine- mediated signaling.
(A and B) Proteome profiler mouse chemokine (A) and cytokine (B) array original blots using plasma isolated from basal (no treatment), DSS, and AOM/DSS treatment groups. Representative spots are highlighted. (C) Quantification of intensity of cytokine and chemokine duplicate spots identifies significantly different proteins under basal conditions (top panel), after DSS treatment (middle panel) and after AOM/DSS treatment (lower panel). Compared with Wt group, *$p<0.05$ (Student's t-test).

In addition to plasma, colon tissues from DSS treated mice were also collected, fixed and stained for different markers of immune cells as described above. Consistent to

AOM/DSS treatment, we found that loss of Prx4 reduced infiltration of $CD86^+$ M1 macrophages, $CD163^+$ M2 macrophages, $CD138^+$ plasma cells, $CD4^+$ T cells, and $CD8^+$ T cells in $Prx4^{-/-}$ colon (Figure 3.10). Thus, Prx4 protects mice against DSS-induced inflammation by modulating cytokines and chemokines.

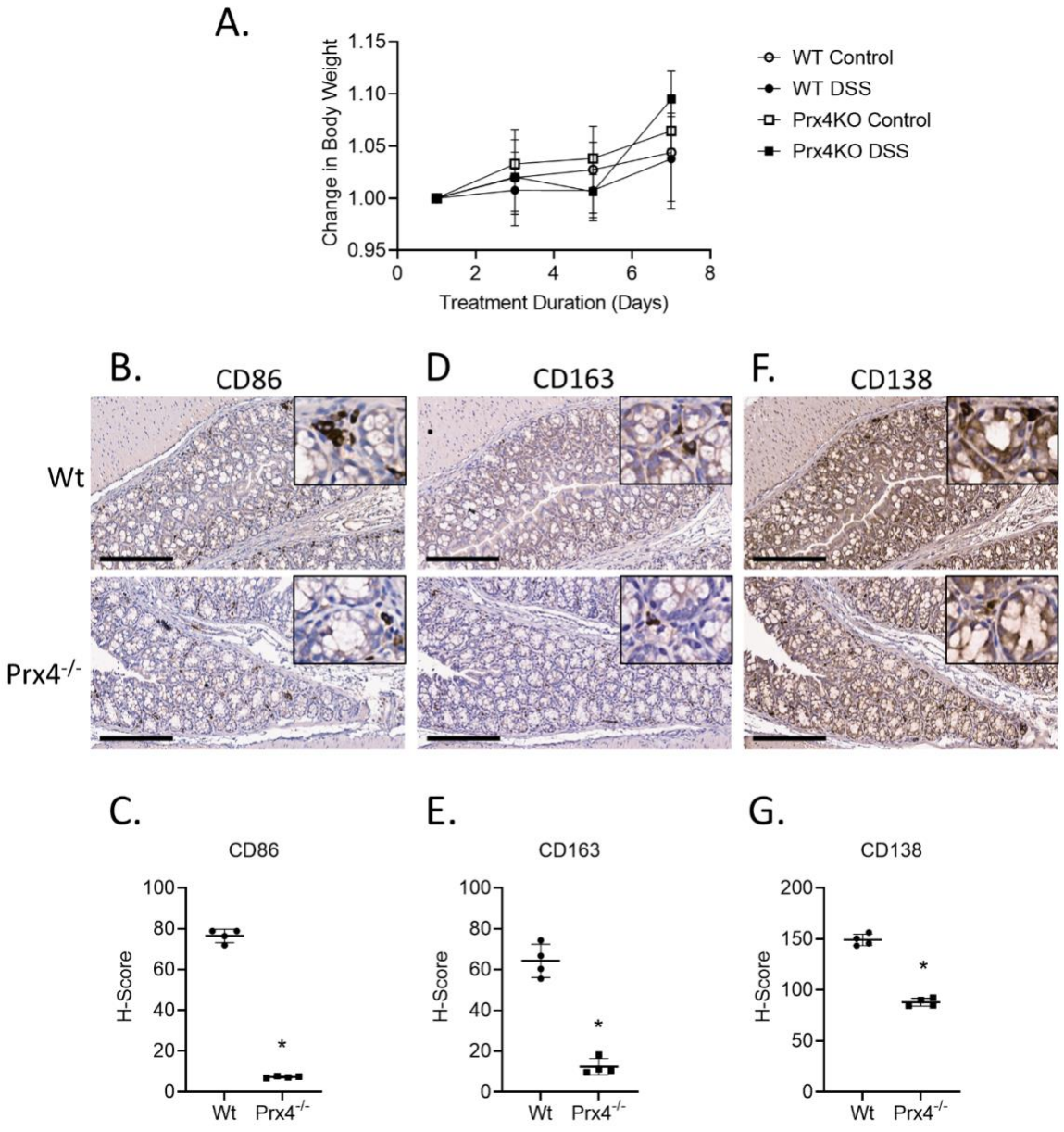

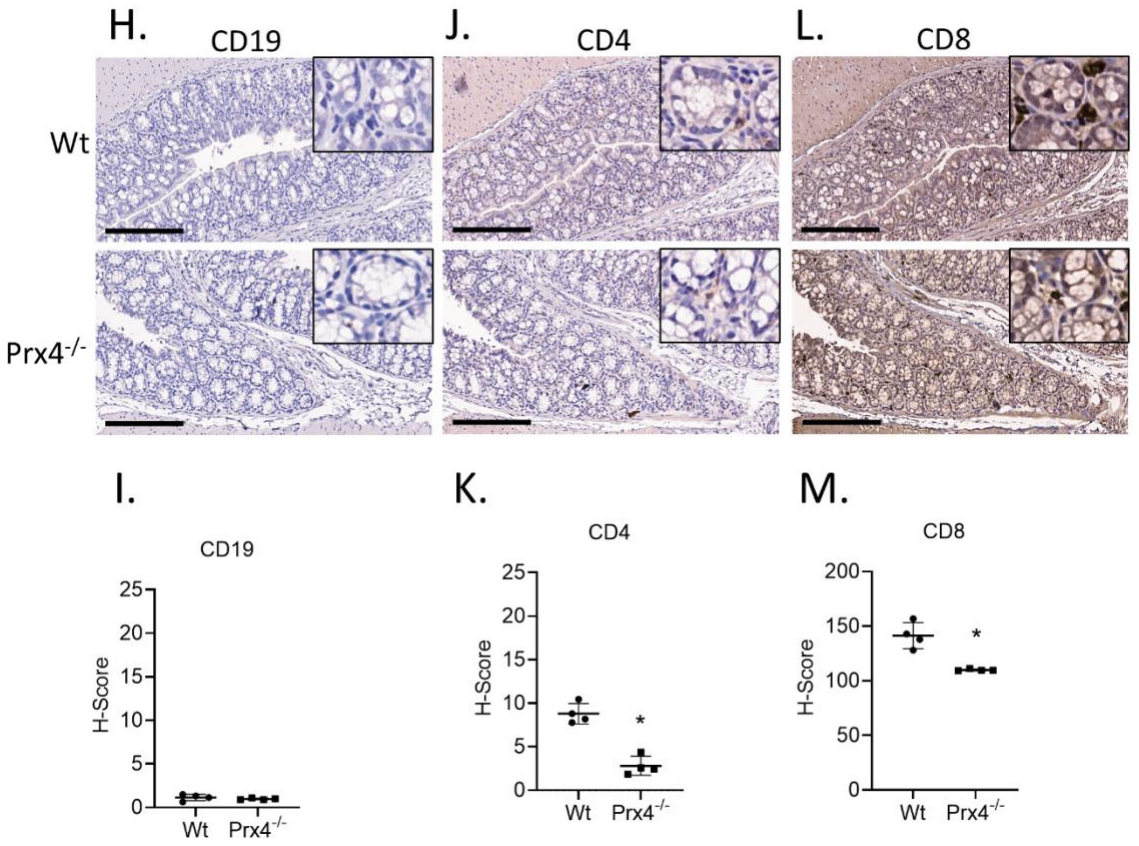

Figure 3.10 Prx4 knockout colons have lower immune cell infiltration compared to wildtype after DSS treatment.

(A) Change to initial body weight of DSS-treated or untreated (control) wildtype and Prx4 knockout mice. Decreased macrophage infiltration in Prx4 knockout colon as indicated by staining of M1 macrophage marker CD86 (B and C) and M2 macrophage marker CD163 (D and E). (F and G) IHC staining of CD138 indicates lower presence of plasma cells in Prx4 knockout colon. (H and I) Comparable naïve B cells infiltration as indicated by staining of CD19. (J and K) Lower levels of CD4+ staining was detected in Prx4 knockout compared to Wt. (L and M) IHC staining of CD8 shows decreased recruitment of cytotoxic T cells in Prx4KO group. Compared with Wt group, *$p<0.05$ (Student's t-test). Bar = 200 μm.

3.3 Discussion

It has been well recognized that strains of inbred mice do not bear same genetics due to polymorphisms and multiple layers of regulatory elements. Such distinctions in genetics lead to significant variations in susceptibility to tumorigenesis among different mouse strains even exposed to the same tightly controlled protocol of carcinogen(s) [238,

249]. Among them, FVB/N mouse has been reported to be highly sensitive to carcinogen-induced cancer development, such as DMBA/TPA-induced skin cancer AOM/DSS-induced colon cancer, and urethane-induced lung cancer [250-252]. Previously we have shown that $Srx^{-/-}$ mice are resistant to AOM/DSS-induced colon tumorigenesis, identified that Prx4 is the major downstream substrate of Srx, and the integrity of the Srx-Prx4 axis is required for cancer malignancy [138, 226, 235].

In the present study, we aimed to identify the function of Prx4 in colon carcinogenesis. AOM/DSS model was again used to induce colon cancer development in wildtype and Prx4 null mice in FVB/N background. We demonstrated that the absence of this gene provided resistance to chemically-induced tumor formation. $Prx4^{-/-}$ group had lower tumor incidence, multiplicity, volume and tumor burden than wildtype mice. In mechanistic studies, we found that Prx4 knockout led to higher intra-tumoral cell death likely due to increased oxidative stress. The knockout of Prx4 also decreased infiltration of inflammatory cells into the tumor microenvironment and resulted in downregulation of PD-1 in tumor stroma. Thus, loss of Prx4 protects mice against AOM/DSS-induced colon tumorigenesis.

Our results presented here are in accordance with several previously published studies that have examined the role of Prx4 in inflammation and cancer. It has been reported that Prx4 can activate NF-κB, a master regulator of inflammation, in T cells and macrophages [43, 112]. We have previously demonstrated that Srx contributes to tumorigenesis in chemically- induced models of colon cancer and skin cancer [226, 237]. Srx null tumors in both studies had comparable cell proliferation but significantly higher apoptosis than wildtype tumors. In addition, loss of Srx reduced macrophage infiltration in

colon tumors. Similarly, in urethane-induced lung cancer, Prx4 promoted chemically induced lung tumorigenesis. Human Prx4 expressing transgenic mice had more tumors than non-transgenic control mice [141]. The tumors in transgenic groups also had lower oxidative stress and higher macrophage infiltration. Furthermore, Prx4 has been suggested to promote progression of prostate cancer, pancreatic cancer, hepatocellular carcinoma and colorectal cancer [131, 147, 156, 166]. Thus, our study further confirms the pro-inflammatory and oncogenic role of Prx4 in colorectal cancer.

The loss of Prx4 providing resistance to DSS-induced inflammation fits the general trend observed when antioxidant enzymes are depleted in colitis models: Loss of Prx1, Prx2, Prx6 and the combined loss of GPx1 and Catalase all improved colitis in mouse and rat models [125, 253-255]. (Exceptions to this observation include GPx2 knockout and Gpx1 and GPx2 double knockout mouse models which highlight the protective role of selenium [256, 257]). This trend suggests that appropriately increased oxidative environment (as indicated by two of these studies) upon silencing of antioxidant enzymes suppresses inflammatory response. In our study, whether oxidation of Prx4 occurred in wildtype tumors are DSS and AOM/DSS treatment was not examined. Measuring Prx4 oxidation levels would help shed light on the contribution of redox function of Prx4 on inflammation and tumorigenesis. Moreover, it would be interesting to examine the role of Prxs and other antioxidants in the production and maturation of immune cells under normal conditions as well as in response to carcinogens, tumor promoters. Similarly, it might be worth re-evaluating clinical studies that examined the effects of antioxidant rich diet or supplements on patients at risk of inflammatory bowel disease and colorectal cancer. The effect these treatments had on oxidative damage must be examined in samples from past

interventions as well as in future studies. This would help clarify if the intervening 'antioxidants' are actually performing redox functions in vivo and whether diet recommendations need updating.

Prx4 loss caused upregulation of several pro-inflammatory and anti-inflammatory cytokines after DSS and AOM/DSS treatment. As mentioned above, Prx4 modulates NF-κB signaling, and many of the cytokines differentially expressed in our study are known targets of this transcription factor [258-260]. We observed increased plasma EGF and MMP-9 in Prx4KO mice compared to wildtype. The reason for this upregulation is not clear. We have shown previously that loss of Srx contributes to reduction of EGFR signaling and MMP-9 protein expression [138, 235]. It is possible that loss of Prx4 has a similar effect on these proteins and signaling pathways, resulting in a feedback loop which causes high circulation levels. Further studies are necessary to address the function of these upregulations in normal physiology. Among the cytokines differentially expressed in Prx4KO mice upon DSS treatment, increased Endoglin and Fetuin A and decreased PDGF-BB have been associated previously with reduced inflammation of the colon. Endoglin heterozygous mice were more sensitive to DSS treatment compared to wildtype mice resulting in higher VEGF levels and angiogenesis [261]. In addition, in human subjects, increased serum Fetuin A is inversely associated with inflammatory bowel disease (IBD), suggesting a protective role for this protein [262]. IBD patients have also been reported to have higher plasma PDGF-BB compared to healthy controls [263]. However, even though Prx4 deficiency is protective overall against colitis, there was upregulation of two proteins positively associated with gastrointestinal inflammation, namely Serpin F1, M-CSF and

IGFBP-1 [264-266]. Targeting these proteins along with Prx4 could further strengthen resistance against colitis and tumor formation.

After AOM/DSS treatment, plasma EGF was significantly higher in $Prx4^{-/-}$ group although the difference between wildtype and $Prx4^{-/-}$ plasma was reduced compared to basal conditions. Plasma EGF are significantly higher in cancer patients than those with benign colorectal conditions [267]. In addition, IGFBP-1, which was reduced in Prx4KO mice, is inversely associated with colorectal cancer in human subjects [268, 269]. High KC mRNA is also inversely associated with overall survival of stage IV patients (but there were no correlations to survival in stage II and III patients) [270]. Therefore, whether these cytokines serve pro-tumor or anti-tumor functions in Prx4KO mice is not clear. It might be worthwhile to conduct studies targeting one or more of these proteins along with Prx4 depletion to shed more light on their combined contribution to colon carcinogenesis. Meanwhile, I-TAC, which is upregulated in $Prx4^{-/-}$ group, is reported to have a protective role against colon cancer. Bioinformatics analysis shows I-TAC transcript is higher in stages I and II of CRC compared to stages III and IV, and high I-TAC is associated with better overall survival of patients [271, 272]. Thus, upregulation of these chemokines at least partially contributed to reduced colon tumor formation in Prx4KO mice.

Prx4 is upregulated in human IBD, and it has been suggested as a potential diagnostic marker for IBD [96]. However, whether Prx4 contributes directly to IBD progression or is a secondary response to altered intestinal microenvironment is not fully understood. Our results indicate that Prx4 promotes DSS-induced inflammation. However, these findings contrast with other data reporting an anti-inflammatory role of Prx4 after DSS [97]. The most notable discrepancy between this work and previous report were in

the type of mouse strains used. Specifically, Takagi et al. utilized male mice of C57BL/6 background whereas this study utilized both male and female mice of FVB/N background. Different strains of mice have different responsiveness to DSS [273]. In addition to genetic differences between the mice, the differences in mouse microbiome- result of housing in different institutions- also likely contributed to the inconsistency [274]. It remains critical for future studies to evaluate the effects of these factors in the function of Prx4.

Overall, our results show an important role of antioxidant Prx4 in regulating colon carcinogenesis. Knockdown of Prx4 provides resistance to tumor formation by reducing inflammation and promoting cell death without affecting cell proliferation. This identifies Prx4 as a potential therapeutic target for prevention and treatment of colorectal cancer. Regulation of Prx4 expression in patients at high risk of inflammation-driven cancer through dietary supplements or other preventive agents may prove useful to block or delay the early stages of cancer. Similarly, identification of Prx4-specific inhibitors to target increased apoptosis of tumor cells in combination with radiation or chemotherapy could enhance the outcome of cancer treatment.

CHAPTER 4. PEROXIREDOXIN IV PROMOTES THE PROGRESSION OF COLORECTAL CANCER

4.1 Introduction

Colorectal cancer (CRC) is the third most common cancer and the third leading cause of cancer deaths in the US [275]. CRC is the development of polyps on the inner lining (mucosa) of colon or rectum into malignant cancer. Risk factors for colorectal cancer include old age, family history, inflammatory bowel disease, diabetes, smoking and alcohol intake. Colonoscopy is a screening method commonly used to detect CRC at early stage. It is critical to detect cancers including CRC at early stage because this is when surgery and treatments work best. Early stage malignant polyps can be resected endoscopically. In cases where there are too many tumors or tumors cannot all be removed during colonoscopy, surgery to remove part of the colon is performed [276]. Chemoradiotherapy is often used in combination with surgery to reduce the risk of recurrence. As tumor becomes malignant, tumor cells migrate through blood vessels or lymph vessels. Metastasis into lymph nodes or other organs makes treatment much more difficult. Patients with metastatic CRC are treated with several lines of therapies involving two or three chemotherapy drugs, anti-EGFR, anti-VEGF antibodies and immunotherapy [276]. Despite recent advances, the 5-year survival rate for patients with distant metastatic CRC is only 10% [277]. Therefore, further research is necessary to understand and develop more effective treatments for advanced CRC.

We have shown previously that the enzyme Srx promotes both the initiation and progression of colorectal cancer. In azoxymethane (AOM)/ Dextran sulfate sodium (DSS)-induced CRC, Srx knockout mice were found to be more resistant to colon tumor formation compared to wildtype mice [226]. Loss of Srx increased intratumoral apoptosis and

decreased inflammatory cell infiltration. Similarly, in vitro and in vivo studies demonstrate that Srx promotes CRC migration, invasion and metastasis [235]. Srx has the highest binding affinity for Prx4 relative to other typical 2-Cys Prxs [138]. We have also discovered upon AOM/DSS treatment that Prx4 promotes colorectal tumor formation in mouse model [172]. Loss of Prx4 leads to increased cell death through lipid peroxidation and lower infiltration of inflammatory cells in the Prx4 knockout tumors compared to wildtype. Therefore, the next logical questions to ask are whether and how Prx4 promote colorectal cancer progression.

Literature survey shows that high Prx4 expression is positively correlated with increased metastasis and shorter survival of patients [145, 146]. To better examine this association and to study the causal role of Prx4 in CRC progression, we used loss-of-function and gain-of-function approaches. We established cell lines with stable knockdown and overexpression of Prx4. Subsequent in vitro studies show that Prx4 knockdown cell lines have lower migration and invasion rate than control cell lines. In orthotopic implantation model, HCT116 Prx4 knockdown cells metastasized had significantly lower rate than shNT cells. RNA Sequencing and GSEA analysis identified several signaling pathways significantly altered in knockdown cells which was validated in vitro. Our results confirm that Prx4 enhances invasion and metastasis of CRC. Thus, our findings provide novel insights regarding the role of Prx4 in human colon cancer pathogenesis.

4.2 Results

4.2.1 Prx4 is highly expressed in tumor specimens from colon adenocarcinoma

We first examined the expression of Prx4 transcripts in normal and tumor colorectal tissues. Analysis of RNA-Sequencing datasets from TCGA using UALCAN website shows

that Prx4 mRNA is upregulated in colon adenocarcinoma (COAD) samples compared to normal colon (Figure 4.1A). Stage1 - Stage 4 COAD all had higher Prx4 transcripts than normal colon, but there was no increase in Prx4 levels with increasing COAD stage (Figure 4.1B). Similarly, analysis of proteomics data using UALCAN shows that Prx4 protein is also upregulated in colon adenocarcinoma compared to normal colon (Figure 4.1C). Consistently, higher Prx4 protein levels were detected in Stage 2 and Stage 3 of COAD relative to normal (Figure 4.1D). We also analyzed Prx4 expression in TCGA rectum adenocarcinoma (READ) samples. We observed higher Prx4 mRNA levels in overall primary READ tumor as well as stages 1 – 4 of READ compared to normal rectum (Figure 4.1E,F). Thus, bioinformatics analysis of publicly available datasets indicates that Prx4 is upregulated at mRNA and protein levels in colorectal cancer patients.

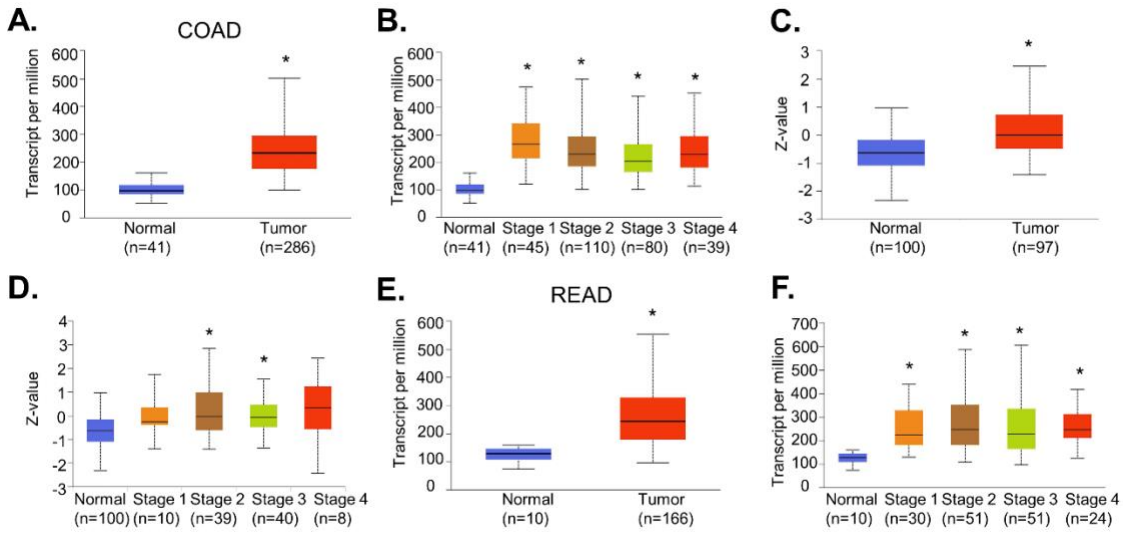

Figure 4.1. Bioinformatics analysis of Prx4 transcript levels and protein levels in colorectal cancer patients.

(A) Prx4 transcript in normal and colon adenocarcinoma (COAD) tissues. (B) Prx4 transcript in normal colon and different stages of COAD tissues. (C) Prx4 protein in normal and COAD tissues. (D) Prx4 protein in normal and different stages of COAD tissues. (E) Prx4 transcript in normal and rectum adenocarcinoma (READ) tissues. (F) Prx4 transcript in normal and different stages of READ tissues. *p<0.05 (t-test).

We wanted to confirm this finding in additional patient samples. A tissue microarray method based on the established IHC protocol was used to detect Prx4 in normal colon (n=19), Crohn's disease (n= 9), Ulcerative Colitis (n= 4), normal adjacent to tumor (n=19), benign tumor (n=15), malignant tumor of stages I, II and III (n=35) and metastasized tumor (n=20) from human subjects (Figure 4.2A). Prx4 staining was analyzed by board certified pathologist. Prx4 is expressed in normal colon with high expression in the epithelial cells of the crypt. We also confirmed that Prx4 is upregulated in malignant tumors stages 1 – 3 compared to normal colon (Figure 4.2A,B). No significant changes in Prx4 expression were observed in Ulcerative colitis and Crohn's disease or in metastatic tumor samples relative to normal colon tissue. We also performed western blot to examine expression of Prx4 in human colorectal cancer cell lines SW620, SW480, RKO, LOVO, HT29, HCT116 and GEO. There was high expression of Prx4 in all colorectal cancer cell lines examined (Figure 4.2C). Together these data validate our bioinformatic analysis and demonstrate that Prx4 is highly expressed in CRC cells.

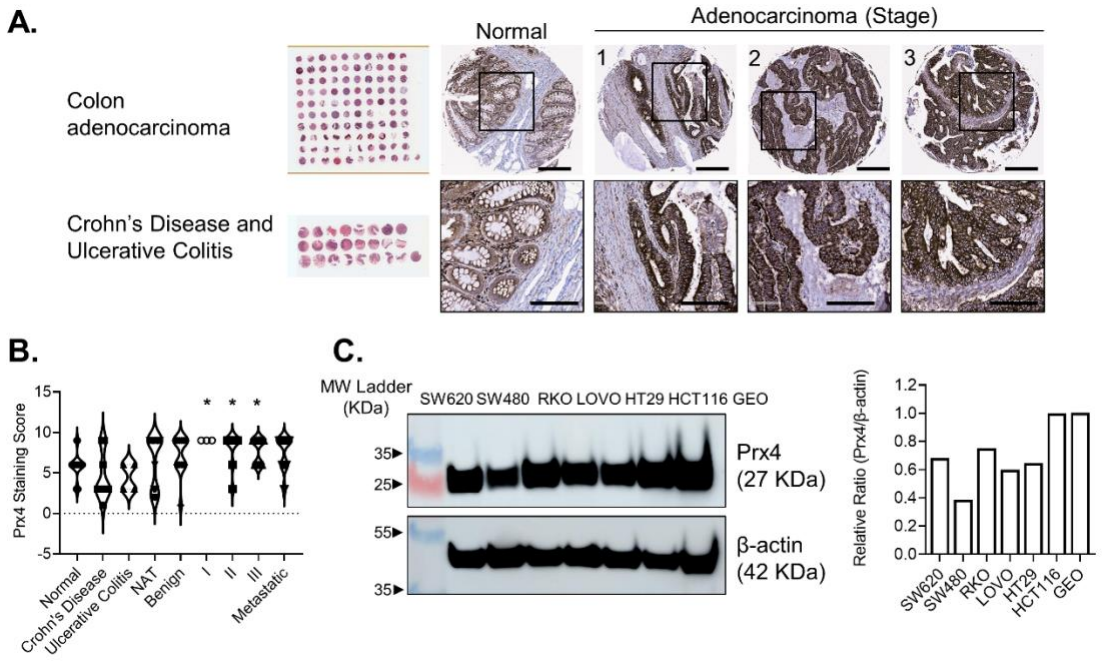

Figure 4.2. Examination of Prx4 protein levels in patient specimens of colon cancer and colon cancer cell lines.

(A) Tissue microarray slides with image of hematoxylin and eosin (H&E) staining (left panel) and representative images of anti-Prx4 staining of normal colon and colon adenocarcinoma. The scale bars represent 300 μm (individual tumor), and 100 μm (zoomed in). (B) Anti-Prx4 staining positivity and intensity were quantitatively scored by board-certified pathologist and normal group (n=19) was compared to Crohn's Disease (n=9), Ulcerative Colitis (n=4), Normal adjacent tumor (NAT) (n=19), Benign tumor (n=15), Stage I (n= 3), Stage II (n= 19), Stage III (n=12) and Metastatic Tumor (n=20). *$p<0.05$ (Two-way ANOVA). (C) Prx4 levels in colorectal cancer-derived cell lines measured by Western blot.

4.2.2 Prx4 knockdown reduces migration and invasion of colon cancer cell lines

Next, we wanted to identify the function of Prx4 upregulation. Previously we have demonstrated that depletion of Srx in CRC cell lines reduces cell migration and invasion [235]. We wanted to examine if this was true for Prx4 as well. Therefore, stable knockdown of Prx4 was performed in HCT116 and RKO cell lines. The targeting efficiency of shPrx4 as well as the specificity of anti-Prx4 antibody has been described in previous studies in our lab [131, 138]. Depletion of Prx4 was confirmed using Western blot (Figure 4.3A,B). Cell migration is important for physiological processes such as embryonic development

and wound repair as well as for tumor metastasis. The role of Prx4 in colorectal cancer cell migration was investigated using two assays. In wound healing assay, confluent cells were scratched using 200 μL pipet tip after overnight serum starvation, washed, and imaged at different intervals. The area of wound was measured using ImageJ software. In this assay, we discovered that wound healing was slower in shPrx4 cells than shNT cells (Figure 4.3C,D). In the second assay, the movement of individual shNT and shPrx4 cells was tracked using Cytation5 and analyzed using Cell tracker software. Again, Prx4 knockdown cells were found to have slower rate of movement and had shorter distance travelled than shNT cells (Figure 4.3E,F). Thus, loss of Prx4 reduces migration of human CRC cell lines in vitro.

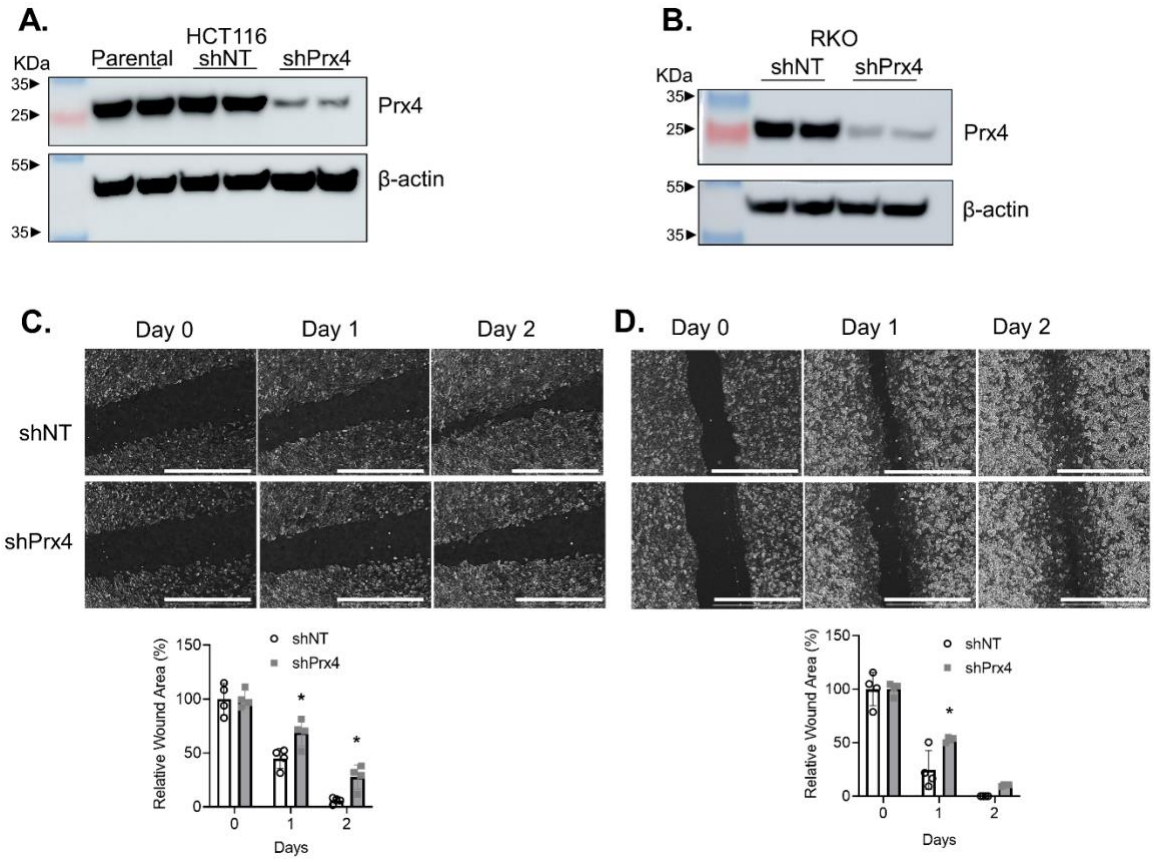

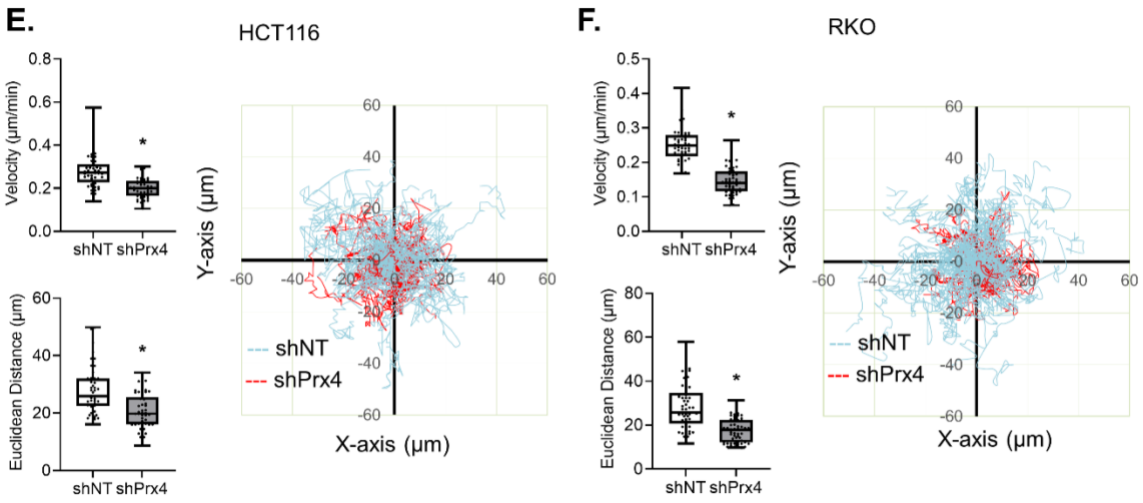

Figure 4.3. Knockdown of Prx4 in CRC cells decreases their ability of to migrate. Western Blot results showing stable knockdown of Prx4 using shRNA in (A) HCT116 and (B) RKO cell lines. Wound healing assay in (C) HCT116 and (D) RKO cell lines. Bar =1000 μm. Quantification is shown below the images. Cell movement tracking analysis of (E) HCT116 and (F) RKO cells performed using CellTracker software. Velocity and distance were calculated from tracking of at least 50 cells in each group. Cell movement routes are shown below the graphs. Compared to shNT, *p<0.05 (Student's t-test).

Cell invasion is another important physiological process where cells become motile and migrate through extracellular matrix. Cell invasion occurs naturally during development and repair, but it is also utilized by cancer cells to metastasize to secondary sites. Colorectal cancer cells frequently spread to liver via the portal circulation, and they may also metastasize to lungs, brain, etc. Therefore, we asked if Prx4 regulates invasion of CRC cells. In transwell invasion assay, shNT and shPrx4 cells resuspended in serum-free medium were allowed to invade through Matrigel in response to 10% FBS for 48 hours. Subsequent staining and image analysis showed that fewer shPrx4 cells had invaded through Matrigel than shNT cells (Figure 4.4A,B). This indicates reduction of invasiveness in CRC cells upon Prx4 depletion. To further solidify our findings, we performed 3D spheroid invasion assay. In this assay, cells were induced to form spheroids, invasion

matrix was added to promote gel formation around the spheroids and culture medium containing 20% FBS (chemoattractant) and TPA (inducer of cell invasion) were added. Images of cellular spheroids and spindle-like projections were captured using Cytation5 and analyzed using ImageJ. Consistent with classic transwell assay, 3D spheroid invasion assay also shows that Prx4-depleted cells have lower invasion rate than control cells in HCT116 cell line (Figure 4.4C,D). Interestingly, RKO cells detached from the cell spheres towards chemoattractants, and the number of detached cells was higher in shPrx4 group Figure 4.4D. Finally, to further characterize the process of invasion, we performed invadopodia formation assay. Invadopodia are actin-rich protrusions used by cancer cells to invade surrounding matrix through proteolysis. The colocalization of cortactin with F-actin is a commonly used marker of invadopodia formation [278]. Quantification of stained cells shows that colocalization of cortactin and F-actin is much more prevalent in shNT cells than shPrx4 cells, indicating reduced invadopodia formation in shPrx4 cells (Figure 4.4E,F).

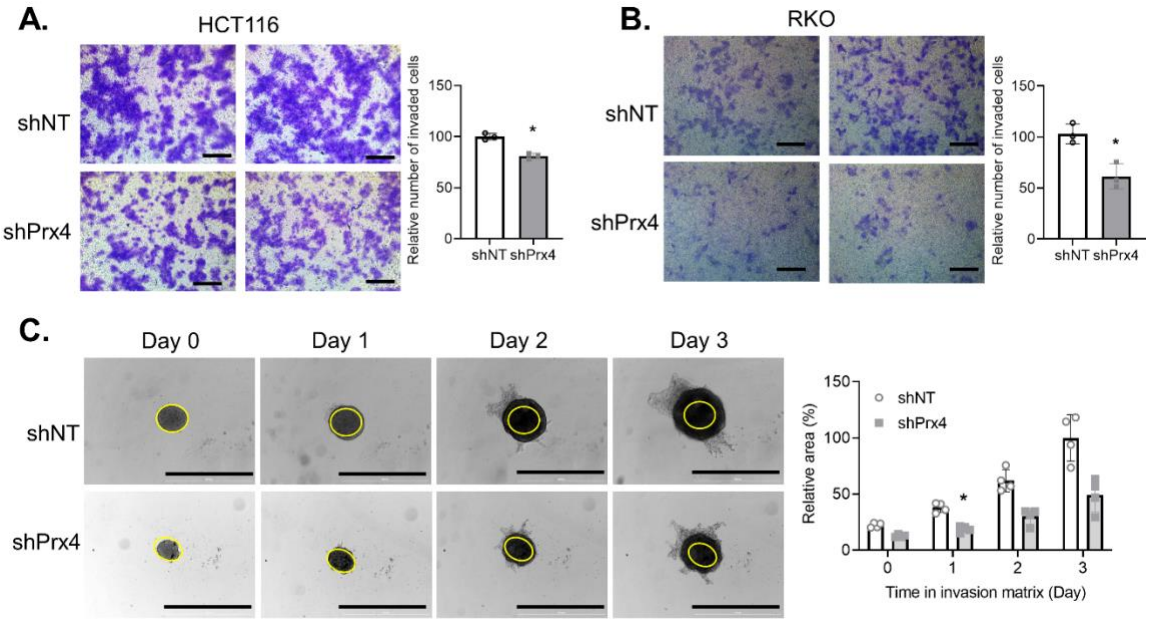

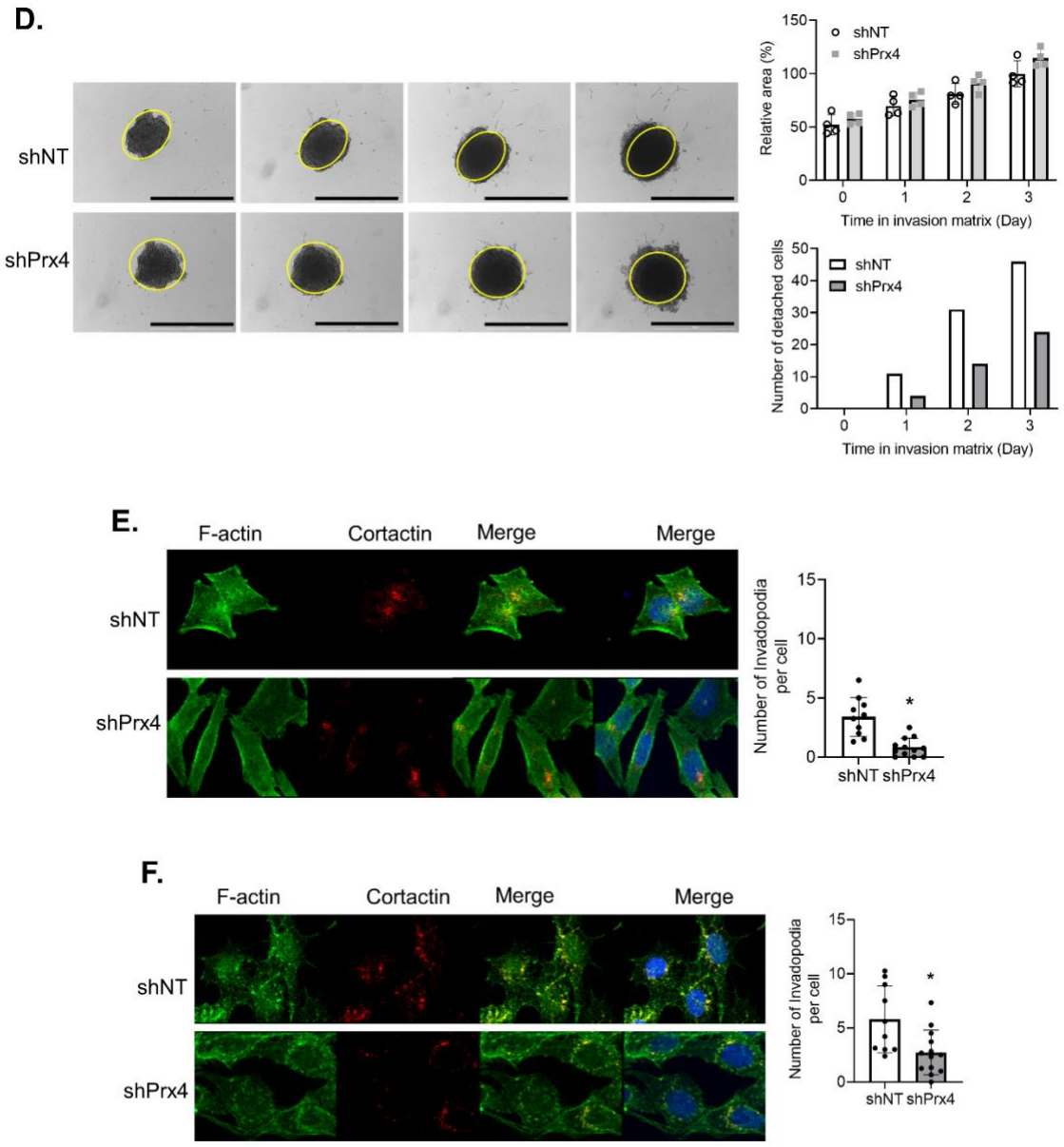

Figure 4.4. Knockdown of Prx4 in CRC cells decreases their ability of to invade. Transwell cell invasion assay using (A) HCT116 and (B) RKO cell lines. Bar =200 μm. Quantification is shown in bar graph on the right. 3D spheroid invasion assay using (C) HCT116 and (D) RKO cell lines. Bar =1000 μm. Quantification is shown on the right. Representative confocal imaging (E) HCT116 and (F) RKO cells indicate presence of invadopodia characterized by the co-staining of F-actin (green) and cortactin (red). Bar graph on the right shows average number of invadopodia from three independent experiments. Compared to shNT, *$p<0.05$ (Student's t-test).

To further validate our results, additional experiments were performed. Cell proliferation assay using CCK-8 kit showed no significant difference between shNT and

shPrx4 cells in both HCT116 and RKO (Figure 4.5A,B, respectively). Stable overexpression of Prx4 was performed in HT29 cell line (Figure 4.5C) and several of the experiments above were repeated. Prx4-Flag cells and Vector control cells had comparable rate of wound healing (Figure 4.5D). Prx4-Flag cells were more efficient than Vector control cells at wound healing, although the difference was not statistically significant (Figure 4.5E). Together, these data suggest that loss of Prx4 reduces invadopodia formation and hence the invasiveness of human CRC cell lines in vitro.

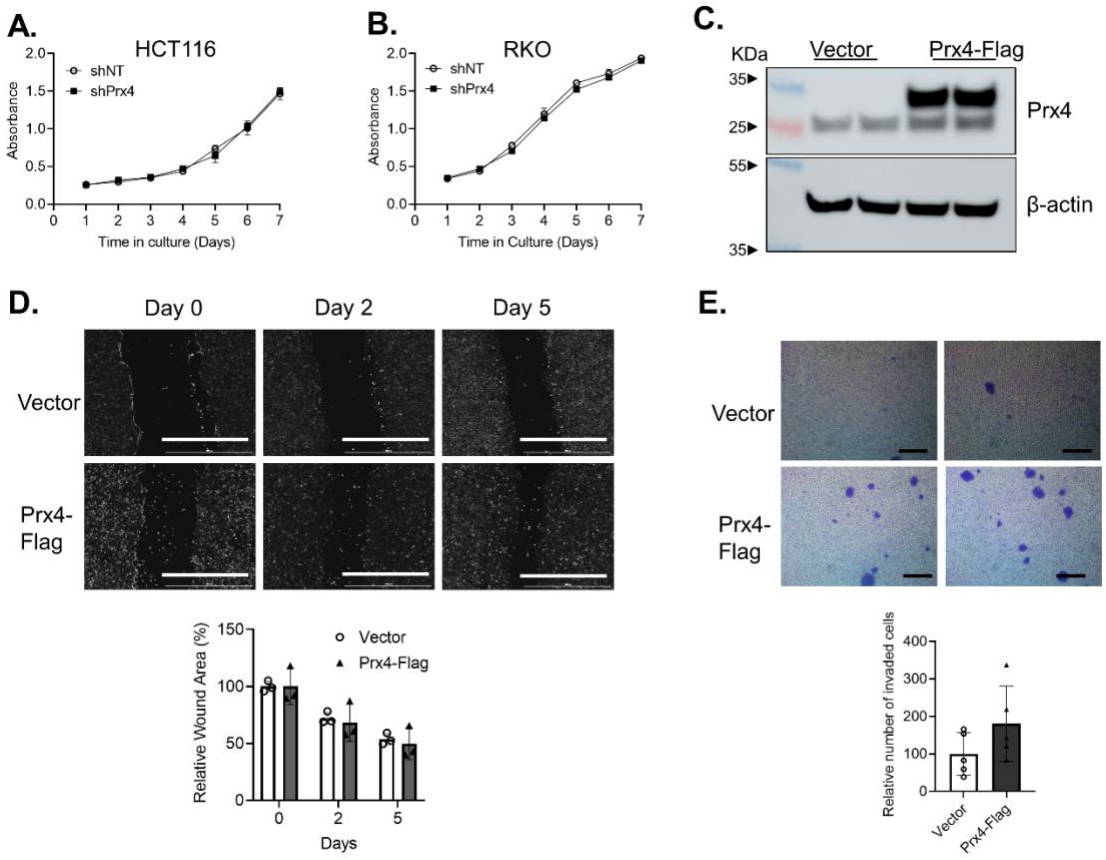

Figure 4.5. Knockdown of Prx4 does not affect cell proliferation of HCT116 and RKO and overexpression of Prx4 increases migration and invasion in HT29.
Cell proliferation curve of (A) HCT116 and (B) RKO cell lines. (C) Western Blot results showing stable knockdown of Prx4 using shRNA in HT29. (D) Wound healing assay using HT29 Vector Control and HT29 Prx4-Flag cell lines. Bar =1000 μm. Quantification is shown in bar graph below the images. (E) Transwell cell invasion assay using HT29 Vector Control and HT29 Prx4-Flag cell lines. Bar =200 μm. Quantification is shown below the images. Compared to shNT, *$p<0.05$ (Student's t-test).

4.2.3 Prx4 knockdown reduces metastasis of human colon cancer cell lines in NSG mice in vivo

From cell culture studies, we found that Prx4 is critical for migration and invasion of CRC cell lines HCT116 and RKO. Previous studies have reported positive correlation between Prx4 expression and invasion and metastasis [145, 146]. However, whether manipulation of Prx4 in HCT116 cells affects metastasis in vivo has not been studied. Therefore, we implanted HCT116 shNT and shPrx4 cells into the cecum wall of NSG mice to examine the ability of these cells to grow and metastasize in vivo (Figure 4.6A). 4 weeks after injection, the mice were humanely euthanized and tissues were collected. Compared with mice injected with shNT cells, the rate of metastasis in mice injected with shPrx4 cells was significantly reduced. Fixed tissues from each group were randomly chosen and tissue slides were obtained by sequential sectioning. H&E staining and histopathology analysis were performed. Microscopic analysis of H&E stained slides confirmed that the numbers of metastasized tumor nodules in lungs (Figure 4.6B) and livers (Figure 4.6C) was higher in shNT group than shPrx4 group (Figure 4.6D). These data suggest that Prx4 positively contributes to metastasis in vivo, which is consistent with the observation that knockdown of Prx4 leads to reduced migration and invasion of HCT116 cells in vitro.

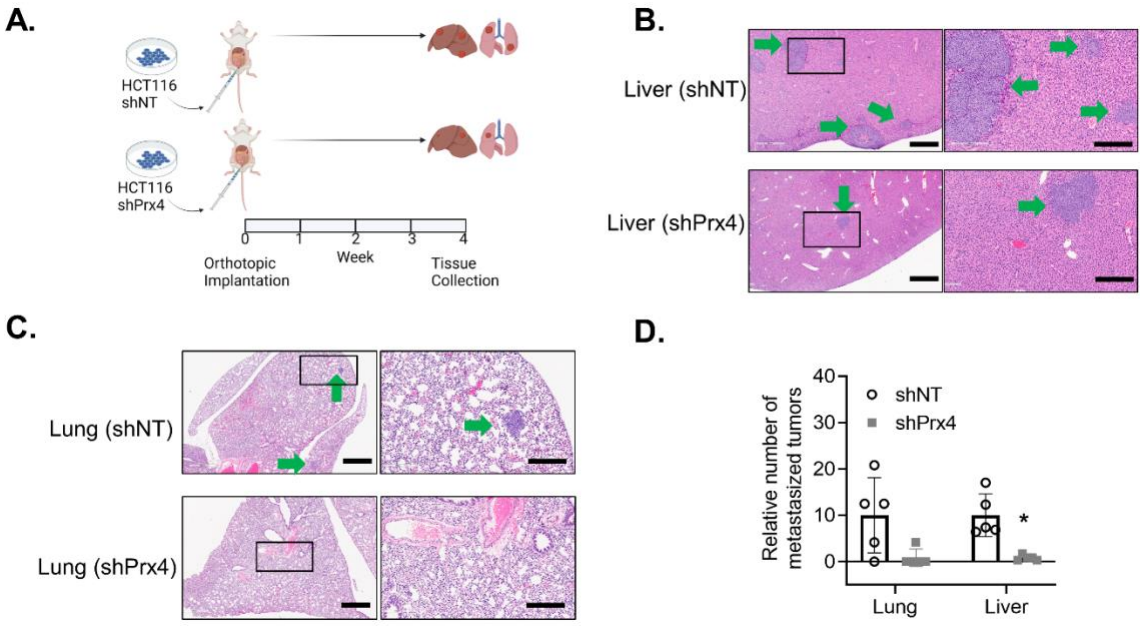

Figure 4.6. Knockdown of Prx4 in HCT116 cells reduces metastasis in vivo in a mouse orthotopic implantation model.
(A) Schematic presentation of the orthotopic injection protocol. Hematoxylin and eosin (H&E) staining and microscopic tumor metastasis found in the liver (B) and lung (C) of mice injected with HCT116 shNT and shPrx4 cells. Arrows heads indicate tumor metastasis (bar = 800 μm) and black square indicates the spot zoomed in (bar = 300μm). (D) Quantitative analysis of data from B and C. Compared to shNT, *p<0.05 (Student's t-test).

4.2.4 RNA sequencing and GSEA analysis

To identify the underlying mechanisms through which Prx4 contributes to malignant phenotype, we performed RNA-Sequencing analysis using HCT116 shNT and shPrx4 cells. The similarity among the three independent samples used in each group is shown in Figure 4.7A. Upon comparing the RNA profiles of shNT cell lines to their shPrx4 counterparts, 185 genes were identified as differentially expressed genes including Prx4 but not other Prxs (Figure 4.7B–D). Gene Set Enrichment Analysis using Hallmark gene sets to identify gene sets enriched in shPrx4 cell lines detected changes in pathways such as TNFα signaling via NFκB, p53 pathway, and apoptosis (Figure 4.7E). Of these,

immunoblotting was used to validate the TNFα signaling via NF-κB pathway. HCT116, RKO and HT29 cell lines were treated with increasing concentrations of TNFα for 24 hours. Western blot results confirm that NF-κB family protein p-p65 is increased in Prx4 knockdown cells and decreased in Prx4 overexpression cells (Figure 4.8A–C). Activation of NF-κB upon loss of Prx4 observed here is consistent with what is reported in literature [30].

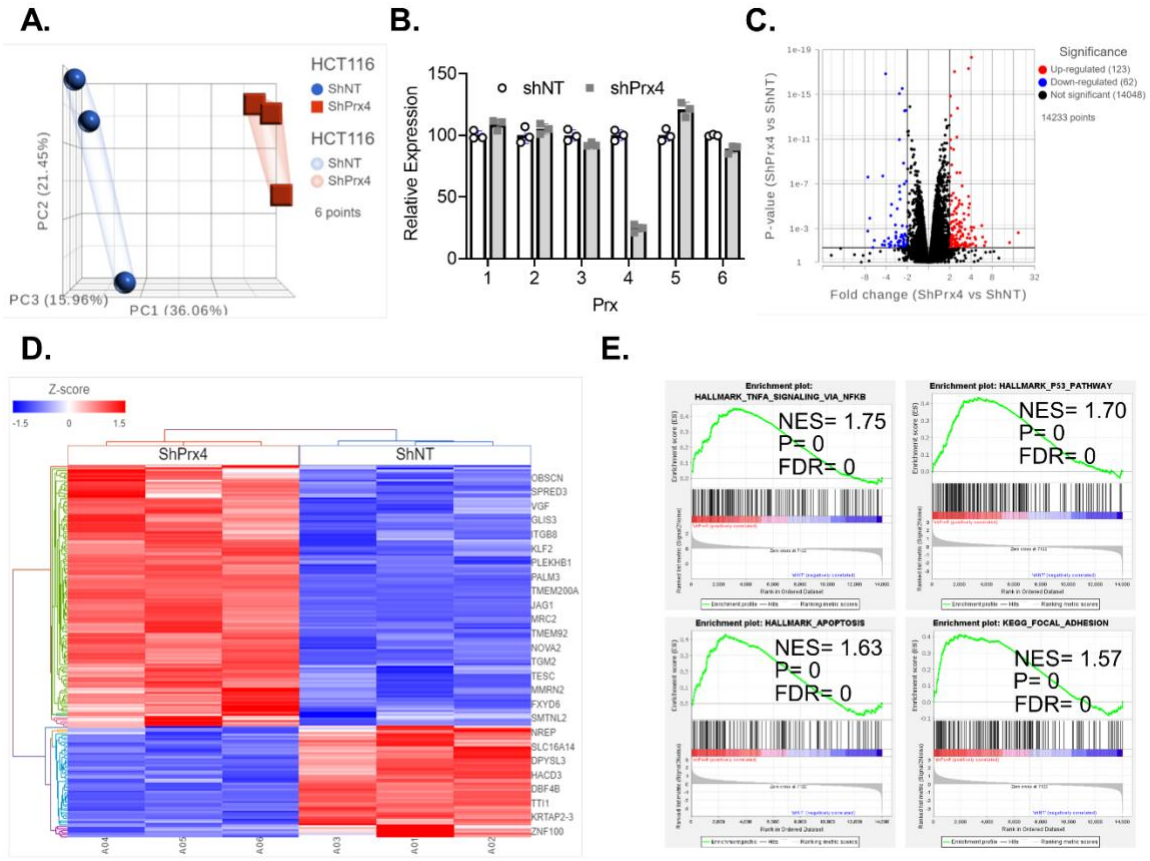

Figure 4.7. RNA Sequencing of HCT116 shNT and shPrx4 cells.
(A) Principal component analysis (PCA) RNA-seq data from shNT and shPrx4 (n = 3 per group) shows the relatedness between samples. (B) Relative transcript levels of Prx family members in HCT116 shNT and shPrx4 cells per RNA Sequencing results. (C) Red dots indicate genes that are expressed at least 2- fold higher in shPrx4 cells; blue dots indicate genes that expressed at least 2-fold lower in shPrx4 cells; black dots indicate genes that show no significant difference between shNT and shPrx4 cells. (D) Comparison of differential expressed genes with significant P value indicates clustering pattern of genes upregulated (red) and downregulated (blue) in shPrx4 cells. (E) GSEA

revealed that differentially expressed genes in shPrx4 cells leads to activation of several signaling pathways.

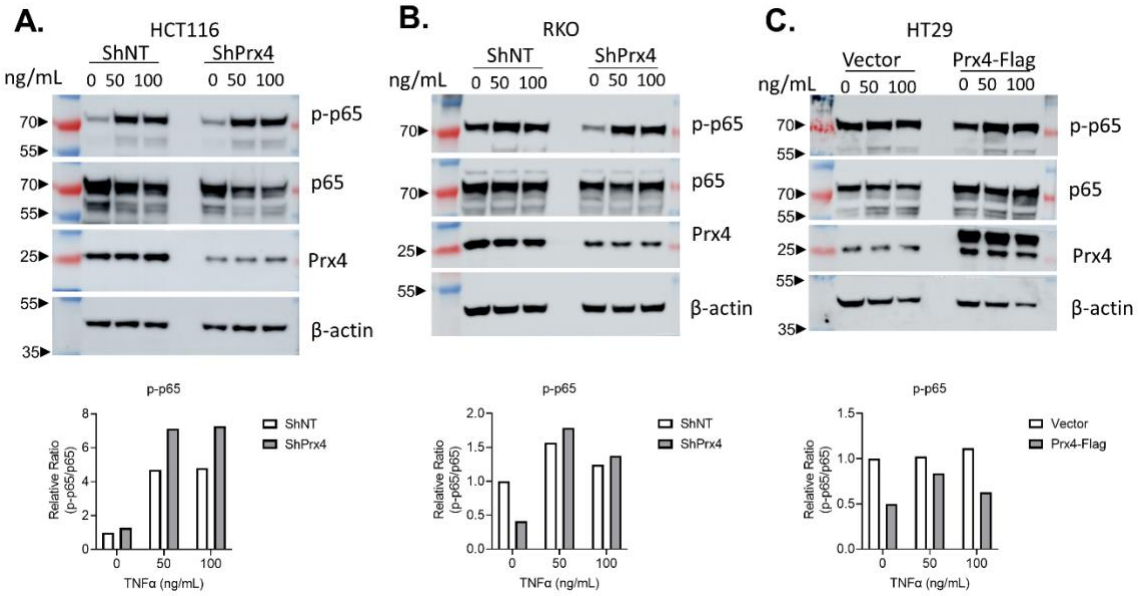

Figure 4.8. Loss of Prx4 activates NF-κB signaling in colon cancer cell lines.
Western blot results of p65 (RelA) and phospho-p65 (Ser536) proteins 24 hours post TNFα treatment in (A) HCT116, (B) RKO and (C) HT29. Quantification is shown on bar graphs.

4.2.5 Loss of Prx4 upregulates DKK1 and increases focal adhesion

Leading edge analysis of enriched gene sets with nominal p-value less than 0.1 was performed to identify leading edge genes in common between these gene sets. Dickkopf-1 (DKK1) was identified to be one of common leading edge genes (Figure 4.9A). It is well-established that Wnt/β-catenin signaling contributes to tumorigenesis and metastasis in CRC [279, 280]. DKK1 binds to LRP6 and causes its endocytosis, thus preventing activation of Wnt/β-catenin pathway. Overexpression of DKK1 has been shown to impair migration and invasion of HCT116 cells [281]. Therefore, we decided to investigate this alteration in expression of DKK1 upon Prx4 knockdown. The upregulation of DKK1 expression was first validated by monitoring the mRNA and protein levels of DKK1 using

qRT-PCR and Western blot respectively (Figure 4.9B-D). Prx4 knockdown was also found to decrease β-catenin protein expression (Figure 4.9C). In HT29 cells, DKK1 was downregulated in HT29 Prx4 overexpression cells compared to Vector control cells, although β-catenin expression was not altered (Figure 4.9D). When HCT116 cells were treated with increasing concentrations of Wnt3a conditioned medium collected from HEK293T, we detected lower increase in phosphorylation of LRP6 (S1490) in shPrx4 cells compared to shNT cells, suggesting Prx4 depletion-induced upregulation of DKK1 is indeed capable of Wnt signaling inhibition (Figure 4.9E). These data suggest that Prx4 suppresses DKK1 and enhances activation of Wnt signaling to promote colorectal cancer progression.

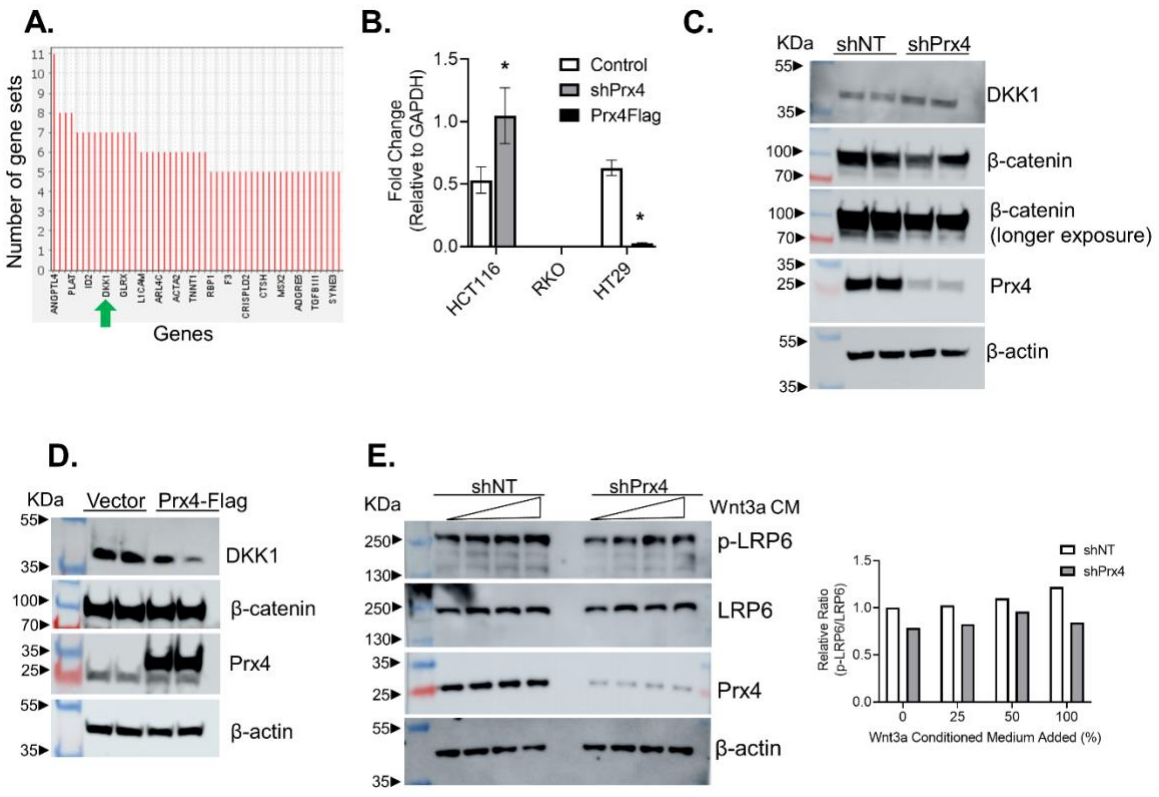

Figure 4.9. DKK1 is upregulated in Prx4 knockdown cells.
(A) Leading edge analysis shows genes that contributed the most to enriched gene sets. DKK1 is highlighted with green arrowhead. (B) Quantitative real-time PCR was used to

measure the levels of DKK1 mRNA in HCT116, RKO and HT29 cell lines. (C) Western Blot results showing expression of DKK1 and β-catenin in HCT116 shNT and shPrx4 cell lysates. (D) Western Blot results showing expression of DKK1 and β-catenin in HT29 Vector control and Prx4-Flag cell lysates. (E) Western Blot results showing expression of phospho-LRP6 Ser1490 and total LRP6 in HCT116 shNT and shPrx4 cells after treatment with Wnt3a conditioned medium for 24 hours. Quantification is shown in bar graph on the right.

RNA-Sequencing and GSEA analysis revealed enrichment of focal adhesion (FA) signaling in HCT116 shPrx4 compared to HCT116 shNT cells (Figure 4.7E). Integrins mediate attachment of cells to extracellular matrix through focal adhesions. Focal adhesions connect cells to the ECM and transmit ECM-derived signals to cellular pathways. During cell migration, focal adhesions are continuously assembled and disassembled to generate forces for cell movement. Therefore, the role of Prx4 expression levels in focal adhesion was examined. Cell-matrix adhesion was measured by seeding cells into fibronectin-coated dishes, allowed to adhere for 20 minutes, gently washed, and the number of adhered cells counted using CellTiter-Glo. In this assay, Prx4 depleted cells were found to have stronger adhesion while Prx4 overexpression cells had lower adhesion than control cells (Figure 4.10A,B). Focal Adhesion Kinase (FAK) localizes to FAs and plays a major role in their assembly and disassembly. Autophosphorylation of Y397 residue of FAK in response to integrin clustering initiates assembly of FAs. FAK is even more important for disassembly of FAs such that inhibition of FAK stabilizes steady-state FAs [282, 283]. To confirm that FAK plays a role in Prx4-mediated cell adhesion, HCT116 shNT and shPrx4 cells were seeded onto Fibronectin coated or uncoated wells for 1 hour and activation of FAK was compared. Western blot results show that phosphorylation of Y397 increases in the presence of fibronectin and increases even more significantly when cells have lower levels of Prx4 (Figure 4.10C). To examine the role of DKK1 in focal

adhesion, DKK1 knockdown was first performed using increasing concentrations of esiRNA (Figure 4.10D). Next, the adhesion of HCT116 shNT and shPrx4 cells to fibronectin was re-measured after 48 hours treatment with 400 ng/mL siCon control or esiDKK1. Decrease in DKK1 levels significantly reduced adhesion of cells to the matrix in both shNT and shPrx4 cells (Figure 4.10E). To confirm that DKK1 upregulation in the absence of Prx4 contributes to malignant phenotype, HCT116 shNT and shPrx4 cells were also treated with siRNA negative control or esiRNA against DKK1 for 48 hours, and migration and invasion assays were performed. Depletion of DKK1 increased the rate of cell migration in both shNT and shPrx4 cell lines (Figure 4.10F). In addition, the difference in migration between shNT and shPrx4 cells was no longer significant upon depletion of DKK1 (Figure 4.10F). In matrigel invasion assay, depletion of DKK1 partially rescued invasiveness of shPrx4 cells (Figure 4.10G). This suggests that DKK1 plays an important role in increasing focal adhesion and decreasing migration and invasion of colon cancer cells.

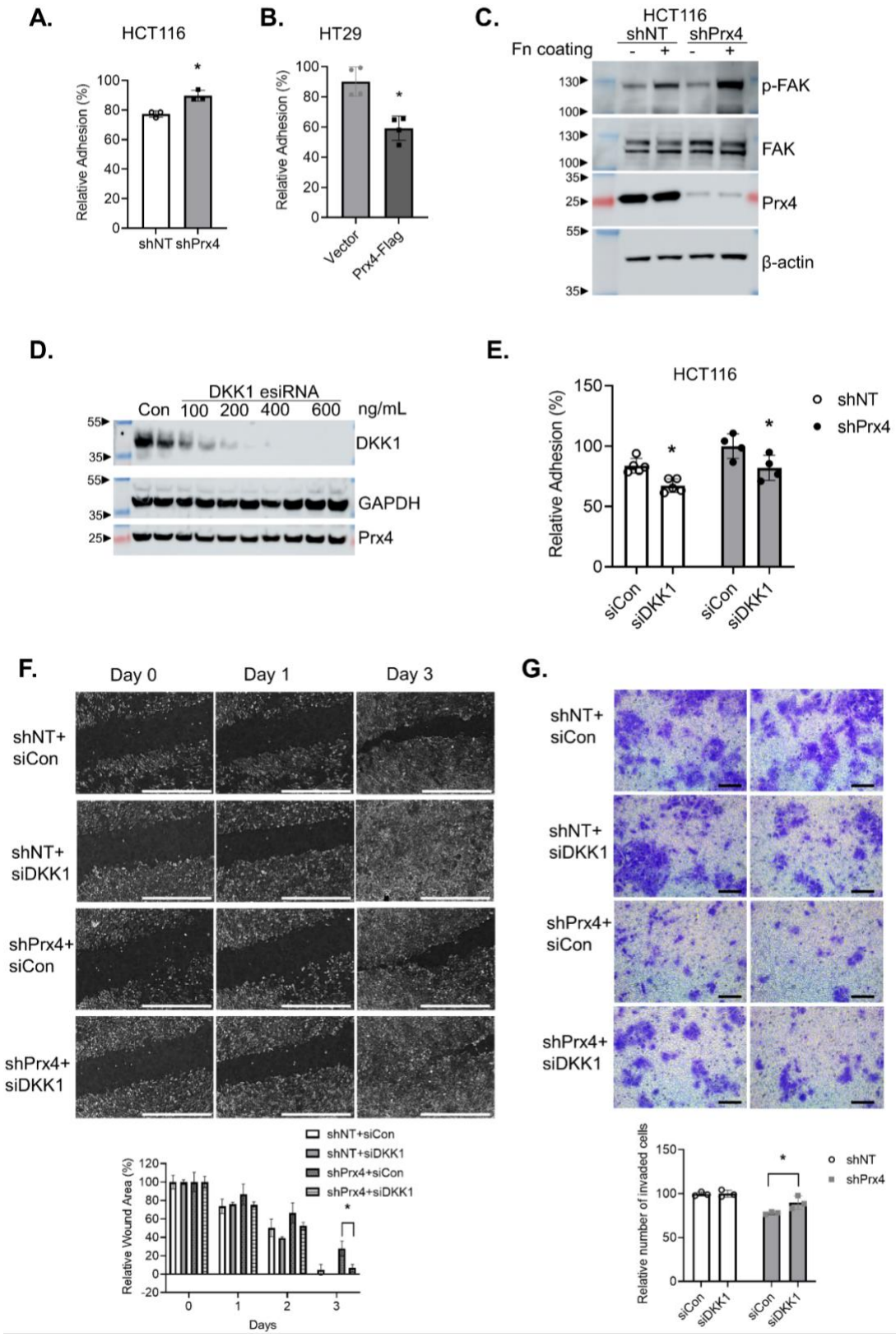

Figure 4.10. Knockdown of Prx4 increases focal adhesion which is reverted by depletion of DKK1.

(A) Cell adhesion assay of HCT116 shNT and shPrx4 cells in fibronectin-coated cell culture dish. (B) Cell adhesion assay of HT29 Vector control and Prx4-Flag cells in fibronectin-coated cell culture dish. (C) Western blot results of HCT116 shNT and shPrx4 cells seeded into fibronectin coated or uncoated cell culture dish and harvested after 1 hour. (D) Western Blot results showing expression of DKK1 after treatment with siRNA negative control and increasing concentrations of DKK1 esiRNA for 48 hours. 400ng/mL was selected for use in subsequent experiments. (E) Cell adhesion assay of HCT116 shNT siCon or siDKK1 (left) and HCT116 shPrx4 siCon or siDKK1 (right) cells in fibronectin-coated cell culture dish. Compared to siCon, *$p<0.05$ (Two-way ANOVA) (F) Wound healing assay after treatment of HCT116 with negative control siRNA or DKK1 esiRNA for 48 hours. Bar =1000 μm. (G) Transwell cell invasion assay after treatment of HCT116 with negative control siRNA or DKK1 esiRNA. Two replicates shown for each group. Bar =200 μm. Compared to shNT, *$p<0.05$ (Two-way ANOVA).

4.3 Discussion

In this study, we aimed to learn whether and how Prx4 facilitates metastasis of CRC. Loss of Prx4 significantly decreased migration and invasion of CRC cell lines HCT116 and RKO. We also discovered that decreased invasiveness upon loss of Prx4 is due to reduced invadopodia formation. Implantation of HCT116 shNT and shPrx4 cells into the cecum wall of NSG mice revealed that shPrx4 cell metastasized to the lungs and livers at much lower rate than shNT cells. DKK1 is upregulated and β-catenin is downregulated when Prx4 is depleted in HCT116 cells. We found that depletion of DKK1 in shPrx4 cells reversed migration, adhesion and invasion phenotypes. Thus, Prx4 facilitates metastasis of CRC at least partially by suppressing DKK1 expression.

These observations are supported by previously published studies. There is a positive correlation between Prx4 protein expression in CRC tissues and the depth of invasion, lymph node metastasis, tumor stage and shorter survival [145]. Verifying and building on the correlation suggested by this study, we performed loss-of-function and gain-of-function studies to establish the causal role of Prx4 on CRC progression using in vitro and in vivo models. Similarly, we previously discovered that depletion of Srx

decreases migration, invasion and metastasis of CRC cell lines [235, 284]. Even though Prx4 is the preferred substrate of Srx, Srx function in CRC progression occurred in a Prx4-independent manner. Here, we have shown that loss of Prx4 produces identical phenotype as loss of Srx, although this occurs through a different mechanism. Therefore, combined targeting of Srx and Prx4 (or their downstream targets Fascin and DKK1 respectively) could provide additive or synergistic effects on the treatment of CRC. Furthermore, it has been reported previously that overexpression of DKK1 impairs migration and invasion of HCT116 cells [281, 285]. We have shown that one potential mechanism to upregulate the expression of metastasis-suppressor DKK1 is through depletion of Prx4. Thus, our data establishes the causative role of Prx4 in colorectal cancer progression and identifies loss of DKK1 as one of the major downstream factors.

Prx4 also has oncogenic role in other cancers [30]. Prx4 is associated with bone metastasis of prostate cancer and breast cancer. Knockdown of Prx4 in MDA-MB-231 cells reduced osteoclast formation in vitro [129]. Similarly, knockdown of Prx4 in prostate cancer cell line PC3 decreased the ability of cancer cells to induce osteoclastogenesis in vitro and osteolysis in vivo [129]. In glioma orthotopic transplantation model where neurosphere-forming GBM cells from Mut6 mouse were injected into the striatum of normal mice, knockdown of Prx4 increased survival of recipient mice by 35% [158]. Finally, in pancreatic cancer, Prx4 is associated with liver metastases and shorter survival of patients [166]. Orthotopic implantation of human cancer cell lines MIA PaCa-2 and PANC-1 in mice pancreases showed that loss of Prx4 increased disease-free survival. Thus, Prx4 is positively associated with metastasis of colorectal cancer as well as other cancers.

Inflammatory bowel disease including Ulcerative colitis and Crohn's disease is a major risk factor for development of colorectal cancer. In IHC of COAD tissue microarray, no significant changes in Prx4 staining were observed in Ulcerative colitis and Crohn's disease samples relative to normal colon tissue. This is in contrast to a proteomics study which identified Prx4 as one of the upregulated proteins in UC [96]. However, both of these studies had a relatively small sample size of IBD samples. Therefore, further investigation needs to be completed with a larger sample size to clarify the expression levels of Prx4 in IBD. In addition, even if its total expression is unchanged, alterations in the enzymatic activity of Prx4 could contribute to different severities of colitis. The oxidation state of Prx4 (sulfinic acid vs. sulfonic acid forms) can be determined as a measure of its antioxidant enzyme activity. Similarly, while our study hints at a role for Prx4 in inflammation, additional studies are necessary. We have shown previously that Prx4 can affect secretion of cytokines and chemokines to increase inflammatory cell infiltration into colon and colon tumors [172]. One of the possible mechanisms by which Prx4 regulates inflammation is through transcription factor NF-κB as indicated by RNA-Sequencing of HCT116 cells. In several colon cancer models, NF-κB has been reported to negatively regulate β-catenin activity in Wnt-dependent and -independent manner [286-288]. In our orthotopic implantation model, human CRC cells HCT116 shNT and shPrx4 cells were injected into immunodeficient NSG mice. Therefore, a full overview of Prx4-regulated inflammation in metastasis is not possible. Immunocompetent syngeneic mouse model could be used in future studies to address this limitation. Thus, detailed mechanistic studies are warranted to define the role of Prx4 in immune cell function in colitis and CRC progression.

Another limitation of our study is that the reduced activation of LRP6 in Prx4 knockdown cells was only demonstrated in HCT116. This experiment needs to be conducted in additional models with and without activating mutations in Wnt/β-catenin pathway proteins. Such experiments would clarify β-catenin degradation-dependent and -independent effects of Prx4-DKK1 axis in CRC progression. The expression of DKK1 increased at mRNA and protein level after knockdown of Prx4. As shown in Figure 4.10, such upregulation of DKK1 contributes to the reduced migration and invasion phenotypes of CRC. However, the mechanism by which Prx4 loss induces DKK1 expression is not understood. Identification of the epigenetic or genetic changes responsible for DKK1 upregulation would help design strategies to translate this into clinic. Additionally, while we used cell adhesion assay to provide a snapshot of focal adhesion formation and stability, live-cell imaging to monitor the turnover of foal adhesions is also necessary to further illuminate the role of Prx4 in cell-matrix adhesions. The detailed mechanism of how Prx4 or DKK1 regulate focal adhesion, including whether redox signaling or Wnt/ β-catenin signaling pathways are involved, needs to be addressed. Having established that Prx4 contributes to CRC progression through changes in DKK1 and focal adhesion pathways, in future studies, we can target Srx and Prx4 expression and enzyme activities and/or DKK1, focal adhesion pathways for improved treatment of CRC. In addition, we identified numerous other signaling pathways significantly altered upon Prx4 knockdown such as activation of NF-κB, p53 and increased apoptosis. In vitro and in vivo studies are needed to further delineate the contribution of each of these pathways to Prx4-mediated CRC progression.

In summary, we demonstrated in this study that knockdown of Prx4 in CRC cell lines decreases migration, invasion in vitro and metastasis in vivo. Prx4 suppresses DKK1 expression and decreases focal adhesion to promote these oncogenic phenotypes. This study identifies Prx4 as a therapeutic target for CRC treatment. Prx4 inhibition or suppression of expression could prove highly useful in combination with existing treatments to improve outcome for patients.

CHAPTER 5. SUMMARY

5.1 Summary and future directions

The results presented in this dissertation demonstrate that Peroxiredoxin IV (Prx4) promotes initiation of colorectal cancer. Treatment of wildtype and Prx4 null mice with Azoxymethane/ Dextran sulfate sodium (AOM/DSS) resulted in lower tumor incidence, multiplicity, volume and tumor burden in Prx4 knockout mice compared to wildtype mice. Mechanistic studies revealed that loss of Prx4 leads to increased cell death through lipid peroxidation and lower infiltration of inflammatory cells in the knockout tumors compared to wildtype. Our findings reported in chapter four demonstrate that Prx4 promotes progression of colorectal cancer. Knockdown of Prx4 in HCT116 and RKO cell lines resulted in decreased cell migration and invasion in vitro and decreased metastasis in vivo. mRNA sequencing followed by Gene Set Enrichment Analysis (GSEA) identified several signaling pathways significantly altered in Prx4 knockdown cells. Of these, upregulation of DKK1 and its contribution to suppression of malignant phenotypes was validated through rescue experiments. These results, along with those previously reported in literature, are summarized in Figure 5.1. These different contributions of Prx4 to colorectal cancer development need to be characterized further. For example, it is not clear which biochemical functions of Prx4- antioxidant or protein chaperone or both- are involved in suppressing DKK1 expression and modulating cytokine secretion. In addition, the cellular compartments in which Prx4 regulates these different pathways is not yet clear.

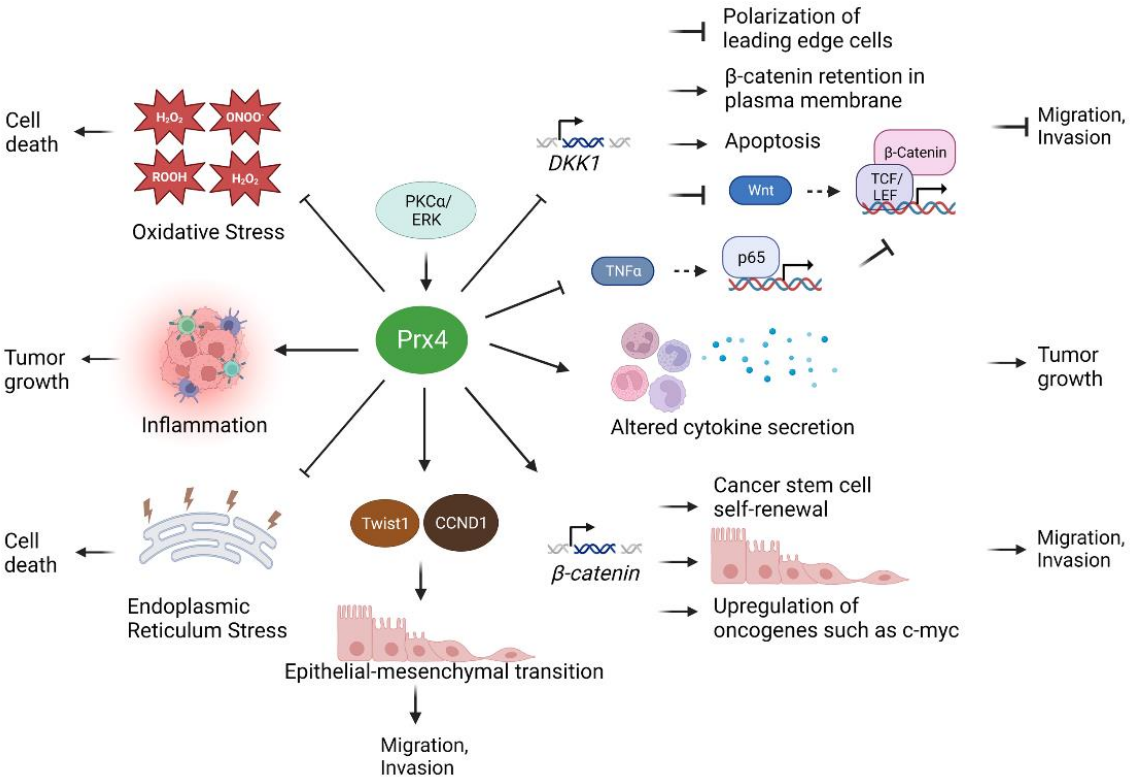

Figure 5.1. Prx4 promotes colorectal cancer formation and metastasis.
PKCα/ERK pathway causes upregulation of Prx4. Increased Prx4 promotes AOM/DSS-induced colorectal tumor formation by increasing inflammation and protecting dysplastic cells against cell death. Increase in Prx4 also promotes migration and invasion of colorectal cancer due in part to suppression of DKK1 and β-catenin transcription.

Based on our findings that Prx4 promotes inflammatory tumor microenvironment, the next questions we need to ask are whether myeloid cell-specific or lymphoid cell-specific knockout of Prx4 is enough to replicate results of whole-body knockout in an in vivo colon carcinogenesis model. In Prx4 knockout mice, we observed decreased presence of both macrophages and lymphocytes after DSS and AOM/DSS treatment. We also demonstrated that macrophages and plasma cells express high levels of Prx4. ROS play a critical role in activation of B-cell receptor and T-cell receptor signaling [289]. Myeloid cells are a major source of oxidants in tumor microenvironment, and these cells also alter redox state in tumor cells via cytokine secretion [290, 291]. It is likely that expression level

of Prx4 affects the ROS-mediated signaling in these cell types. However, whether Prx4 affects their function through other mechanisms (such as through protein folding) needs to be inspected. Myeloid-specific or lymphoid-specific depletion of Prx4 would illuminate these mechanisms and help us identify specific cell types and signaling pathways to be targeted for clinical treatment. One limitation of our study is that we only examined major types of immune cells in DSS treated colons and AOM/DSS treated tumors. In future studies, a more holistic approach (such as flow cytometry and/or single cell RNA-Sequencing) should be utilized to comprehensively characterize the immune microenvironment in CRC tumors. Further studies also need to be conducted to understand the role of Prx4 in inhibiting tumor-extrinsic inflammatory triggers while promoting tumor-associated inflammation.

AOM/DSS model utilized here is ideally used to model non-hereditary, inflammation-driven CRC. Therefore, our findings apply best to colitis-associated cancer, and caution must be taken when translating the findings to other subtypes of CRC. Further studies must be conducted in other mouse models, such as mouse with mutations in the *Apc* gene, to investigate the function of Prx4 in development of sporadic and familial colon cancer. This model is especially relevant now that Prx4 is known to regulate transcription of Wnt signaling inhibitor DKK1. In addition, another limitation of our study is that the effect of Prx4 loss on host microbiota was not studied. Intestinal bacteria play an important role not only in metabolic activation of pro-carcinogen AOM and increasing the severity of colitis upon DSS-induced epithelial injury, but also in metastasis of intestinal tumors [227, 292-294]. Therefore, it is critical that future studies address how Prx4 modulates intestinal microbiota at basal conditions and in different stages of CRC.

Prx4 is frequently upregulated in cancers including colorectal cancer. We have clearly shown that increased Prx4 is advantageous to cancer formation and survival. This highlights the urgent need for development of inhibitors for expression and activity of Prx4. It is not an easy task to find an inhibitor that is specific for Prx4-specific thiols without targeting other thiols, although the search is ongoing. Unfortunately, the process of Prx4 upregulation is also not well-understood. Any epigenetic modifications as well as transcription factors responsible for increase in Prx4 in CRC are yet be determined. Huang et al. have suggested involvement of EGFR- Protein Kinase Cα pathway in transcription of Prx4, but detailed mechanistic studies must be conducted to delineate the process of Prx4 upregulation [147]. Therefore, identification of Prx4 expression and/or enzyme activity inhibitors to target increased cell death of tumor cells could enhance the outcome of cancer treatment upon combination with radiation or chemotherapy.

As mentioned previously, Prx4 is secreted into the ECM. A major limitation of our study is that the role of extracellular Prx4 in cancer development was not considered. This gap in knowledge must be addressed in future studies. First, we need to determine the mechanism and functions of secreted Prx4 in normal physiological conditions. Then, whether secreted Prx4 serves pro-cancer function or anti-cancer function can be examined. It would also be interesting to study the levels of secreted Prx4 and their correlations with CRC stages and/or treatments. If a positive correlation is detected, use of serum Prx4 as a novel non-invasive biomarker could be explored. Thus, there is an urgent need to study the functions of extracellular Prx4.

In summary, our study has led to a better understanding of the contribution of Prx4 in colorectal cancer development. This dissertation has demonstrated that Prx4 promotes

inflammation-associated colorectal tumor formation through increased inflammation and that Prx4 promotes migration and invasion of colorectal cancer through suppression of DKK1. Thus, our study identifies Prx4 as an important therapeutic target for prevention and treatment of colorectal cancer.

APPENDIX

Abbreviations

AOM	azoxymethane
AR	androgen receptor
CHOP	ccaat-enhancer-binding protein homologous protein
COAD	colon adenocarcinoma
COX	cyclooxygenase
CRC	colorectal cancer
CREB	camp response element-binding protein
CSC	cancer stem cells
DAB	3,3′-diaminobenzidine
DCFH-DA	2'-7'-dichlorodihydrofluorescein diacetate
DKK1	dickkopf1
DKO	double knockout
DMBA	7,12-dimethylbenz[a]anthracene
DSS	dextran sulfate sodium
ECM	extracellular matrix
EGFR	epidermal growth factor receptor
EMT	epithelial to mesenchymal transition
ER	endoplasmic reticulum
FAK	focal adhesion kinase
GSEA	gene set enrichment analysis
GSH	glutathione
HCC	hepatocellular carcinoma
IBD	inflammatory bowel disease
IGFBP	insulin-like growth factor-binding protein
IHC	immunohistochemistry
NSCLC	non-small cell lung cancer
PDGF	platelet-derived growth factor
PDI	protein disulfide isomerase
PRX	peroxiredoxin
PTEN	phosphatase and tensin homolog
QSOX	quiescin q6 sulfhydryl oxidase
READ	rectum adenocarcinoma
RIPA	radioimmunoprecipitation
RNS	reactive nitrogen species
ROS	reactive oxygen species
SRX	sulfiredoxin
TBARS	thiobarbituric acid reactive substances
TXNDC	thioredoxin domain containing protein
UALCAN	university of alabama at birmingham cancer data analysis portal
UC	ulcerative colitis
UPR	unfolded protein response

REFERENCES

1. Pizzorno, J., Glutathione! *Integrative medicine (Encinitas, Calif.)* **2014,** 13, (1), 8-12.
2. Fridovich, I., Superoxide radical and superoxide dismutases. *Annu Rev Biochem* **1995,** 64, 97-112.
3. Glorieux, C.; Calderon, P. B., Catalase, a remarkable enzyme: targeting the oldest antioxidant enzyme to find a new cancer treatment approach. *Biological chemistry* **2017,** 398, (10), 1095-1108.
4. Brigelius-Flohé, R.; Maiorino, M., Glutathione peroxidases. *Biochim Biophys Acta* **2013,** 1830, (5), 3289-303.
5. Nogoceke, E.; Gommel, D. U.; Kiess, M.; Kalisz, H. M.; Flohé, L., A unique cascade of oxidoreductases catalyses trypanothione-mediated peroxide metabolism in Crithidia fasciculata. *Biological chemistry* **1997,** 378, (8), 827-36.
6. Bryk, R.; Griffin, P.; Nathan, C., Peroxynitrite reductase activity of bacterial peroxiredoxins. *Nature* **2000,** 407, (6801), 211-5.
7. Hillas, P. J.; del Alba, F. S.; Oyarzabal, J.; Wilks, A.; Ortiz De Montellano, P. R., The AhpC and AhpD antioxidant defense system of Mycobacterium tuberculosis. *J Biol Chem* **2000,** 275, (25), 18801-9.
8. Milev, N. B.; Rhee, S. G.; Reddy, A. B., Cellular Timekeeping: It's Redox o'Clock. *Cold Spring Harbor perspectives in biology* **2018,** 10, (5).
9. Troussicot, L.; Burmann, B. M.; Molin, M., Structural determinants of multimerization and dissociation in 2-Cys peroxiredoxin chaperone function. *Structure* **2021,** 29, (7), 640-654.
10. Kim, K.; Kim, I. H.; Lee, K. Y.; Rhee, S. G.; Stadtman, E. R., The isolation and purification of a specific "protector" protein which inhibits enzyme inactivation by a thiol/Fe(III)/O2 mixed-function oxidation system. *J Biol Chem* **1988,** 263, (10), 4704-11.
11. Tartaglia, L. A.; Storz, G.; Brodsky, M. H.; Lai, A.; Ames, B. N., Alkyl hydroperoxide reductase from Salmonella typhimurium. Sequence and homology to thioredoxin reductase and other flavoprotein disulfide oxidoreductases. *J Biol Chem* **1990,** 265, (18), 10535-40.
12. Chae, H. Z.; Chung, S. J.; Rhee, S. G., Thioredoxin-dependent peroxide reductase from yeast. *J Biol Chem* **1994,** 269, (44), 27670-8.
13. Edgar, R. S.; Green, E. W.; Zhao, Y.; van Ooijen, G.; Olmedo, M.; Qin, X.; Xu, Y.; Pan, M.; Valekunja, U. K.; Feeney, K. A.; Maywood, E. S.; Hastings, M. H.; Baliga, N. S.; Merrow, M.; Millar, A. J.; Johnson, C. H.; Kyriacou, C. P.; O'Neill, J. S.; Reddy, A. B., Peroxiredoxins are conserved markers of circadian rhythms. *Nature* **2012,** 485, (7399), 459-64.
14. Nelson, K. J.; Knutson, S. T.; Soito, L.; Klomsiri, C.; Poole, L. B.; Fetrow, J. S., Analysis of the peroxiredoxin family: using active-site structure and sequence information for global classification and residue analysis. *Proteins* **2011,** 79, (3), 947-64.
15. NCBI Resource Coordinators, Database resources of the National Center for Biotechnology Information. *Nucleic Acids Res* **2018,** 46, (D1), D8-d13.

16. Cao, Z.; Lindsay, J. G., The Peroxiredoxin Family: An Unfolding Story. *Subcell Biochem* **2017,** 83, 127-147.
17. Jiang, H.; Thapa, P.; Hao, Y.; Ding, N.; Alshahrani, A.; Wei, Q., Protein Disulfide Isomerases Function as the Missing Link Between Diabetes and Cancer. *Antioxid Redox Signal* **2022**.
18. Schröder, E.; Ponting, C. P., Evidence that peroxiredoxins are novel members of the thioredoxin fold superfamily. *Protein science : a publication of the Protein Society* **1998,** 7, (11), 2465-8.
19. Zeida, A.; Reyes, A. M.; Lebrero, M. C.; Radi, R.; Trujillo, M.; Estrin, D. A., The extraordinary catalytic ability of peroxiredoxins: a combined experimental and QM/MM study on the fast thiol oxidation step. *Chemical communications (Cambridge, England)* **2014,** 50, (70), 10070-3.
20. Seo, M. S.; Kang, S. W.; Kim, K.; Baines, I. C.; Lee, T. H.; Rhee, S. G., Identification of a new type of mammalian peroxiredoxin that forms an intramolecular disulfide as a reaction intermediate. *J Biol Chem* **2000,** 275, (27), 20346-54.
21. Shau, H.; Kim, A., Identification of natural killer enhancing factor as a major antioxidant in human red blood cells. *Biochem Biophys Res Commun* **1994,** 199, (1), 83-8.
22. Woo, H. A.; Yim, S. H.; Shin, D. H.; Kang, D.; Yu, D. Y.; Rhee, S. G., Inactivation of peroxiredoxin I by phosphorylation allows localized H(2)O(2) accumulation for cell signaling. *Cell* **2010,** 140, (4), 517-28.
23. Chang, T. S.; Jeong, W.; Choi, S. Y.; Yu, S.; Kang, S. W.; Rhee, S. G., Regulation of peroxiredoxin I activity by Cdc2-mediated phosphorylation. *J Biol Chem* **2002,** 277, (28), 25370-6.
24. Goemaere, J.; Knoops, B., Peroxiredoxin distribution in the mouse brain with emphasis on neuronal populations affected in neurodegenerative disorders. *The Journal of comparative neurology* **2012,** 520, (2), 258-80.
25. Peskin, A. V.; Dickerhof, N.; Poynton, R. A.; Paton, L. N.; Pace, P. E.; Hampton, M. B.; Winterbourn, C. C., Hyperoxidation of peroxiredoxins 2 and 3: rate constants for the reactions of the sulfenic acid of the peroxidatic cysteine. *J Biol Chem* **2013,** 288, (20), 14170-14177.
26. Bolduc, J. A.; Nelson, K. J.; Haynes, A. C.; Lee, J.; Reisz, J. A.; Graff, A. H.; Clodfelter, J. E.; Parsonage, D.; Poole, L. B.; Furdui, C. M.; Lowther, W. T., Novel hyperoxidation resistance motifs in 2-Cys peroxiredoxins. *J Biol Chem* **2018,** 293, (30), 11901-11912.
27. Cox, A. G.; Winterbourn, C. C.; Hampton, M. B., Mitochondrial peroxiredoxin involvement in antioxidant defence and redox signalling. *Biochem J* **2009,** 425, (2), 313-25.
28. Matsumoto, A.; Okado, A.; Fujii, T.; Fujii, J.; Egashira, M.; Niikawa, N.; Taniguchi, N., Cloning of the peroxiredoxin gene family in rats and characterization of the fourth member. *FEBS Lett* **1999,** 443, (3), 246-50.
29. Okado-Matsumoto, A.; Matsumoto, A.; Fujii, J.; Taniguchi, N., Peroxiredoxin IV is a secretable protein with heparin-binding properties under reduced conditions. *J Biochem* **2000,** 127, (3), 493-501.

30. Thapa, P.; Ding, N.; Hao, Y.; Alshahrani, A.; Jiang, H.; Wei, Q., Essential Roles of Peroxiredoxin IV in Inflammation and Cancer. *Molecules (Basel, Switzerland)* **2022,** 27, (19).
31. De Simoni, S.; Goemaere, J.; Knoops, B., Silencing of peroxiredoxin 3 and peroxiredoxin 5 reveals the role of mitochondrial peroxiredoxins in the protection of human neuroblastoma SH-SY5Y cells toward MPP+. *Neuroscience letters* **2008,** 433, (3), 219-24.
32. Knoops, B.; Goemaere, J.; Van der Eecken, V.; Declercq, J. P., Peroxiredoxin 5: structure, mechanism, and function of the mammalian atypical 2-Cys peroxiredoxin. *Antioxid Redox Signal* **2011,** 15, (3), 817-29.
33. Sorokina, E. M.; Feinstein, S. I.; Milovanova, T. N.; Fisher, A. B., Identification of the amino acid sequence that targets peroxiredoxin 6 to lysosome-like structures of lung epithelial cells. *American journal of physiology. Lung cellular and molecular physiology* **2009,** 297, (5), L871-80.
34. Fisher, A. B., Peroxiredoxin 6: a bifunctional enzyme with glutathione peroxidase and phospholipase A_2 activities. *Antioxid Redox Signal* **2011,** 15, (3), 831-44.
35. Wu, Y.; Feinstein, S. I.; Manevich, Y.; Chowdhury, I.; Pak, J. H.; Kazi, A.; Dodia, C.; Speicher, D. W.; Fisher, A. B., Mitogen-activated protein kinase-mediated phosphorylation of peroxiredoxin 6 regulates its phospholipase A(2) activity. *Biochem J* **2009,** 419, (3), 669-79.
36. Woo, H. A.; Jeong, W.; Chang, T. S.; Park, K. J.; Park, S. J.; Yang, J. S.; Rhee, S. G., Reduction of cysteine sulfinic acid by sulfiredoxin is specific to 2-cys peroxiredoxins. *J Biol Chem* **2005,** 280, (5), 3125-8.
37. Sievers, F.; Wilm, A.; Dineen, D.; Gibson, T. J.; Karplus, K.; Li, W.; Lopez, R.; McWilliam, H.; Remmert, M.; Söding, J.; Thompson, J. D.; Higgins, D. G., Fast, scalable generation of high-quality protein multiple sequence alignments using Clustal Omega. *Molecular systems biology* **2011,** 7, 539.
38. Goujon, M.; McWilliam, H.; Li, W.; Valentin, F.; Squizzato, S.; Paern, J.; Lopez, R., A new bioinformatics analysis tools framework at EMBL-EBI. *Nucleic Acids Res* **2010,** 38, (Web Server issue), W695-9.
39. Madeira, F.; Park, Y. M.; Lee, J.; Buso, N.; Gur, T.; Madhusoodanan, N.; Basutkar, P.; Tivey, A. R. N.; Potter, S. C.; Finn, R. D.; Lopez, R., The EMBL-EBI search and sequence analysis tools APIs in 2019. *Nucleic Acids Res* **2019,** 47, (W1), W636-w641.
40. Fujii, J.; Ikeda, Y.; Kurahashi, T.; Homma, T., Physiological and pathological views of peroxiredoxin 4. *Free Radic Biol Med* **2015,** 83, 373-9.
41. Yim, S. H.; Kim, Y. J.; Oh, S. Y.; Fujii, J.; Zhang, Y.; Gladyshev, V. N.; Rhee, S. G., Identification and characterization of alternatively transcribed form of peroxiredoxin IV gene that is specifically expressed in spermatids of postpubertal mouse testis. *J Biol Chem* **2011,** 286, (45), 39002-12.
42. Tavender, T. J.; Sheppard, A. M.; Bulleid, N. J., Peroxiredoxin IV is an endoplasmic reticulum-localized enzyme forming oligomeric complexes in human cells. *Biochem J* **2008,** 411, (1), 191-9.
43. Haridas, V.; Ni, J.; Meager, A.; Su, J.; Yu, G. L.; Zhai, Y.; Kyaw, H.; Akama, K. T.; Hu, J.; Van Eldik, L. J.; Aggarwal, B. B., TRANK, a novel cytokine that activates NF-kappa B and c-Jun N-terminal kinase. *J Immunol* **1998,** 161, (1), 1-6.

44. Kakihana, T.; Araki, K.; Vavassori, S.; Iemura, S.; Cortini, M.; Fagioli, C.; Natsume, T.; Sitia, R.; Nagata, K., Dynamic regulation of Ero1α and peroxiredoxin 4 localization in the secretory pathway. *J Biol Chem* **2013,** 288, (41), 29586-94.
45. Tempio, T.; Orsi, A.; Sicari, D.; Valetti, C.; Yoboue, E. D.; Anelli, T.; Sitia, R., A virtuous cycle operated by ERp44 and ERGIC-53 guarantees proteostasis in the early secretory compartment. *iScience* **2021,** 24, (3), 102244.
46. Wang, X.; Wang, L.; Wang, X.; Sun, F.; Wang, C. C., Structural insights into the peroxidase activity and inactivation of human peroxiredoxin 4. *Biochem J* **2012,** 441, (1), 113-8.
47. Cao, Z.; Tavender, T. J.; Roszak, A. W.; Cogdell, R. J.; Bulleid, N. J., Crystal structure of reduced and of oxidized peroxiredoxin IV enzyme reveals a stable oxidized decamer and a non-disulfide-bonded intermediate in the catalytic cycle. *J Biol Chem* **2011,** 286, (49), 42257-66.
48. Tavender, T. J.; Springate, J. J.; Bulleid, N. J., Recycling of peroxiredoxin IV provides a novel pathway for disulphide formation in the endoplasmic reticulum. *Embo j* **2010,** 29, (24), 4185-97.
49. Rabilloud, T.; Heller, M.; Gasnier, F.; Luche, S.; Rey, C.; Aebersold, R.; Benahmed, M.; Louisot, P.; Lunardi, J., Proteomics analysis of cellular response to oxidative stress. Evidence for in vivo overoxidation of peroxiredoxins at their active site. *J Biol Chem* **2002,** 277, (22), 19396-401.
50. Roussel, X.; Béchade, G.; Kriznik, A.; Van Dorsselaer, A.; Sanglier-Cianferani, S.; Branlant, G.; Rahuel-Clermont, S., Evidence for the formation of a covalent thiosulfinate intermediate with peroxiredoxin in the catalytic mechanism of sulfiredoxin. *J Biol Chem* **2008,** 283, (33), 22371-82.
51. Mishra, M.; Jiang, H.; Wu, L.; Chawsheen, H. A.; Wei, Q., The sulfiredoxin-peroxiredoxin (Srx-Prx) axis in cell signal transduction and cancer development. *Cancer Lett* **2015,** 366, (2), 150-9.
52. Elko, E. A.; Manuel, A. M.; White, S.; Zito, E.; van der Vliet, A.; Anathy, V.; Janssen-Heininger, Y. M. W., Oxidation of peroxiredoxin-4 induces oligomerization and promotes interaction with proteins governing protein folding and endoplasmic reticulum stress. *J Biol Chem* **2021,** 296, 100665.
53. Bonnichsen, R. K.; Chance, B.; Theorell, H., Catalase Activity. *Acta Chemica Scandinavica* **1947,** 1, 685-709.
54. Winterbourn, C. C., The biological chemistry of hydrogen peroxide. *Methods in enzymology* **2013,** 528, 3-25.
55. Nguyen, V. D.; Saaranen, M. J.; Karala, A. R.; Lappi, A. K.; Wang, L.; Raykhel, I. B.; Alanen, H. I.; Salo, K. E.; Wang, C. C.; Ruddock, L. W., Two endoplasmic reticulum PDI peroxidases increase the efficiency of the use of peroxide during disulfide bond formation. *Journal of molecular biology* **2011,** 406, (3), 503-15.
56. Hatahet, F.; Ruddock, L. W., Protein disulfide isomerase: a critical evaluation of its function in disulfide bond formation. *Antioxid Redox Signal* **2009,** 11, (11), 2807-50.
57. Tu, B. P.; Weissman, J. S., The FAD- and O(2)-dependent reaction cycle of Ero1-mediated oxidative protein folding in the endoplasmic reticulum. *Mol Cell* **2002,** 10, (5), 983-94.

58. Gross, E.; Sevier, C. S.; Heldman, N.; Vitu, E.; Bentzur, M.; Kaiser, C. A.; Thorpe, C.; Fass, D., Generating disulfides enzymatically: reaction products and electron acceptors of the endoplasmic reticulum thiol oxidase Ero1p. *Proc Natl Acad Sci U S A* **2006,** 103, (2), 299-304.
59. Sato, Y.; Kojima, R.; Okumura, M.; Hagiwara, M.; Masui, S.; Maegawa, K.; Saiki, M.; Horibe, T.; Suzuki, M.; Inaba, K., Synergistic cooperation of PDI family members in peroxiredoxin 4-driven oxidative protein folding. *Sci Rep* **2013,** 3, 2456.
60. Zito, E.; Hansen, H. G.; Yeo, G. S.; Fujii, J.; Ron, D., Endoplasmic reticulum thiol oxidase deficiency leads to ascorbic acid depletion and noncanonical scurvy in mice. *Mol Cell* **2012,** 48, (1), 39-51.
61. Moon, J. C.; Kim, G. M.; Kim, E. K.; Lee, H. N.; Ha, B.; Lee, S. Y.; Jang, H. H., Reversal of 2-Cys peroxiredoxin oligomerization by sulfiredoxin. *Biochem Biophys Res Commun* **2013,** 432, (2), 291-5.
62. Pattwell, D.; Ashton, T.; McArdle, A.; Griffiths, R. D.; Jackson, M. J., Ischemia and reperfusion of skeletal muscle lead to the appearance of a stable lipid free radical in the circulation. *American journal of physiology. Heart and circulatory physiology* **2003,** 284, (6), H2400-4.
63. Pattwell, D. M.; McArdle, A.; Morgan, J. E.; Patridge, T. A.; Jackson, M. J., Release of reactive oxygen and nitrogen species from contracting skeletal muscle cells. *Free Radic Biol Med* **2004,** 37, (7), 1064-72.
64. Salzano, S.; Checconi, P.; Hanschmann, E. M.; Lillig, C. H.; Bowler, L. D.; Chan, P.; Vaudry, D.; Mengozzi, M.; Coppo, L.; Sacre, S.; Atkuri, K. R.; Sahaf, B.; Herzenberg, L. A.; Herzenberg, L. A.; Mullen, L.; Ghezzi, P., Linkage of inflammation and oxidative stress via release of glutathionylated peroxiredoxin-2, which acts as a danger signal. *Proc Natl Acad Sci U S A* **2014,** 111, (33), 12157-62.
65. Manabe, Y.; Takagi, M.; Nakamura-Yamada, M.; Goto-Inoue, N.; Taoka, M.; Isobe, T.; Fujii, N. L., Redox proteins are constitutively secreted by skeletal muscle. *The journal of physiological sciences : JPS* **2014,** 64, (6), 401-9.
66. Wadley, A. J.; Keane, G.; Cullen, T.; James, L.; Vautrinot, J.; Davies, M.; Hussey, B.; Hunter, D. J.; Mastana, S.; Holliday, A.; Petersen, S. V.; Bishop, N. C.; Lindley, M. R.; Coles, S. J., Characterization of extracellular redox enzyme concentrations in response to exercise in humans. *J Appl Physiol (1985)* **2019,** 127, (3), 858-866.
67. Shi, H.; Liu, J.; Zhu, P.; Wang, H.; Zhao, Z.; Sun, G.; Li, J., Expression of peroxiredoxins in the human testis, epididymis and spermatozoa and their role in preventing H2O2-induced damage to spermatozoa. *Folia Histochem Cytobiol* **2018,** 56, (3), 141-150.
68. Iuchi, Y.; Okada, F.; Tsunoda, S.; Kibe, N.; Shirasawa, N.; Ikawa, M.; Okabe, M.; Ikeda, Y.; Fujii, J., Peroxiredoxin 4 knockout results in elevated spermatogenic cell death via oxidative stress. *Biochem J* **2009,** 419, (1), 149-58.
69. Tasaki, E.; Matsumoto, S.; Tada, H.; Kurahashi, T.; Zhang, X.; Fujii, J.; Utsumi, T.; Iuchi, Y., Protective role of testis-specific peroxiredoxin 4 against cellular oxidative stress. *J Clin Biochem Nutr* **2017,** 60, (3), 156-161.
70. O'Flaherty, C.; de Souza, A. R., Hydrogen peroxide modifies human sperm peroxiredoxins in a dose-dependent manner. *Biology of reproduction* **2011,** 84, (2), 238-47.

71. Sasagawa, I.; Matsuki, S.; Suzuki, Y.; Iuchi, Y.; Tohya, K.; Kimura, M.; Nakada, T.; Fujii, J., Possible involvement of the membrane-bound form of peroxiredoxin 4 in acrosome formation during spermiogenesis of rats. *Eur J Biochem* **2001,** 268, (10), 3053-61.
72. Matsuki, S.; Sasagawa, I.; Iuchi, Y.; Fujii, J., Impaired expression of peroxiredoxin 4 in damaged testes by artificial cryptorchidism. *Redox report : communications in free radical research* **2002,** 7, (5), 276-8.
73. Homma, T.; Kurahashi, T.; Ishii, N.; Shirasawa, N.; Fujii, J., Testis-specific peroxiredoxin 4 variant is not absolutely required for spermatogenesis and fertility in mice. *Sci Rep* **2020,** 10, (1), 17934.
74. Ma, W. W.; Hu, M. T.; Gao, L.; Gao, C.; Qin, G.; Liu, J. Y.; Meng, Y.; Cui, Y. G., [Peroxiredoxin 4 protects the testis from heat stress]. *Zhonghua nan ke xue = National journal of andrology* **2020,** 26, (2), 99-105.
75. Khorami Sarvestani, S.; Shojaeian, S.; Vanaki, N.; Ghresi-Fard, B.; Amini, M.; Gilany, K.; Soltanghoraee, H.; Arefi, S.; Jeddi-Tehrani, M.; Zarnani, A. H., Proteome profiling of human placenta reveals developmental stage-dependent alterations in protein signature. *Clinical proteomics* **2021,** 18, (1), 18.
76. Yi, Q.; Meng, C.; Cai, L. B.; Cui, Y. G.; Liu, J. Y.; Meng, Y., Peroxiredoxin 4, a new oxidative stress marker in follicular fluid, may predict in vitro fertilization and embryo transfer outcomes. *Annals of translational medicine* **2020,** 8, (17), 1049.
77. Choi, Y. S.; Cho, S.; Seo, S. K.; Park, J. H.; Kim, S. H.; Lee, B. S., Alteration in the intrafollicular thiol-redox system in infertile women with endometriosis. *Reproduction (Cambridge, England)* **2015,** 149, (2), 155-62.
78. Mazloomi, S.; Khodadadi, I.; Alizadeh, N.; Shafiee, G., Association of glutamate cystein ligase (GCL) activity Peroxiredoxin 4 (prxR4) and apelin levels in women with preeclampsia. *Pregnancy hypertension* **2021,** 23, 163-168.
79. Wang, S.; Zheng, Y.; Li, J.; Yu, Y.; Zhang, W.; Song, M.; Liu, Z.; Min, Z.; Hu, H.; Jing, Y.; He, X.; Sun, L.; Ma, L.; Esteban, C. R.; Chan, P.; Qiao, J.; Zhou, Q.; Izpisua Belmonte, J. C.; Qu, J.; Tang, F.; Liu, G. H., Single-Cell Transcriptomic Atlas of Primate Ovarian Aging. *Cell* **2020,** 180, (3), 585-600.e19.
80. Qian, Y.; Shao, L.; Yuan, C.; Jiang, C. Y.; Liu, J.; Gao, C.; Gao, L.; Cui, Y. G.; Jiang, S. W.; Liu, J. Y.; Meng, Y., Implication of Differential Peroxiredoxin 4 Expression with Age in Ovaries of Mouse and Human for Ovarian Aging. *Curr Mol Med* **2016,** 16, (3), 243-51.
81. Liang, X.; Yan, Z.; Ma, W.; Qian, Y.; Zou, X.; Cui, Y.; Liu, J.; Meng, Y., Peroxiredoxin 4 protects against ovarian ageing by ameliorating D-galactose-induced oxidative damage in mice. *Cell death & disease* **2020,** 11, (12), 1053.
82. Yamada, S.; Guo, X., Peroxiredoxin 4 (PRDX4): Its critical in vivo roles in animal models of metabolic syndrome ranging from atherosclerosis to nonalcoholic fatty liver disease. *Pathol Int* **2018,** 68, (2), 91-101.
83. Gateva, A.; Assyov, Y.; Velikova, T.; Kamenov, Z., Increased peroxiredoxin 4 levels in patients with prediabetes compared to normal glucose tolerance subjects. *Clinical endocrinology* **2016,** 85, (4), 551-5.
84. Ding, Y.; Yamada, S.; Wang, K. Y.; Shimajiri, S.; Guo, X.; Tanimoto, A.; Murata, Y.; Kitajima, S.; Watanabe, T.; Izumi, H.; Kohno, K.; Sasaguri, Y., Overexpression of peroxiredoxin 4 protects against high-dose streptozotocin-induced diabetes by

suppressing oxidative stress and cytokines in transgenic mice. *Antioxid Redox Signal* **2010,** 13, (10), 1477-90.

85. Tran, D. T.; Pottekat, A.; Mir, S. A.; Loguercio, S.; Jang, I.; Campos, A. R.; Scully, K. M.; Lahmy, R.; Liu, M.; Arvan, P.; Balch, W. E.; Kaufman, R. J.; Itkin-Ansari, P., Unbiased Profiling of the Human Proinsulin Biosynthetic Interaction Network Reveals a Role for Peroxiredoxin 4 in Proinsulin Folding. *Diabetes* **2020,** 69, (8), 1723-1734.
86. Homma, T.; Kurahashi, T.; Lee, J.; Nabeshima, A.; Yamada, S.; Fujii, J., Double Knockout of Peroxiredoxin 4 (Prdx4) and Superoxide Dismutase 1 (Sod1) in Mice Results in Severe Liver Failure. *Oxid Med Cell Longev* **2018,** 2018, 2812904.
87. Caillard, A.; Sadoune, M.; Cescau, A.; Meddour, M.; Gandon, M.; Polidano, E.; Delcayre, C.; Da Silva, K.; Manivet, P.; Gomez, A. M.; Cohen-Solal, A.; Vodovar, N.; Li, Z.; Mebazaa, A.; Samuel, J. L., QSOX1, a novel actor of cardiac protection upon acute stress in mice. *J Mol Cell Cardiol* **2018,** 119, 75-86.
88. Ibarrola, J.; Arrieta, V.; Sadaba, R.; Martinez-Martinez, E.; Garcia-Pena, A.; Alvarez, V.; Fernandez-Celis, A.; Gainza, A.; Santamaria, E.; Fernandez-Irigoyen, J.; Cachofeiro, V.; Zalba, G.; Fay, R.; Rossignol, P.; Lopez-Andres, N., Galectin-3 down-regulates antioxidant peroxiredoxin-4 in human cardiac fibroblasts: a new pathway to induce cardiac damage. *Clin Sci (Lond)* **2018,** 132, (13), 1471-1485.
89. Tian, Y.; Lv, W.; Lu, C.; Jiang, Y.; Yang, X.; Song, M., Galectin-3 inhibition attenuates doxorubicin-induced cardiac dysfunction by upregulating the expression of peroxiredoxin-4. *Canadian journal of physiology and pharmacology* **2020,** 98, (10), 700-707.
90. Rowe, D. D.; Leonardo, C. C.; Hall, A. A.; Shahaduzzaman, M. D.; Collier, L. A.; Willing, A. E.; Pennypacker, K. R., Cord blood administration induces oligodendrocyte survival through alterations in gene expression. *Brain research* **2010,** 1366, 172-88.
91. Huang, Y.; Wang, J.; Cai, J.; Qiu, Y.; Zheng, H.; Lai, X.; Sui, X.; Wang, Y.; Lu, Q.; Zhang, Y.; Yuan, M.; Gong, J.; Cai, W.; Liu, X.; Shan, Y.; Deng, Z.; Shi, Y.; Shu, Y.; Zhang, L.; Qiu, W.; Peng, L.; Ren, J.; Lu, Z.; Xiang, A. P., Targeted homing of CCR2-overexpressing mesenchymal stromal cells to ischemic brain enhances post-stroke recovery partially through PRDX4-mediated blood-brain barrier preservation. *Theranostics* **2018,** 8, (21), 5929-5944.
92. Majd, S.; Power, J. H. T., Oxidative Stress and Decreased Mitochondrial Superoxide Dismutase 2 and Peroxiredoxins 1 and 4 Based Mechanism of Concurrent Activation of AMPK and mTOR in Alzheimer's Disease. *Current Alzheimer research* **2018,** 15, (8), 764-776.
93. Kam, M. K.; Lee, D. G.; Kim, B.; Lee, H. S.; Lee, S. R.; Bae, Y. C.; Lee, D. S., Peroxiredoxin 4 ameliorates amyloid beta oligomer-mediated apoptosis by inhibiting ER-stress in HT-22 hippocampal neuron cells. *Cell biology and toxicology* **2019,** 35, (6), 573-588.
94. Kang, J. H.; Kim, M. H.; Lee, H. J.; Huh, J. W.; Lee, H. S.; Lee, D. S., Peroxiredoxin 4 attenuates glutamate-induced neuronal cell death through inhibition of endoplasmic reticulum stress. *Free Radic Res* **2020,** 54, (4), 207-220.
95. Schrotter, A.; Pfeiffer, K.; El Magraoui, F.; Platta, H. W.; Erdmann, R.; Meyer, H. E.; Egensperger, R.; Marcus, K.; Muller, T., The amyloid precursor protein (APP)

family members are key players in S-adenosylmethionine formation by MAT2A and modify BACE1 and PSEN1 gene expression-relevance for Alzheimer's disease. *Molecular & cellular proteomics : MCP* **2012,** 11, (11), 1274-88.
96. Poulsen, N. A.; Andersen, V.; Møller, J. C.; Møller, H. S.; Jessen, F.; Purup, S.; Larsen, L. B., Comparative analysis of inflamed and non-inflamed colon biopsies reveals strong proteomic inflammation profile in patients with ulcerative colitis. *BMC gastroenterology* **2012,** 12, 76.
97. Takagi, T.; Homma, T.; Fujii, J.; Shirasawa, N.; Yoriki, H.; Hotta, Y.; Higashimura, Y.; Mizushima, K.; Hirai, Y.; Katada, K.; Uchiyama, K.; Naito, Y.; Itoh, Y., Elevated ER stress exacerbates dextran sulfate sodium-induced colitis in PRDX4-knockout mice. *Free Radic Biol Med* **2019,** 134, 153-164.
98. Rao, Z.; Wang, S.; Wang, J., Peroxiredoxin 4 inhibits IL-1β-induced chondrocyte apoptosis via PI3K/AKT signaling. *Biomed Pharmacother* **2017,** 90, 414-420.
99. Chang, X.; Cui, Y.; Zong, M.; Zhao, Y.; Yan, X.; Chen, Y.; Han, J., Identification of proteins with increased expression in rheumatoid arthritis synovial tissues. *The Journal of rheumatology* **2009,** 36, (5), 872-80.
100. Aihaiti, Y.; Tuerhong, X.; Zheng, H.; Cai, Y.; Yang, M.; Xu, P., Peroxiredoxin 4 regulates tumor-cell-like characteristics of fibroblast-like synoviocytes in rheumatoid arthritis through PI3k/Akt signaling pathway. *Clinical immunology (Orlando, Fla.)* **2022,** 237, 108964.
101. Han, K.; Du, S. S.; Wang, H.; Qiao, J. J.; Zhang, X.; Wang, P.; Shen, F. H., [Differential expression of PRDX4 in alveolar macrophages of patients with silicosis]. *Zhonghua lao dong wei sheng zhi ye bing za zhi = Zhonghua laodong weisheng zhiyebing zazhi = Chinese journal of industrial hygiene and occupational diseases* **2021,** 39, (1), 17-19.
102. Bertolotti, M.; Yim, S. H.; Garcia-Manteiga, J. M.; Masciarelli, S.; Kim, Y. J.; Kang, M. H.; Iuchi, Y.; Fujii, J.; Vene, R.; Rubartelli, A.; Rhee, S. G.; Sitia, R., B-to plasma-cell terminal differentiation entails oxidative stress and profound reshaping of the antioxidant responses. *Antioxid Redox Signal* **2010,** 13, (8), 1133-44.
103. Yamaguchi, R.; Guo, X.; Zheng, J.; Zhang, J.; Han, J.; Shioya, A.; Uramoto, H.; Mochizuki, T.; Yamada, S., Peroxiredoxin 4 improved aging-related delayed wound healing in mice. *The Journal of investigative dermatology* **2021**.
104. Greten, F. R.; Eckmann, L.; Greten, T. F.; Park, J. M.; Li, Z. W.; Egan, L. J.; Kagnoff, M. F.; Karin, M., IKKbeta links inflammation and tumorigenesis in a mouse model of colitis-associated cancer. *Cell* **2004,** 118, (3), 285-96.
105. Popivanova, B. K.; Kitamura, K.; Wu, Y.; Kondo, T.; Kagaya, T.; Kaneko, S.; Oshima, M.; Fujii, C.; Mukaida, N., Blocking TNF-alpha in mice reduces colorectal carcinogenesis associated with chronic colitis. *The Journal of clinical investigation* **2008,** 118, (2), 560-70.
106. Dolcet, X.; Llobet, D.; Pallares, J.; Matias-Guiu, X., NF-kB in development and progression of human cancer. *Virchows Arch* **2005,** 446, (5), 475-82.
107. Jin, D. Y.; Chae, H. Z.; Rhee, S. G.; Jeang, K. T., Regulatory role for a novel human thioredoxin peroxidase in NF-kappaB activation. *J Biol Chem* **1997,** 272, (49), 30952-61.

108. Weichart, D.; Gobom, J.; Klopfleisch, S.; Häsler, R.; Gustavsson, N.; Billmann, S.; Lehrach, H.; Seegert, D.; Schreiber, S.; Rosenstiel, P., Analysis of NOD2-mediated proteome response to muramyl dipeptide in HEK293 cells. *J Biol Chem* **2006,** 281, (4), 2380-9.
109. Yu, S.; Mu, Y.; Ao, J.; Chen, X., Peroxiredoxin IV regulates pro-inflammatory responses in large yellow croaker (Pseudosciaena crocea) and protects against bacterial challenge. *J Proteome Res* **2010,** 9, (3), 1424-36.
110. Mu, Y.; Lian, F. M.; Teng, Y. B.; Ao, J.; Jiang, Y. L.; He, Y. X.; Chen, Y.; Zhou, C. Z.; Chen, X., The N-terminal beta-sheet of peroxiredoxin 4 in the large yellow croaker Pseudosciaena crocea is involved in its biological functions. *PLoS One* **2013,** 8, (2), e57061.
111. Radyuk, S. N.; Klichko, V. I.; Michalak, K.; Orr, W. C., The effect of peroxiredoxin 4 on fly physiology is a complex interplay of antioxidant and signaling functions. *Faseb j* **2013,** 27, (4), 1426-38.
112. Zhao, L. X.; Du, J. R.; Zhou, H. J.; Liu, D. L.; Gu, M. X.; Long, F. Y., Differences in Proinflammatory Property of Six Subtypes of Peroxiredoxins and Anti-Inflammatory Effect of Ligustilide in Macrophages. *PLoS One* **2016,** 11, (10), e0164586.
113. Rathinam, V. A.; Fitzgerald, K. A., Inflammasome Complexes: Emerging Mechanisms and Effector Functions. *Cell* **2016,** 165, (4), 792-800.
114. Park, C. H.; Lee, H. S.; Kwak, M. S.; Shin, J. S., Inflammasome-Dependent Peroxiredoxin 2 Secretion Induces the Classical Complement Pathway Activation. *Immune network* **2021,** 21, (5), e36.
115. Cui, S.; Wang, C.; Bai, W.; Li, J.; Pan, Y.; Huang, X.; Yang, H.; Feng, Z.; Xiang, Q.; Fei, L.; Zheng, L.; Huang, J.; Zhang, Q.; Wu, Y.; Chen, Y., CD1d1 intrinsic signaling in macrophages controls NLRP3 inflammasome expression during inflammation. *Science advances* **2020,** 6, (43).
116. He, Y.; Li, S.; Tang, D.; Peng, Y.; Meng, J.; Peng, S.; Deng, Z.; Qiu, S.; Liao, X.; Chen, H.; Tu, S.; Tao, L.; Peng, Z.; Yang, H., Circulating Peroxiredoxin-1 is a novel damage-associated molecular pattern and aggravates acute liver injury via promoting inflammation. *Free Radic Biol Med* **2019,** 137, 24-36.
117. Wang, Y.; Zhao, Y.; Wang, Z.; Sun, R.; Zou, B.; Li, R.; Liu, D.; Lin, M.; Zhou, J.; Ning, S.; Tian, X.; Yao, J., Peroxiredoxin 3 Inhibits Acetaminophen-Induced Liver Pyroptosis Through the Regulation of Mitochondrial ROS. *Frontiers in immunology* **2021,** 12, 652782.
118. Liu, W.; Guo, W.; Zhu, Y.; Peng, S.; Zheng, W.; Zhang, C.; Shao, F.; Zhu, Y.; Hang, N.; Kong, L.; Meng, X.; Xu, Q.; Sun, Y., Targeting Peroxiredoxin 1 by a Curcumin Analogue, AI-44, Inhibits NLRP3 Inflammasome Activation and Attenuates Lipopolysaccharide-Induced Sepsis in Mice. *J Immunol* **2018,** 201, (8), 2403-2413.
119. Vázquez-Medina, J. P.; Tao, J. Q.; Patel, P.; Bannitz-Fernandes, R.; Dodia, C.; Sorokina, E. M.; Feinstein, S. I.; Chatterjee, S.; Fisher, A. B., Genetic inactivation of the phospholipase A(2) activity of peroxiredoxin 6 in mice protects against LPS-induced acute lung injury. *American journal of physiology. Lung cellular and molecular physiology* **2019,** 316, (4), L656-l668.

120. Lipinski, S.; Pfeuffer, S.; Arnold, P.; Treitz, C.; Aden, K.; Ebsen, H.; Falk-Paulsen, M.; Gisch, N.; Fazio, A.; Kuiper, J.; Luzius, A.; Billmann-Born, S.; Schreiber, S.; Nunez, G.; Beer, H. D.; Strowig, T.; Lamkanfi, M.; Tholey, A.; Rosenstiel, P., Prdx4 limits caspase-1 activation and restricts inflammasome-mediated signaling by extracellular vesicles. *Embo j* **2019,** 38, (20), e101266.
121. Minghetti, L., Cyclooxygenase-2 (COX-2) in inflammatory and degenerative brain diseases. *Journal of neuropathology and experimental neurology* **2004,** 63, (9), 901-10.
122. Li, J.; Ruzhi, D.; Hua, X.; Zhang, L.; Lu, F.; Coursey, T. G.; Pflugfelder, S. C.; Li, D. Q., Blueberry Component Pterostilbene Protects Corneal Epithelial Cells from Inflammation via Anti-oxidative Pathway. *Sci Rep* **2016,** 6, 19408.
123. Hua, X.; Deng, R.; Li, J.; Chi, W.; Su, Z.; Lin, J.; Pflugfelder, S. C.; Li, D. Q., Protective Effects of L-Carnitine Against Oxidative Injury by Hyperosmolarity in Human Corneal Epithelial Cells. *Investigative ophthalmology & visual science* **2015,** 56, (9), 5503-11.
124. Zhang, C.; Wang, J.; Qi, Q.; Yang, L.; Sun, P.; Yuan, X., Modulatory effect of fructooligosaccharide against triphenyltin-induced oxidative stress and immune suppression in goldfish (Carassius auratus). *Ecotoxicology and environmental safety* **2021,** 212, 111966.
125. Melhem, H.; Spalinger, M. R.; Cosin-Roger, J.; Atrott, K.; Lang, S.; Wojtal, K. A.; Vavricka, S. R.; Rogler, G.; Frey-Wagner, I., Prdx6 Deficiency Ameliorates DSS Colitis: Relevance of Compensatory Antioxidant Mechanisms. *Journal of Crohn's & colitis* **2017,** 11, (7), 871-884.
126. Ran, X. Q.; Gao, L.; Yan, M.; Kang, C. J., Peroxiredoxin 4 Interacts With Domeless and Participates in Antibacterial Immune Response Through the JAK/STAT Pathway. *Frontiers in immunology* **2022,** 13, 907183.
127. Ummanni, R.; Barreto, F.; Venz, S.; Scharf, C.; Barett, C.; Mannsperger, H. A.; Brase, J. C.; Kuner, R.; Schlomm, T.; Sauter, G.; Sultmann, H.; Korf, U.; Bokemeyer, C.; Walther, R.; Brummendorf, T. H.; Balabanov, S., Peroxiredoxins 3 and 4 are overexpressed in prostate cancer tissue and affect the proliferation of prostate cancer cells in vitro. *J Proteome Res* **2012,** 11, (4), 2452-66.
128. Basu, A.; Banerjee, H.; Rojas, H.; Martinez, S. R.; Roy, S.; Jia, Z.; Lilly, M. B.; De Leon, M.; Casiano, C. A., Differential expression of peroxiredoxins in prostate cancer: consistent upregulation of PRDX3 and PRDX4. *The Prostate* **2011,** 71, (7), 755-65.
129. Rafiei, S.; Tiedemann, K.; Tabaries, S.; Siegel, P. M.; Komarova, S. V., Peroxiredoxin 4: a novel secreted mediator of cancer induced osteoclastogenesis. *Cancer Lett* **2015,** 361, (2), 262-70.
130. Tiedemann, K.; Sadvakassova, G.; Mikolajewicz, N.; Juhas, M.; Sabirova, Z.; Tabaries, S.; Gettemans, J.; Siegel, P. M.; Komarova, S. V., Exosomal Release of L-Plastin by Breast Cancer Cells Facilitates Metastatic Bone Osteolysis. *Translational oncology* **2019,** 12, (3), 462-474.
131. Ding, N.; Jiang, H.; Thapa, P.; Hao, Y.; Alshahrani, A.; Allison, D.; Izumi, T.; Rangnekar, V. M.; Liu, X.; Wei, Q., Peroxiredoxin IV plays a critical role in cancer cell growth and radioresistance through the activation of the Akt/GSK3 signaling pathways. *J Biol Chem* **2022**, 102123.

132. Karihtala, P.; Mantyniemi, A.; Kang, S. W.; Kinnula, V. L.; Soini, Y., Peroxiredoxins in breast carcinoma. *Clinical cancer research : an official journal of the American Association for Cancer Research* **2003,** 9, (9), 3418-24.
133. Wang, G.; Zhong, W. C.; Bi, Y. H.; Tao, S. Y.; Zhu, H.; Zhu, H. X.; Xu, A. M., The Prognosis Of Peroxiredoxin Family In Breast Cancer. *Cancer management and research* **2019,** 11, 9685-9699.
134. Karihtala, P.; Kauppila, S.; Soini, Y.; Arja Jukkola, V., Oxidative stress and counteracting mechanisms in hormone receptor positive, triple-negative and basal-like breast carcinomas. *BMC cancer* **2011,** 11, 262.
135. Mei, J.; Hao, L.; Liu, X.; Sun, G.; Xu, R.; Wang, H.; Liu, C., Comprehensive analysis of peroxiredoxins expression profiles and prognostic values in breast cancer. *Biomarker research* **2019,** 7, 16.
136. Edvardsen, H.; Brunsvig, P. F.; Solvang, H.; Tsalenko, A.; Andersen, A.; Syvanen, A. C.; Yakhini, Z.; Børresen-Dale, A. L.; Olsen, H.; Aamdal, S.; Kristensen, V. N., SNPs in genes coding for ROS metabolism and signalling in association with docetaxel clearance. *The Pharmacogenomics Journal* **2010,** 10, (6), 513-523.
137. Hansen, S. N.; Ehlers, N. S.; Zhu, S.; Thomsen, M. B.; Nielsen, R. L.; Liu, D.; Wang, G.; Hou, Y.; Zhang, X.; Xu, X.; Bolund, L.; Yang, H.; Wang, J.; Moreira, J.; Ditzel, H. J.; Brunner, N.; Schrohl, A. S.; Stenvang, J.; Gupta, R., The stepwise evolution of the exome during acquisition of docetaxel resistance in breast cancer cells. *BMC Genomics* **2016,** 17, 442.
138. Wei, Q.; Jiang, H.; Xiao, Z.; Baker, A.; Young, M. R.; Veenstra, T. D.; Colburn, N. H., Sulfiredoxin-Peroxiredoxin IV axis promotes human lung cancer progression through modulation of specific phosphokinase signaling. *Proc Natl Acad Sci U S A* **2011,** 108, (17), 7004-9.
139. Jiang, H.; Wu, L.; Mishra, M.; Chawsheen, H. A.; Wei, Q., Expression of peroxiredoxin 1 and 4 promotes human lung cancer malignancy. *Am J Cancer Res* **2014,** 4, (5), 445-60.
140. Hwang, J. A.; Song, J. S.; Yu, D. Y.; Kim, H. R.; Park, H. J.; Park, Y. S.; Kim, W. S.; Choi, C. M., Peroxiredoxin 4 as an independent prognostic marker for survival in patients with early-stage lung squamous cell carcinoma. *Int J Clin Exp Pathol* **2015,** 8, (6), 6627-35.
141. Zheng, J.; Guo, X.; Nakamura, Y.; Zhou, X.; Yamaguchi, R.; Zhang, J.; Ishigaki, Y.; Uramoto, H.; Yamada, S., Overexpression of PRDX4 Modulates Tumor Microenvironment and Promotes Urethane-Induced Lung Tumorigenesis. *Oxid Med Cell Longev* **2020,** 2020, 8262730.
142. Hao, C. C.; Luo, J. N.; Xu, C. Y.; Zhao, X. Y.; Zhong, Z. B.; Hu, X. N.; Jin, X. M.; Ge, X., TRIAP1 knockdown sensitizes non-small cell lung cancer to ionizing radiation by disrupting redox homeostasis. *Thoracic cancer* **2020,** 11, (4), 1015-1025.
143. Shioya, A.; Guo, X.; Motono, N.; Mizuguchi, S.; Kurose, N.; Nakada, S.; Aikawa, A.; Ikeda, Y.; Uramoto, H.; Yamada, S., The Combination Of Weak Expression Of PRDX4 And Very High MIB-1 Labelling Index Independently Predicts Shorter Disease-free Survival In Stage I Lung Adenocarcinoma. *Int J Med Sci* **2018,** 15, (10), 1025-1034.

144. Mizutani, K.; Guo, X.; Shioya, A.; Zhang, J.; Zheng, J.; Kurose, N.; Ishibashi, H.; Motono, N.; Uramoto, H.; Yamada, S., The impact of PRDX4 and the EGFR mutation status on cellular proliferation in lung adenocarcinoma. *Int J Med Sci* **2019,** 16, (9), 1199-1206.
145. Yi, N.; Xiao, M. B.; Ni, W. K.; Jiang, F.; Lu, C. H.; Ni, R. Z., High expression of peroxiredoxin 4 affects the survival time of colorectal cancer patients, but is not an independent unfavorable prognostic factor. *Mol Clin Oncol* **2014,** 2, (5), 767-772.
146. Li, M.; Lin, Y. M.; Hasegawa, S.; Shimokawa, T.; Murata, K.; Kameyama, M.; Ishikawa, O.; Katagiri, T.; Tsunoda, T.; Nakamura, Y.; Furukawa, Y., Genes associated with liver metastasis of colon cancer, identified by genome-wide cDNA microarray. *Int J Oncol* **2004,** 24, (2), 305-12.
147. Huang, C. Y.; Lee, K. C.; Tung, S. Y.; Huang, W. S.; Teng, C. C.; Lee, K. F.; Hsieh, M. C.; Kuo, H. C., 2D-DIGE-MS Proteomics Approaches for Identification of Gelsolin and Peroxiredoxin 4 with Lymph Node Metastasis in Colorectal Cancer. *Cancers* **2022,** 14, (13).
148. Ouyang, M.; Luo, Z.; Zhang, W.; Zhu, D.; Lu, Y.; Wu, J.; Yao, X., Protective effect of curcumin against irinotecaninduced intestinal mucosal injury via attenuation of NFkappaB activation, oxidative stress and endoplasmic reticulum stress. *Int J Oncol* **2019,** 54, (4), 1376-1386.
149. Zhu, D. J.; Chen, X. W.; Wang, J. Z.; Ju, Y. L.; Ou Yang, M. Z.; Zhang, W. J., Proteomic analysis identifies proteins associated with curcumin-enhancing efficacy of irinotecan-induced apoptosis of colorectal cancer LOVO cell. *Int J Clin Exp Pathol* **2014,** 7, (1), 1-15.
150. Ribeiro, T.; Lemos, F.; Preto, M.; Azevedo, J.; Sousa, M. L.; Leao, P. N.; Campos, A.; Linder, S.; Vitorino, R.; Vasconcelos, V.; Urbatzka, R., Cytotoxicity of portoamides in human cancer cells and analysis of the molecular mechanisms of action. *PLoS One* **2017,** 12, (12), e0188817.
151. Kobayashi, S.; Hiwasa, T.; Arasawa, T.; Kagaya, A.; Ishii, S.; Shimada, H.; Ito, M.; Suzuki, M.; Kano, M.; Rahmutulla, B.; Kitamura, K.; Sawabe, Y.; Shin, H.; Takiguchi, M.; Nomura, F.; Matsubara, H.; Matsushita, K., Identification of specific and common diagnostic antibody markers for gastrointestinal cancers by SEREX screening using testis cDNA phage library. *Oncotarget* **2018,** 9, (26), 18559-18569.
152. Park, S. Y.; Lee, Y. J.; Park, J.; Kim, T. H.; Hong, S. C.; Jung, E. J.; Ju, Y. T.; Jeong, C. Y.; Park, H. J.; Ko, G. H.; Song, D. H.; Park, M.; Yoo, J.; Jeong, S. H., PRDX4 overexpression is associated with poor prognosis in gastric cancer. *Oncology letters* **2020,** 19, (5), 3522-3530.
153. Worfolk, J. C.; Bell, S.; Simpson, L. D.; Carne, N. A.; Francis, S. L.; Engelbertsen, V.; Brown, A. P.; Walker, J.; Viswanath, Y. K.; Benham, A. M., Elucidation of the AGR2 Interactome in Esophageal Adenocarcinoma Cells Identifies a Redox-Sensitive Chaperone Hub for the Quality Control of MUC-5AC. *Antioxid Redox Signal* **2019,** 31, (15), 1117-1132.
154. Wang, Z.; Hao, Y.; Lowe, A. W., The adenocarcinoma-associated antigen, AGR2, promotes tumor growth, cell migration, and cellular transformation. *Cancer research* **2008,** 68, (2), 492-7.

155. Guo, X.; Noguchi, H.; Ishii, N.; Homma, T.; Hamada, T.; Hiraki, T.; Zhang, J.; Matsuo, K.; Yokoyama, S.; Ishibashi, H.; Fukushige, T.; Kanekura, T.; Fujii, J.; Uramoto, H.; Tanimoto, A.; Yamada, S., The Association of Peroxiredoxin 4 with the Initiation and Progression of Hepatocellular Carcinoma. *Antioxid Redox Signal* **2019,** 30, (10), 1271-1284.
156. Wang, W.; Shen, X. B.; Huang, D. B.; Jia, W.; Liu, W. B.; He, Y. F., Peroxiredoxin 4 suppresses anoikis and augments growth and metastasis of hepatocellular carcinoma cells through the β-catenin/ID2 pathway. *Cellular oncology (Dordrecht)* **2019,** 42, (6), 769-781.
157. Chen, B.; Lan, J.; Xiao, Y.; Liu, P.; Guo, D.; Gu, Y.; Song, Y.; Zhong, Q.; Ma, D.; Lei, P.; Liu, Q., Long noncoding RNA TP53TG1 suppresses the growth and metastasis of hepatocellular carcinoma by regulating the PRDX4/β-catenin pathway. *Cancer Lett* **2021,** 513, 75-89.
158. Kim, T. H.; Song, J.; Alcantara Llaguno, S. R.; Murnan, E.; Liyanarachchi, S.; Palanichamy, K.; Yi, J. Y.; Viapiano, M. S.; Nakano, I.; Yoon, S. O.; Wu, H.; Parada, L. F.; Kwon, C. H., Suppression of peroxiredoxin 4 in glioblastoma cells increases apoptosis and reduces tumor growth. *PLoS One* **2012,** 7, (8), e42818.
159. Kim, T. H.; Song, J.; Kim, S. H.; Parikh, A. K.; Mo, X.; Palanichamy, K.; Kaur, B.; Yu, J.; Yoon, S. O.; Nakano, I.; Kwon, C. H., Piperlongumine treatment inactivates peroxiredoxin 4, exacerbates endoplasmic reticulum stress, and preferentially kills high-grade glioma cells. *Neuro Oncol* **2014,** 16, (10), 1354-64.
160. Hintsala, H. R.; Soini, Y.; Haapasaari, K. M.; Karihtala, P., Dysregulation of redox-state-regulating enzymes in melanocytic skin tumours and the surrounding microenvironment. *Histopathology* **2015,** 67, (3), 348-57.
161. Tome, M. E.; Johnson, D. B.; Rimsza, L. M.; Roberts, R. A.; Grogan, T. M.; Miller, T. P.; Oberley, L. W.; Briehl, M. M., A redox signature score identifies diffuse large B-cell lymphoma patients with a poor prognosis. *Blood* **2005,** 106, (10), 3594-601.
162. Palande, K. K.; Beekman, R.; van der Meeren, L. E.; Beverloo, H. B.; Valk, P. J.; Touw, I. P., The antioxidant protein peroxiredoxin 4 is epigenetically down regulated in acute promyelocytic leukemia. *PLoS One* **2011,** 6, (1), e16340.
163. Mimura, K.; Kua, L. F.; Shimasaki, N.; Shiraishi, K.; Nakajima, S.; Siang, L. K.; Shabbir, A.; So, J.; Yong, W. P.; Kono, K., Upregulation of thioredoxin-1 in activated human NK cells confers increased tolerance to oxidative stress. *Cancer immunology, immunotherapy : CII* **2017,** 66, (5), 605-613.
164. Pedro, N. F.; Biselli, J. M.; Maniglia, J. V.; Santi-Neto, D.; Pavarino, E. C.; Goloni-Bertollo, E. M.; Biselli-Chicote, P. M., Candidate Biomarkers for Oral Squamous Cell Carcinoma: Differential Expression of Oxidative Stress-Related Genes. *Asian Pac J Cancer Prev* **2018,** 19, (5), 1343-1349.
165. Zhang, M.; Hou, M.; Ge, L.; Miao, C.; Zhang, J.; Jing, X.; Shi, N.; Chen, T.; Tang, X., Induction of peroxiredoxin 1 by hypoxia regulates heme oxygenase-1 via NF-κB in oral cancer. *PLoS One* **2014,** 9, (8), e105994.
166. Jain, P.; Dvorkin-Gheva, A.; Mollen, E.; Malbeteau, L.; Xie, M.; Jessa, F.; Dhavarasa, P.; Chung, S.; Brown, K. R.; Jang, G. H.; Vora, P.; Notta, F.; Moffat, J.; Hedley, D.; Boutros, P. C.; Wouters, B. G.; Koritzinsky, M., NOX4 links

metabolic regulation in pancreatic cancer to endoplasmic reticulum redox vulnerability and dependence on PRDX4. *Science advances* **2021,** 7, (19).
167. Horie, K.; Mikami, T.; Yoshida, T.; Sato, Y.; Okayasu, I., Peroxiredoxin 1 expression in active ulcerative colitis mucosa identified by proteome analysis and involvement of thioredoxin based on immunohistochemistry. *Oncology letters* **2018,** 15, (2), 2364-2372.
168. Bostanci, Z.; Mack, R. P., Jr.; Enomoto, L. M.; Alam, S.; Brown, A.; Neumann, C.; Soybel, D. I.; Kelleher, S. L., Marginal zinc intake reduces the protective effect of lactation on mammary gland carcinogenesis in a DMBA-induced tumor model in mice. *Oncology reports* **2016,** 35, (3), 1409-16.
169. Jezierska-Drutel, A.; Attaran, S.; Hopkins, B. L.; Skoko, J. J.; Rosenzweig, S. A.; Neumann, C. A., The peroxidase PRDX1 inhibits the activated phenotype in mammary fibroblasts through regulating c-Jun N-terminal kinases. *BMC cancer* **2019,** 19, (1), 812.
170. Kang, D. H.; Lee, D. J.; Lee, S.; Lee, S. Y.; Jun, Y.; Kim, Y.; Kim, Y.; Lee, J. S.; Lee, D. K.; Lee, S.; Jho, E. H.; Yu, D. Y.; Kang, S. W., Interaction of tankyrase and peroxiredoxin II is indispensable for the survival of colorectal cancer cells. *Nat Commun* **2017,** 8, (1), 40.
171. Hao, Y.; Jiang, H.; Thapa, P.; Ding, N.; Alshahrani, A.; Fujii, J.; Toledano, M. B.; Wei, Q., Critical Role of the Sulfiredoxin-Peroxiredoxin IV Axis in Urethane-Induced Non-Small Cell Lung Cancer. *Antioxidants (Basel)* **2023,** 12, (2).
172. Thapa, P.; Jiang, H.; Ding, N.; Hao, Y.; Alshahrani, A.; Lee, E. Y.; Fujii, J.; Wei, Q., Loss of Peroxiredoxin IV Protects Mice from Azoxymethane/Dextran Sulfate Sodium-Induced Colorectal Cancer Development. *Antioxidants* **2023,** 12, (3), 677.
173. Park, M. H.; Yun, H. M.; Hwang, C. J.; Park, S. I.; Han, S. B.; Hwang, D. Y.; Yoon, D. Y.; Kim, S.; Hong, J. T., Presenilin Mutation Suppresses Lung Tumorigenesis via Inhibition of Peroxiredoxin 6 Activity and Expression. *Theranostics* **2017,** 7, (15), 3624-3637.
174. Ha, B.; Kim, E. K.; Kim, J. H.; Lee, H. N.; Lee, K. O.; Lee, S. Y.; Jang, H. H., Human peroxiredoxin 1 modulates TGF-β1-induced epithelial-mesenchymal transition through its peroxidase activity. *Biochem Biophys Res Commun* **2012,** 421, (1), 33-7.
175. Yang, Y. J.; Baek, J. Y.; Goo, J.; Shin, Y.; Park, J. K.; Jang, J. Y.; Wang, S. B.; Jeong, W.; Lee, H. J.; Um, H. D.; Lee, S. K.; Choi, Y.; Rhee, S. G.; Chang, T. S., Effective Killing of Cancer Cells Through ROS-Mediated Mechanisms by AMRI-59 Targeting Peroxiredoxin I. *Antioxid Redox Signal* **2016,** 24, (8), 453-69.
176. Hong, W. G.; Kim, J. Y.; Cho, J. H.; Hwang, S. G.; Song, J. Y.; Lee, E.; Chang, T. S.; Um, H. D.; Park, J. K., AMRI-59 functions as a radiosensitizer via peroxiredoxin I-targeted ROS accumulation and apoptotic cell death induction. *Oncotarget* **2017,** 8, (69), 114050-114064.
177. Sun, H. H.; Li, Y. L.; Jiang, H.; Yin, X. H.; Jin, X. L., PRDX1 Influences The Occurrence and Progression of Liver Cancer by Inhibiting Mitochondrial Apoptosis Pathway. *Cell journal* **2022,** 24, (11), 657-664.
178. Jiang, Y.; Cao, W.; Wu, K.; Qin, X.; Wang, X.; Li, Y.; Yu, B.; Zhang, Z.; Wang, X.; Yan, M.; Xu, Q.; Zhang, J.; Chen, W., LncRNA LINC00460 promotes EMT in head and neck squamous cell carcinoma by facilitating peroxiredoxin-1 into the

nucleus. *Journal of experimental & clinical cancer research : CR* **2019,** 38, (1), 365.

179. Dasari, C.; Reddy, K. R. K.; Natani, S.; Murthy, T. R. L.; Bhukya, S.; Ummanni, R., Tumor protein D52 (isoform 3) interacts with and promotes peroxidase activity of Peroxiredoxin 1 in prostate cancer cells implicated in cell growth and migration. *Biochimica et biophysica acta. Molecular cell research* **2019,** 1866, (8), 1298-1309.
180. Feng, T.; Zhao, R.; Sun, F.; Lu, Q.; Wang, X.; Hu, J.; Wang, S.; Gao, L.; Zhou, Q.; Xiong, X.; Dong, X.; Wang, L.; Han, B., TXNDC9 regulates oxidative stress-induced androgen receptor signaling to promote prostate cancer progression. *Oncogene* **2020,** 39, (2), 356-367.
181. Li, H. X.; Sun, X. Y.; Yang, S. M.; Wang, Q.; Wang, Z. Y., Peroxiredoxin 1 promoted tumor metastasis and angiogenesis in colorectal cancer. *Pathology, research and practice* **2018,** 214, (5), 655-660.
182. Qu, M.; Li, J.; Hong, Z.; Jia, F.; He, Y.; Yuan, L., The role of human umbilical cord mesenchymal stem cells-derived exosomal microRNA-431-5p in survival and prognosis of colorectal cancer patients. *Mutagenesis* **2022,** 37, (2), 164-171.
183. Xu, S.; Ma, Y.; Tong, Q.; Yang, J.; Liu, J.; Wang, Y.; Li, G.; Zeng, J.; Fang, S.; Li, F.; Xie, X.; Zhang, J., Cullin-5 neddylation-mediated NOXA degradation is enhanced by PRDX1 oligomers in colorectal cancer. *Cell death & disease* **2021,** 12, (3), 265.
184. Bajor, M.; Zych, A. O.; Graczyk-Jarzynka, A.; Muchowicz, A.; Firczuk, M.; Trzeciak, L.; Gaj, P.; Domagala, A.; Siernicka, M.; Zagozdzon, A.; Siedlecki, P.; Kniotek, M.; O'Leary, P. C.; Golab, J.; Zagozdzon, R., Targeting peroxiredoxin 1 impairs growth of breast cancer cells and potently sensitises these cells to prooxidant agents. *British journal of cancer* **2018,** 119, (7), 873-884.
185. Bajor, M.; Graczyk-Jarzynka, A.; Marhelava, K.; Kurkowiak, M.; Rahman, A.; Aura, C.; Russell, N.; Zych, A. O.; Firczuk, M.; Winiarska, M.; Gallagher, W. M.; Zagozdzon, R., Triple Combination of Ascorbate, Menadione and the Inhibition of Peroxiredoxin-1 Produces Synergistic Cytotoxic Effects in Triple-Negative Breast Cancer Cells. *Antioxidants (Basel)* **2020,** 9, (4).
186. Fiskus, W.; Coothankandaswamy, V.; Chen, J.; Ma, H.; Ha, K.; Saenz, D. T.; Krieger, S. S.; Mill, C. P.; Sun, B.; Huang, P.; Mumm, J. S.; Melnick, A. M.; Bhalla, K. N., SIRT2 Deacetylates and Inhibits the Peroxidase Activity of Peroxiredoxin-1 to Sensitize Breast Cancer Cells to Oxidant Stress-Inducing Agents. *Cancer research* **2016,** 76, (18), 5467-78.
187. Skoko, J. J.; Cao, J.; Gaboriau, D.; Attar, M.; Asan, A.; Hong, L.; Paulsen, C. E.; Ma, H.; Liu, Y.; Wu, H.; Harkness, T.; Furdui, C. M.; Manevich, Y.; Morrison, C. G.; Brown, E. T.; Normolle, D.; Spies, M.; Spies, M. A.; Carroll, K.; Neumann, C. A., Redox regulation of RAD51 Cys319 and homologous recombination by peroxiredoxin 1. *Redox biology* **2022,** 56, 102443.
188. Attaran, S.; Skoko, J. J.; Hopkins, B. L.; Wright, M. K.; Wood, L. E.; Asan, A.; Woo, H. A.; Feinberg, A.; Neumann, C. A., Peroxiredoxin-1 Tyr194 phosphorylation regulates LOX-dependent extracellular matrix remodelling in breast cancer. *British journal of cancer* **2021,** 125, (8), 1146-1157.

189. Yang, L.; Hong, Q.; Xu, S. G.; Kuang, X. Y.; Di, G. H.; Liu, G. Y.; Wu, J.; Shao, Z. M.; Yu, S. J., Downregulation of transgelin 2 promotes breast cancer metastasis by activating the reactive oxygen species/nuclear factor-κB signaling pathway. *Mol Med Rep* **2019,** 20, (5), 4045-4258.
190. Wang, R.; Liu, Y.; Liu, L.; Chen, M.; Wang, X.; Yang, J.; Gong, Y.; Ding, B. S.; Wei, Y.; Wei, X., Tumor cells induce LAMP2a expression in tumor-associated macrophage for cancer progression. *EBioMedicine* **2019,** 40, 118-134.
191. Klopotowska, M.; Bajor, M.; Graczyk-Jarzynka, A.; Kraft, A.; Pilch, Z.; Zhylko, A.; Firczuk, M.; Baranowska, I.; Lazniewski, M.; Plewczynski, D.; Goral, A.; Soroczynska, K.; Domagala, J.; Marhelava, K.; Slusarczyk, A.; Retecki, K.; Ramji, K.; Krawczyk, M.; Temples, M. N.; Sharma, B.; Lachota, M.; Netskar, H.; Malmberg, K. J.; Zagozdzon, R.; Winiarska, M., PRDX-1 Supports the Survival and Antitumor Activity of Primary and CAR-Modified NK Cells under Oxidative Stress. *Cancer immunology research* **2022,** 10, (2), 228-244.
192. Chen, Y.; Yang, S.; Zhou, H.; Su, D., PRDX2 Promotes the Proliferation and Metastasis of Non-Small Cell Lung Cancer In Vitro and In Vivo. *BioMed research international* **2020,** 2020, 8359860.
193. Jing, X.; Du, L.; Niu, A.; Wang, Y.; Wang, Y.; Wang, C., Silencing of PRDX2 Inhibits the Proliferation and Invasion of Non-Small Cell Lung Cancer Cells. *BioMed research international* **2020,** 2020, 1276328.
194. Chandimali, N.; Huynh, D. L.; Zhang, J. J.; Lee, J. C.; Yu, D. Y.; Jeong, D. K.; Kwon, T., MicroRNA-122 negatively associates with peroxiredoxin-II expression in human gefitinib-resistant lung cancer stem cells. *Cancer gene therapy* **2019,** 26, (9-10), 292-304.
195. Zhang, Y.; Sun, C.; Xiao, G.; Shan, H.; Tang, L.; Yi, Y.; Yu, W.; Gu, Y., S-nitrosylation of the Peroxiredoxin-2 promotes S-nitrosoglutathione-mediated lung cancer cells apoptosis via AMPK-SIRT1 pathway. *Cell death & disease* **2019,** 10, (5), 329.
196. Wang, W.; Wei, J.; Zhang, H.; Zheng, X.; Zhou, H.; Luo, Y.; Yang, J.; Deng, Q.; Huang, S.; Fu, Z., PRDX2 promotes the proliferation of colorectal cancer cells by increasing the ubiquitinated degradation of p53. *Cell death & disease* **2021,** 12, (6), 605.
197. Peng, L.; Xiong, Y.; Wang, R.; Xiang, L.; Zhou, H.; Fu, Z., The critical role of peroxiredoxin-2 in colon cancer stem cells. *Aging* **2021,** 13, (8), 11170-11187.
198. Wang, R.; Wei, J.; Zhang, S.; Wu, X.; Guo, J.; Liu, M.; Du, K.; Xu, J.; Peng, L.; Lv, Z.; You, W.; Xiong, Y.; Fu, Z., Peroxiredoxin 2 is essential for maintaining cancer stem cell-like phenotype through activation of Hedgehog signaling pathway in colon cancer. *Oncotarget* **2016,** 7, (52), 86816-86828.
199. Cerda, M. B.; Lloyd, R.; Batalla, M.; Giannoni, F.; Casal, M.; Policastro, L., Silencing peroxiredoxin-2 sensitizes human colorectal cancer cells to ionizing radiation and oxaliplatin. *Cancer Lett* **2017,** 388, 312-319.
200. Peng, L.; Jiang, J.; Chen, H. N.; Zhou, L.; Huang, Z.; Qin, S.; Jin, P.; Luo, M.; Li, B.; Shi, J.; Xie, N.; Deng, L. W.; Liou, Y. C.; Nice, E. C.; Huang, C.; Wei, Y., Redox-sensitive cyclophilin A elicits chemoresistance through realigning cellular oxidative status in colorectal cancer. *Cell Rep* **2021,** 37, (9), 110069.

201. Lv, Z.; Wei, J.; You, W.; Wang, R.; Shang, J.; Xiong, Y.; Yang, H.; Yang, X.; Fu, Z., Disruption of the c-Myc/miR-200b-3p/PRDX2 regulatory loop enhances tumor metastasis and chemotherapeutic resistance in colorectal cancer. *Journal of translational medicine* **2017,** 15, (1), 257.
202. Xu, J.; Zhang, S.; Wang, R.; Wu, X.; Zeng, L.; Fu, Z., Knockdown of PRDX2 sensitizes colon cancer cells to 5-FU by suppressing the PI3K/AKT signaling pathway. *Bioscience reports* **2017,** 37, (3).
203. Yu, Y.; Chen, D.; Wu, T.; Lin, H.; Ni, L.; Sui, H.; Xiao, S.; Wang, C.; Jiang, S.; Pan, H.; Li, S.; Jin, X.; Xie, C.; Cui, R., Dihydroartemisinin enhances the anti-tumor activity of oxaliplatin in colorectal cancer cells by altering PRDX2-reactive oxygen species-mediated multiple signaling pathways. *Phytomedicine : international journal of phytotherapy and phytopharmacology* **2022,** 98, 153932.
204. Ahmad, A.; Prakash, R.; Khan, M. S.; Altwaijry, N.; Asghar, M. N.; Raza, S. S.; Khan, R., N-Carbamoyl Alanine-Mediated Selective Targeting for CHEK2-Null Colorectal Cancer. *ACS omega* **2022,** 7, (15), 13095-13101.
205. Zhang, S.; Fu, Z.; Wei, J.; Guo, J.; Liu, M.; Du, K., Peroxiredoxin 2 is involved in vasculogenic mimicry formation by targeting VEGFR2 activation in colorectal cancer. *Medical oncology (Northwood, London, England)* **2015,** 32, (1), 414.
206. Zheng, X.; Wei, J.; Li, W.; Li, X.; Wang, W.; Guo, J.; Fu, Z., PRDX2 removal inhibits the cell cycle and autophagy in colorectal cancer cells. *Aging* **2020,** 12, (16), 16390-16409.
207. Shi, J.; Zhou, L.; Huang, H. S.; Peng, L.; Xie, N.; Nice, E.; Fu, L.; Jiang, C.; Huang, C., Repurposing Oxiconazole against Colorectal Cancer via PRDX2-mediated Autophagy Arrest. *International journal of biological sciences* **2022,** 18, (9), 3747-3761.
208. Zhu, J.; Wu, C.; Li, H.; Yuan, Y.; Wang, X.; Zhao, T.; Xu, J., DACH1 inhibits the proliferation and invasion of lung adenocarcinoma through the downregulation of peroxiredoxin 3. *Tumour biology : the journal of the International Society for Oncodevelopmental Biology and Medicine* **2016,** 37, (7), 9781-8.
209. Myers, C. R., Enhanced targeting of mitochondrial peroxide defense by the combined use of thiosemicarbazones and inhibitors of thioredoxin reductase. *Free Radic Biol Med* **2016,** 91, 81-92.
210. Chen, H. C.; Long, M.; Gao, Z. W.; Liu, C.; Wu, X. N.; Yang, L.; Dong, K.; Zhang, H. Z., Silencing of B7-H4 induces intracellular oxidative stress and inhibits cell viability of breast cancer cells via downregulating PRDX3. *Neoplasma* **2022,** 69, (4), 940-947.
211. Song, I. S.; Jeong, Y. J.; Jeong, S. H.; Heo, H. J.; Kim, H. K.; Bae, K. B.; Park, Y. H.; Kim, S. U.; Kim, J. M.; Kim, N.; Ko, K. S.; Rhee, B. D.; Han, J., FOXM1-Induced PRX3 Regulates Stemness and Survival of Colon Cancer Cells via Maintenance of Mitochondrial Function. *Gastroenterology* **2015,** 149, (4), 1006-16.e9.
212. Kim, B.; Kim, Y. S.; Ahn, H. M.; Lee, H. J.; Jung, M. K.; Jeong, H. Y.; Choi, D. K.; Lee, J. H.; Lee, S. R.; Kim, J. M.; Lee, D. S., Peroxiredoxin 5 overexpression enhances tumorigenicity and correlates with poor prognosis in gastric cancer. *Int J Oncol* **2017,** 51, (1), 298-306.

213. Sato, K.; Shi, L.; Ito, F.; Ohara, Y.; Motooka, Y.; Tanaka, H.; Mizuno, M.; Hori, M.; Hirayama, T.; Hibi, H.; Toyokuni, S., Non-thermal plasma specifically kills oral squamous cell carcinoma cells in a catalytic Fe(II)-dependent manner. *J Clin Biochem Nutr* **2019,** 65, (1), 8-15.
214. Sun, H. N.; Guo, X. Y.; Xie, D. P.; Wang, X. M.; Ren, C. X.; Han, Y. H.; Yu, N. N.; Huang, Y. L.; Kwon, T., Knockdown of Peroxiredoxin V increased the cytotoxicity of non-thermal plasma-treated culture medium to A549 cells. *Aging* **2022,** 14, (9), 4000-4013.
215. Chen, X.; Cao, X.; Xiao, W.; Li, B.; Xue, Q., PRDX5 as a novel binding partner in Nrf2-mediated NSCLC progression under oxidative stress. *Aging* **2020,** 12, (1), 122-137.
216. Cao, X.; Chen, X. M.; Xiao, W. Z.; Li, B.; Zhang, B.; Wu, Q.; Xue, Q., ROS-mediated hypomethylation of PRDX5 promotes STAT3 binding and activates the Nrf2 signaling pathway in NSCLC. *International journal of molecular medicine* **2021,** 47, (2), 573-582.
217. Ahn, H. M.; Yoo, J. W.; Lee, S.; Lee, H. J.; Lee, H. S.; Lee, D. S., Peroxiredoxin 5 promotes the epithelial-mesenchymal transition in colon cancer. *Biochem Biophys Res Commun* **2017,** 487, (3), 580-586.
218. Liu, Y.; Kwon, T.; Kim, J. S.; Chandimali, N.; Jin, Y. H.; Gong, Y. X.; Xie, D. P.; Han, Y. H.; Jin, M. H.; Shen, G. N.; Jeong, D. K.; Lee, D. S.; Cui, Y. D.; Sun, H. N., Peroxiredoxin V Reduces β-Lapachone-induced Apoptosis of Colon Cancer Cells. *Anticancer research* **2019,** 39, (7), 3677-3686.
219. Chandimali, N.; Sun, H. N.; Kong, L. Z.; Zhen, X.; Liu, R.; Kwon, T.; Lee, D. S., Shikonin-induced Apoptosis of Colon Cancer Cells Is Reduced by Peroxiredoxin V Expression. *Anticancer research* **2019,** 39, (11), 6115-6123.
220. Li, H.; Zhang, D.; Li, B.; Zhen, H.; Chen, W.; Men, Q., PRDX6 Overexpression Promotes Proliferation, Invasion, and Migration of A549 Cells in vitro and in vivo. *Cancer management and research* **2021,** 13, 1245-1255.
221. Xu, J.; Su, Q.; Gao, M.; Liang, Q.; Li, J.; Chen, X., Differential Expression And Effects Of Peroxiredoxin-6 On Drug Resistance And Cancer Stem Cell-Like Properties In Non-Small Cell Lung Cancer. *OncoTargets and therapy* **2019,** 12, 10477-10486.
222. Li, B. Z.; Bai, H. H.; Tan, F. W.; Gao, Y. B.; He, J., Identification of peroxiredoxin 6 as a potential lung-adenocarcinoma biomarker for predicting chemotherapy response by proteomic analysis. *Journal of biological regulators and homeostatic agents* **2021,** 35, (2), 537-546.
223. Chen, C.; Gong, L.; Liu, X.; Zhu, T.; Zhou, W.; Kong, L.; Luo, J., Identification of peroxiredoxin 6 as a direct target of withangulatin A by quantitative chemical proteomics in non-small cell lung cancer. *Redox biology* **2021,** 46, 102130.
224. Huang, W. S.; Huang, C. Y.; Hsieh, M. C.; Kuo, Y. H.; Tung, S. Y.; Shen, C. H.; Hsieh, Y. Y.; Teng, C. C.; Lee, K. C.; Lee, K. F.; Kuo, H. C., Expression of PRDX6 Correlates with Migration and Invasiveness of Colorectal Cancer Cells. *Cellular physiology and biochemistry : international journal of experimental cellular physiology, biochemistry, and pharmacology* **2018,** 51, (6), 2616-2630.
225. Planson, A. G.; Palais, G.; Abbas, K.; Gerard, M.; Couvelard, L.; Delaunay, A.; Baulande, S.; Drapier, J. C.; Toledano, M. B., Sulfiredoxin protects mice from

lipopolysaccharide-induced endotoxic shock. *Antioxid Redox Signal* **2011,** 14, (11), 2071-80.
226. Wei, Q.; Jiang, H.; Baker, A.; Dodge, L. K.; Gerard, M.; Young, M. R.; Toledano, M. B.; Colburn, N. H., Loss of sulfiredoxin renders mice resistant to azoxymethane/dextran sulfate sodium-induced colon carcinogenesis. *Carcinogenesis* **2013,** 34, (6), 1403-10.
227. Okayasu, I.; Hatakeyama, S.; Yamada, M.; Ohkusa, T.; Inagaki, Y.; Nakaya, R., A novel method in the induction of reliable experimental acute and chronic ulcerative colitis in mice. *Gastroenterology* **1990,** 98, (3), 694-702.
228. Euhus, D. M.; Hudd, C.; LaRegina, M. C.; Johnson, F. E., Tumor measurement in the nude mouse. *Journal of surgical oncology* **1986,** 31, (4), 229-34.
229. Thaker, A. I.; Shaker, A.; Rao, M. S.; Ciorba, M. A., Modeling colitis-associated cancer with azoxymethane (AOM) and dextran sulfate sodium (DSS). *Journal of visualized experiments : JoVE* **2012**, (67).
230. Tseng, W.; Leong, X.; Engleman, E., Orthotopic mouse model of colorectal cancer. *Journal of visualized experiments : JoVE* **2007**, (10), 484.
231. Siegel, R. L.; Miller, K. D.; Fuchs, H. E.; Jemal, A., Cancer statistics, 2022. *CA Cancer J Clin* **2022,** 72, (1), 7-33.
232. Siegel, R. L.; Fedewa, S. A.; Anderson, W. F.; Miller, K. D.; Ma, J.; Rosenberg, P. S.; Jemal, A., Colorectal Cancer Incidence Patterns in the United States, 1974-2013. *Journal of the National Cancer Institute* **2017,** 109, (8).
233. Chaiswing, L.; St Clair, W. H.; St Clair, D. K., Redox Paradox: A Novel Approach to Therapeutics-Resistant Cancer. *Antioxid Redox Signal* **2018,** 29, (13), 1237-1272.
234. Zito, E.; Melo, E. P.; Yang, Y.; Wahlander, A.; Neubert, T. A.; Ron, D., Oxidative protein folding by an endoplasmic reticulum-localized peroxiredoxin. *Mol Cell* **2010,** 40, (5), 787-97.
235. Jiang, H.; Wu, L.; Chen, J.; Mishra, M.; Chawsheen, H. A.; Zhu, H.; Wei, Q., Sulfiredoxin Promotes Colorectal Cancer Cell Invasion and Metastasis through a Novel Mechanism of Enhancing EGFR Signaling. *Molecular cancer research : MCR* **2015,** 13, (12), 1554-66.
236. Biteau, B.; Labarre, J.; Toledano, M. B., ATP-dependent reduction of cysteine-sulphinic acid by S. cerevisiae sulphiredoxin. *Nature* **2003,** 425, (6961), 980-4.
237. Wu, L.; Jiang, H.; Chawsheen, H. A.; Mishra, M.; Young, M. R.; Gerard, M.; Toledano, M. B.; Colburn, N. H.; Wei, Q., Tumor promoter-induced sulfiredoxin is required for mouse skin tumorigenesis. *Carcinogenesis* **2014,** 35, (5), 1177-84.
238. Suzuki, R.; Kohno, H.; Sugie, S.; Nakagama, H.; Tanaka, T., Strain differences in the susceptibility to azoxymethane and dextran sodium sulfate-induced colon carcinogenesis in mice. *Carcinogenesis* **2006,** 27, (1), 162-9.
239. Heng, T. S.; Painter, M. W., The Immunological Genome Project: networks of gene expression in immune cells. *Nature immunology* **2008,** 9, (10), 1091-4.
240. Boutilier, A. J.; Elsawa, S. F., Macrophage Polarization States in the Tumor Microenvironment. *Int J Mol Sci* **2021,** 22, (13).
241. Downs-Canner, S. M.; Meier, J.; Vincent, B. G.; Serody, J. S., B Cell Function in the Tumor Microenvironment. *Annual review of immunology* **2022,** 40, 169-193.

242. Terzić, J.; Grivennikov, S.; Karin, E.; Karin, M., Inflammation and colon cancer. *Gastroenterology* **2010,** 138, (6), 2101-2114.e5.
243. Noy, R.; Pollard, J. W., Tumor-associated macrophages: from mechanisms to therapy. *Immunity* **2014,** 41, (1), 49-61.
244. Feng, M.; Zhao, Z.; Yang, M.; Ji, J.; Zhu, D., T-cell-based immunotherapy in colorectal cancer. *Cancer Lett* **2021,** 498, 201-209.
245. Ziegler, S. F., Division of labour by CD4(+) T helper cells. *Nature reviews. Immunology* **2016,** 16, (7), 403.
246. Zhang, N.; Bevan, M. J., CD8(+) T cells: foot soldiers of the immune system. *Immunity* **2011,** 35, (2), 161-8.
247. Keir, M. E.; Butte, M. J.; Freeman, G. J.; Sharpe, A. H., PD-1 and its ligands in tolerance and immunity. *Annual review of immunology* **2008,** 26, 677-704.
248. Yamaguchi, H.; Hsu, J. M.; Yang, W. H.; Hung, M. C., Mechanisms regulating PD-L1 expression in cancers and associated opportunities for novel small-molecule therapeutics. *Nature reviews. Clinical oncology* **2022,** 19, (5), 287-305.
249. Cowen, P. N., Strain differences in mice to the carcinogenic action of urethane and its non-carcinogenicity in chicks and guinea-pigs. *British journal of cancer* **1950,** 4, (2), 245-53.
250. Hennings, H.; Glick, A. B.; Lowry, D. T.; Krsmanovic, L. S.; Sly, L. M.; Yuspa, S. H., FVB/N mice: an inbred strain sensitive to the chemical induction of squamous cell carcinomas in the skin. *Carcinogenesis* **1993,** 14, (11), 2353-8.
251. Malkinson, A. M., The genetic basis of susceptibility to lung tumors in mice. *Toxicology* **1989,** 54, (3), 241-71.
252. Nambiar, P. R.; Girnun, G.; Lillo, N. A.; Guda, K.; Whiteley, H. E.; Rosenberg, D. W., Preliminary analysis of azoxymethane induced colon tumors in inbred mice commonly used as transgenic/knockout progenitors. *Int J Oncol* **2003,** 22, (1), 145-50.
253. Wu, N.; Du, X.; Peng, Z.; Zhang, Z.; Cui, L.; Li, D.; Wang, R.; Ma, M., Silencing of peroxiredoxin 1 expression ameliorates ulcerative colitis in a rat model. *J Int Med Res* **2021,** 49, (3), 300060520986313.
254. Won, H. Y.; Jang, E. J.; Lee, K.; Oh, S.; Kim, H. K.; Woo, H. A.; Kang, S. W.; Yu, D. Y.; Rhee, S. G.; Hwang, E. S., Ablation of peroxiredoxin II attenuates experimental colitis by increasing FoxO1-induced Foxp3+ regulatory T cells. *J Immunol* **2013,** 191, (8), 4029-37.
255. Kim, H. R.; Lee, A.; Choi, E. J.; Kie, J. H.; Lim, W.; Lee, H. K.; Moon, B. I.; Seoh, J. Y., Attenuation of experimental colitis in glutathione peroxidase 1 and catalase double knockout mice through enhancing regulatory T cell function. *PLoS One* **2014,** 9, (4), e95332.
256. Krehl, S.; Loewinger, M.; Florian, S.; Kipp, A. P.; Banning, A.; Wessjohann, L. A.; Brauer, M. N.; Iori, R.; Esworthy, R. S.; Chu, F. F.; Brigelius-Flohé, R., Glutathione peroxidase-2 and selenium decreased inflammation and tumors in a mouse model of inflammation-associated carcinogenesis whereas sulforaphane effects differed with selenium supply. *Carcinogenesis* **2012,** 33, (3), 620-8.
257. Esworthy, R. S.; Kim, B. W.; Chow, J.; Shen, B.; Doroshow, J. H.; Chu, F. F., Nox1 causes ileocolitis in mice deficient in glutathione peroxidase-1 and -2. *Free Radic Biol Med* **2014,** 68, 315-25.

258. Botella, L. M.; Sánchez-Elsner, T.; Sanz-Rodriguez, F.; Kojima, S.; Shimada, J.; Guerrero-Esteo, M.; Cooreman, M. P.; Ratziu, V.; Langa, C.; Vary, C. P.; Ramirez, J. R.; Friedman, S.; Bernabéu, C., Transcriptional activation of endoglin and transforming growth factor-beta signaling components by cooperative interaction between Sp1 and KLF6: their potential role in the response to vascular injury. *Blood* **2002,** 100, (12), 4001-10.
259. Hohensinner, P. J.; Kaun, C.; Rychli, K.; Niessner, A.; Pfaffenberger, S.; Rega, G.; de Martin, R.; Maurer, G.; Ullrich, R.; Huber, K.; Wojta, J., Macrophage colony stimulating factor expression in human cardiac cells is upregulated by tumor necrosis factor-alpha via an NF-kappaB dependent mechanism. *Journal of thrombosis and haemostasis : JTH* **2007,** 5, (12), 2520-8.
260. Au, P. Y.; Martin, N.; Chau, H.; Moemeni, B.; Chia, M.; Liu, F. F.; Minden, M.; Yeh, W. C., The oncogene PDGF-B provides a key switch from cell death to survival induced by TNF. *Oncogene* **2005,** 24, (19), 3196-205.
261. Jerkic, M.; Peter, M.; Ardelean, D.; Fine, M.; Konerding, M. A.; Letarte, M., Dextran sulfate sodium leads to chronic colitis and pathological angiogenesis in Endoglin heterozygous mice. *Inflammatory bowel diseases* **2010,** 16, (11), 1859-70.
262. Ma, P.; Feng, Y. C., Decreased serum fetuin-A levels and active inflammatory bowel disease. *The American journal of the medical sciences* **2014,** 348, (1), 47-51.
263. Krzystek-Korpacka, M.; Neubauer, K.; Matusiewicz, M., Platelet-derived growth factor-BB reflects clinical, inflammatory and angiogenic disease activity and oxidative stress in inflammatory bowel disease. *Clinical biochemistry* **2009,** 42, (16-17), 1602-9.
264. Wiercinska-Drapalo, A.; Jaroszewicz, J.; Parfieniuk, A.; Lapinski, T. W.; Rogalska, M.; Prokopowicz, D., Pigment epithelium-derived factor in ulcerative colitis: possible relationship with disease activity. *Regulatory peptides* **2007,** 140, (1-2), 1-4.
265. Makiyama, K.; Tomonaga, M.; Nakamuta, K.; Oda, H.; Itsuno, M.; Hara, K., Serum concentration of macrophage colony stimulating factor (M-CSF) in patients with inflammatory bowel disease. *Gastroenterologia Japonica* **1993,** 28, (5), 740.
266. Baricević, I.; Jones, D. R.; Nikolić, J. A.; Nedić, O., Gastrointestinal inflammation and the circulating IGF system in humans. *Hormone and metabolic research = Hormon- und Stoffwechselforschung = Hormones et metabolisme* **2006,** 38, (1), 22-7.
267. Grieco, M. J.; Shantha Kumara, H. M.; Baxter, R.; Dujovny, N.; Kalady, M. F.; Cekic, V.; Luchtefeld, M.; Whelan, R. L., Minimally invasive colorectal resection is associated with a rapid and sustained decrease in plasma levels of epidermal growth factor (EGF) in the colon cancer setting. *Surgical endoscopy* **2010,** 24, (10), 2617-22.
268. Le Marchand, L.; Wang, H.; Rinaldi, S.; Kaaks, R.; Vogt, T. M.; Yokochi, L.; Decker, R., Associations of plasma C-peptide and IGFBP-1 levels with risk of colorectal adenoma in a multiethnic population. *Cancer epidemiology, biomarkers & prevention : a publication of the American Association for Cancer Research, cosponsored by the American Society of Preventive Oncology* **2010,** 19, (6), 1471-7.

269. Kaaks, R.; Toniolo, P.; Akhmedkhanov, A.; Lukanova, A.; Biessy, C.; Dechaud, H.; Rinaldi, S.; Zeleniuch-Jacquotte, A.; Shore, R. E.; Riboli, E., Serum C-peptide, insulin-like growth factor (IGF)-I, IGF-binding proteins, and colorectal cancer risk in women. *Journal of the National Cancer Institute* **2000,** 92, (19), 1592-600.
270. le Rolle, A. F.; Chiu, T. K.; Fara, M.; Shia, J.; Zeng, Z.; Weiser, M. R.; Paty, P. B.; Chiu, V. K., The prognostic significance of CXCL1 hypersecretion by human colorectal cancer epithelia and myofibroblasts. *Journal of translational medicine* **2015,** 13, 199.
271. Lu, C.; Zhang, X.; Luo, Y.; Huang, J.; Yu, M., Identification of CXCL10 and CXCL11 as the candidate genes involving the development of colitis-associated colorectal cancer. *Frontiers in genetics* **2022,** 13, 945414.
272. Cao, Y.; Jiao, N.; Sun, T.; Ma, Y.; Zhang, X.; Chen, H.; Hong, J.; Zhang, Y., CXCL11 Correlates With Antitumor Immunity and an Improved Prognosis in Colon Cancer. *Frontiers in cell and developmental biology* **2021,** 9, 646252.
273. Mähler, M.; Bristol, I. J.; Leiter, E. H.; Workman, A. E.; Birkenmeier, E. H.; Elson, C. O.; Sundberg, J. P., Differential susceptibility of inbred mouse strains to dextran sulfate sodium-induced colitis. *The American journal of physiology* **1998,** 274, (3), G544-51.
274. Reinoso Webb, C.; den Bakker, H.; Koboziev, I.; Jones-Hall, Y.; Rao Kottapalli, K.; Ostanin, D.; Furr, K. L.; Mu, Q.; Luo, X. M.; Grisham, M. B., Differential Susceptibility to T Cell-Induced Colitis in Mice: Role of the Intestinal Microbiota. *Inflammatory bowel diseases* **2018,** 24, (2), 361-379.
275. Siegel, R. L.; Miller, K. D.; Wagle, N. S.; Jemal, A., Cancer statistics, 2023. *CA Cancer J Clin* **2023,** 73, (1), 17-48.
276. Dekker, E.; Tanis, P. J.; Vleugels, J. L. A.; Kasi, P. M.; Wallace, M. B., Colorectal cancer. *Lancet (London, England)* **2019,** 394, (10207), 1467-1480.
277. Haggar, F. A.; Boushey, R. P., Colorectal cancer epidemiology: incidence, mortality, survival, and risk factors. *Clinics in colon and rectal surgery* **2009,** 22, (4), 191-7.
278. Tokui, N.; Yoneyama, M. S.; Hatakeyama, S.; Yamamoto, H.; Koie, T.; Saitoh, H.; Yamaya, K.; Funyu, T.; Nakamura, T.; Ohyama, C.; Tsuboi, S., Extravasation during bladder cancer metastasis requires cortactin-mediated invadopodia formation. *Mol Med Rep* **2014,** 9, (4), 1142-6.
279. Jardé, T.; Evans, R. J.; McQuillan, K. L.; Parry, L.; Feng, G. J.; Alvares, B.; Clarke, A. R.; Dale, T. C., In vivo and in vitro models for the therapeutic targeting of Wnt signaling using a Tet-OΔN89β-catenin system. *Oncogene* **2013,** 32, (7), 883-93.
280. Shibata, H.; Toyama, K.; Shioya, H.; Ito, M.; Hirota, M.; Hasegawa, S.; Matsumoto, H.; Takano, H.; Akiyama, T.; Toyoshima, K.; Kanamaru, R.; Kanegae, Y.; Saito, I.; Nakamura, Y.; Shiba, K.; Noda, T., Rapid colorectal adenoma formation initiated by conditional targeting of the Apc gene. *Science* **1997,** 278, (5335), 120-3.
281. Qi, L.; Sun, B.; Liu, Z.; Li, H.; Gao, J.; Leng, X., Dickkopf-1 inhibits epithelial-mesenchymal transition of colon cancer cells and contributes to colon cancer suppression. *Cancer science* **2012,** 103, (4), 828-35.
282. Ilić, D.; Furuta, Y.; Kanazawa, S.; Takeda, N.; Sobue, K.; Nakatsuji, N.; Nomura, S.; Fujimoto, J.; Okada, M.; Yamamoto, T., Reduced cell motility and enhanced

focal adhesion contact formation in cells from FAK-deficient mice. *Nature* **1995,** 377, (6549), 539-44.
283. Webb, D. J.; Donais, K.; Whitmore, L. A.; Thomas, S. M.; Turner, C. E.; Parsons, J. T.; Horwitz, A. F., FAK-Src signalling through paxillin, ERK and MLCK regulates adhesion disassembly. *Nat Cell Biol* **2004,** 6, (2), 154-61.
284. Jiang, H.; Thapa, P.; Ding, N.; Hao, Y.; Alshahrani, A.; Wang, C.; Evers, B. M.; Wei, Q., Sulfiredoxin Promotes Cancer Cell Invasion through Regulation of the miR143-Fascin Axis. *Mol Cell Biol* **2022,** 42, (5), e0005122.
285. Jia, Y.; Chen, L.; Guo, S.; Li, Y., Baicalin induced colon cancer cells apoptosis through miR-217/DKK1-mediated inhibition of Wnt signaling pathway. *Mol Biol Rep* **2019,** 46, (2), 1693-1700.
286. Cho, H. H.; Song, J. S.; Yu, J. M.; Yu, S. S.; Choi, S. J.; Kim, D. H.; Jung, J. S., Differential effect of NF-kappaB activity on beta-catenin/Tcf pathway in various cancer cells. *FEBS Lett* **2008,** 582, (5), 616-22.
287. Gwak, J.; Park, S.; Cho, M.; Song, T.; Cha, S. H.; Kim, D. E.; Jeon, Y. J.; Shin, J. G.; Oh, S., Polysiphonia japonica extract suppresses the Wnt/beta-catenin pathway in colon cancer cells by activation of NF-kappaB. *International journal of molecular medicine* **2006,** 17, (6), 1005-10.
288. Lamberti, C.; Lin, K. M.; Yamamoto, Y.; Verma, U.; Verma, I. M.; Byers, S.; Gaynor, R. B., Regulation of beta-catenin function by the IkappaB kinases. *J Biol Chem* **2001,** 276, (45), 42276-86.
289. Bassoy, E. Y.; Walch, M.; Martinvalet, D., Reactive Oxygen Species: Do They Play a Role in Adaptive Immunity? *Front Immunol* **2021,** 12, 755856.
290. Pang, B.; Zhou, X.; Yu, H.; Dong, M.; Taghizadeh, K.; Wishnok, J. S.; Tannenbaum, S. R.; Dedon, P. C., Lipid peroxidation dominates the chemistry of DNA adduct formation in a mouse model of inflammation. *Carcinogenesis* **2007,** 28, (8), 1807-13.
291. Coussens, L. M.; Werb, Z., Inflammation and cancer. *Nature* **2002,** 420, (6917), 860-7.
292. Pozharisski, K. M.; Kapustin, Y. M.; Likhachev, A. J.; Shaposhnikov, J. D., The mechanism of carcinogenic action of 1,2-dimethylhydrazine (SDMH) in rats. *International journal of cancer* **1975,** 15, (4), 673-83.
293. Ohkusa, T.; Yamada, M.; Takenaga, T.; Kitazume, C.; Yamamoto, N.; Sasabe, M.; Takashimizu, I.; Tamura, Y.; Sakamoto, E.; Kurosawa, H.; et al., [Protective effect of metronidazole in experimental ulcerative colitis induced by dextran sulfate sodium]. *Nihon Shokakibyo Gakkai zasshi = The Japanese journal of gastro-enterology* **1987,** 84, (10), 2337-46.
294. Rooks, M. G.; Garrett, W. S., Gut microbiota, metabolites and host immunity. *Nat Rev Immunol* **2016,** 16, (6), 341-52.

VITA

Pratik Thapa

Education

2018 - 2023	Ph.D. student, Toxicology and Cancer Biology, University of Kentucky, Lexington, KY
2014 - 2018	B.S. Chemistry, University of Louisville, Louisville, KY

Professional Positions

2018 - present	Graduate Research Assistant, University of Kentucky, Lexington, KY
2016 - 2017	Undergraduate Research Assistant, Department of Biology, University of Louisville, Louisville, KY

Scholastic and Professional Honors

April 2022	Markey Cancer Center Scientist in Training Travel Award, AACR Annual Meeting 2022
April 2021	ASBMB Graduate Student Travel Award, Annual Meeting 2021
January 2020 – January 2022	T32ES07266 T-32 Molecular Mechanism of Toxicity Training Grant, University of Kentucky, Lexington, KY
May 2018	Special Citation for Outstanding Academic Performance, Department of Chemistry, University of Louisville
August 2016 – May 2017	Undergraduate Research Scholar Grant, University of Louisville, Louisville, KY
December 2014 – May 2018	Dean’s List, University of Louisville, Louisville, KY

Publications

1. Chawsheen HA, Jiang H, Ying Q, Ding N, **Thapa P**, Wei Q. The redox regulator sulfiredoxin forms a complex with thioredoxin domain-containing 5 protein in response to ER stress in lung cancer cells. J Biol Chem. 2019 May 31;294(22):8991-9006. doi: 10.1074/jbc.RA118.005804. Epub 2019 Apr 18. PMID: 31000628; PMCID: PMC6552416.
2. Jiang H, **Thapa P**, Ding N, Hao Y, Alshahrani A, Wang C, Evers BM, Wei Q. Sulfiredoxin Promotes Cancer Cell Invasion through Regulation of the miR143-Fascin Axis. Mol Cell Biol. 2022 May 19;42(5):e0005122. doi: 10.1128/mcb.00051-22. Epub 2022 Apr 12. PMID: 35412358; PMCID: PMC9119116.
3. Ding N, Jiang H, **Thapa P**, Hao Y, Alshahrani A, Allison D, Izumi T, Rangnekar VM, Liu X, Wei Q. Peroxiredoxin IV plays a critical role in cancer cell growth and radioresistance through the activation of the Akt/GSK3 signaling pathways. J Biol Chem. 2022 Jun 10:102123. doi: 10.1016/j.jbc.2022.102123. Epub ahead of print. PMID: 35697073.
4. Jiang H, **Thapa P**, Hao Y, Ding N, Alshahrani A, Wei Q. Protein Disulfide Isomerases Function as the Missing Link Between Diabetes and Cancer. Antioxid Redox Signal. 2022 Aug 23. doi: 10.1089/ars.2022.0098. Epub ahead of print. PMID: 36000195.
5. **Thapa P**, Ding N, Hao Y, Alshahrani A, Jiang H, Wei Q. Essential Roles of Peroxiredoxin IV in Inflammation and Cancer. Molecules. 2022 Oct 2;27(19):6513. doi: 10.3390/molecules27196513. PMID: 36235049; PMCID: PMC9573489.
6. Hao Y, Jiang H, **Thapa P**, Ding N, Alshahrani A, Fujii J, Toledano MB, Wei Q. Critical Role of the Sulfiredoxin-Peroxiredoxin IV Axis in Urethane-Induced Non-Small Cell Lung Cancer. Antioxidants. 2023; 12(2):367. https://doi.org/10.3390/antiox12020367
7. **Thapa P**, Jiang H, Ding N, Hao Y, Alshahrani A, Lee EY, Fujii J, Wei Q. Loss of Peroxiredoxin IV Protects Mice from Azoxymethane/Dextran Sulfate Sodium-Induced Colorectal Cancer Development. Antioxidants. 2023; 12(3):677. https://doi.org/10.3390/antiox12030677
8. **Thapa P**, Jiang H, Ding N, Hao Y, Alshahrani A, Lee EY, Wei Q. Peroxiredoxin IV promotes colon cancer progression. *Submitted.*
9. **Thapa P**, Jiang H, Ding N, Hao Y, Alshahrani A, Wei Q. The Role of Peroxiredoxins in Cancer Development. *Submitted.*